STUDY OF THE PENETRATION OF POSITRONS AND ELECTRONS IN DIFFERENT MATERIALS

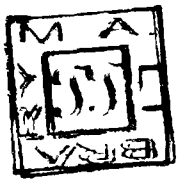

ABSTRACT

THESIS

SUBMITTED TO ALIGARH MUSLIM UNIVERSITY, ALIGARH
IN PARTIAL FULFILMENT FOR THE
AWARD OF THE DEGREE OF

DOCTOR OF PHILOSOPHY

in

PHYSICS

by

TEJA SINGH GILL

M. Sc., M. Phil (Aligarh)

DEPARTMENT OF PHYSICS
ALIGARH MUSLIM UNIVERSITY, ALIGARH.

APRIL 1988

ABSTRACT

This thesis presents new experimental data on newly defined 'straggling free practical' ranges and mass absorption coefficients of positrons and electrons of energy E_{max} lying between 250 KeV to 1.88 MeV in a large number of elemental materials, including the rare earth metals for which these are the first such investigations. While proposing a new definition of the 'straggling free practical range', attempts have been made to establish the meaning of this range which could account for the salient features of the interaction of positrons and electrons with the atoms of the medium they traverse. A new and simple method has been developed for viewing the percentage of transmitted beam intensity theoretically as a function of the thickness of the absorbing material through which the beam passage takes place. A meaningful comparison of the theoretical and experimental data on mass absorption coefficients and ranges has been presented.

The contents of the thesis have been divided in five parts.

The first Chapter deals with the present status of the problem of penetration of positrons and electrons in diffe materials. A summary of the various experimental approaches for the determination of ranges of positrons and electrons is presented. It is observed that most of the measurements are

in few materials and mostly in Aluminium only. These earlier measurements of ranges by different techniques differ from one another because of the use of different conventional definitions of range and the geometrical arrangements of the set-up used. A brief review of the various theoretical approaches on the electron and positron penetration and ranges is also presented in this Chapter.

The second Chapter deals with the upto date developments of the theories of the inelastic processes and the multiple scattering phenomenon followed by the conclusive discussion on the effects of straggling.

In the third Chapter the experimental techniques and measurements of straggling free ranges and mass absorption coefficients of positrons and electrons in a large number of materials and at different energies are presented. A new definition of the 'straggling free practical range' is proposed. A critical investigation of the geometry effect has been reported. A simple empirical relation for the straggling free ranges of these particles is found by subjecting the present experimental data to the least squares fit method. A meaningful comparison of the mass absorption coefficients and straggling free practical ranges, of positrons and electrons has been made. The experimental values of the ranges have been compared with the theoretical values and the limitations of the theoretical calculations have been pointed out.

In the fourth Chapter a new theoretical method to reproduce the transmission curves theoretically has been developed. It is impossible, to build-up the transmission curves and hence to get any information about the absorption coefficients, on the basis of the existing theoretical approaches. The values of the ranges and the mass absorption coefficients realized from theoretically constructed curves at different energies and in a large number of materials, have been compared with the experimental values.

In the fifth and last Chapter a simple attempt has been made to deal with the limitations of the earlier theoretical approach, listed in Chapter first and third. The treatment of the inclusion of the higher order terms in the elastic scattering expression, though not very rigorous, provides a good improvement of the results on ranges. The inclusion of the effects of the diffusion phenomenon on the ranges of positrons and electrons have also been investigated. The final results have been compared with experimental values for few cases at few energies.

It can be concluded that the results of the present investigations confirm that there is a difference between the transmission behaviour of positrons and electrons.

STUDY OF THE PENETRATION OF POSITRONS AND ELECTRONS IN DIFFERENT MATERIALS

THESIS

SUBMITTED TO ALIGARH MUSLIM UNIVERSITY, ALIGARH
IN PARTIAL FULFILMENT FOR THE
AWARD OF THE DEGREE OF

DOCTOR OF PHILOSOPHY

in

PHYSICS

by

TEJA SINGH GILL

M. Sc., M. Phil (Aligarh)

DEPARTMENT OF PHYSICS
ALIGARH MUSLIM UNIVERSITY, ALIGARH.

APRIL 1988

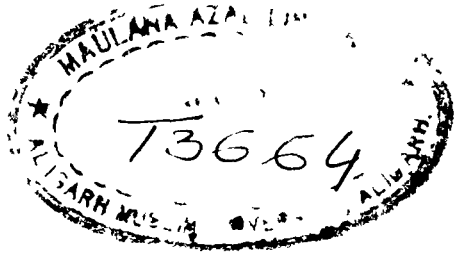

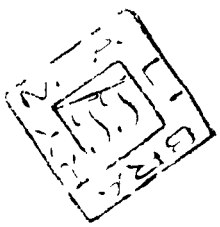

C_E_R_T_I_F_I_C_A_T_E

Certified that the work reported in this thesis is the original work of Mr. Teja Singh Gill, done under my supervision.

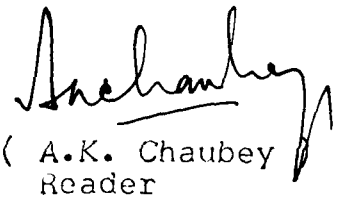

(A.K. Chaubey
Reader
Department of Physics
Aligarh Muslim University
Aligarh, India.

A_C_K_N_O_W_L_E_D_G_E_M_E_N_T_S

I thank late Prof. M.L. Sehgal, Physics Department, Aligarh Muslim University, Aligarh, under whose supervision this work was initiated but the thesis could not be submitted due to his sad demise in December, 1985.

I shall like to express my deep sense of gratitude to Dr. A.K. Chaubey, Physics Department, A.M.U., Aligarh, who is supervising this work now, for encouragement to complete this work. Dr. Chaubey has been indeed a constant source of inspiration and advice for completing this work.

I feel impelled to express my indebtedness to Prof. M.Z. Rahman Khan, former Chairman, Department of Physics and Dean, Faculty of Science; and Prof. Mohd. Shafi, Chairman, Department of Physics, A.M.U., Aligarh, for their interest, sympathetic advice and help in circumventing the difficulties that cropped-up from time to time.

I wish to express my thanks to Dr. P.S. Takhar, Royal Military College of Canada, Kingston, Ontario, Canada, who was my co-worker and co-author in some publications, for extending material help in the experimental work.

I am also deeply indebted to Prof. Wasiur Rehman, Pro-Vice-Chancellor, former Dean of the Faculty of Science, Aligarh Muslim University, Aligarh, whose encouragement has been a constant source of inspiration to me for the completion of this work.

My thanks are also due to all my colleagues in the Department and my wife, Surinderjit Gill, for their co-operation during this work.

I gratefully acknowledge the financial assistance from Council of Scientific and Industrial Research, New Delhi, in the beginning of this study.

I also thank Mr. Mohd. Rashid for neat and careful typing of this thesis.

T.S. Gill.

(Teja Singh Gill)

LIST OF PUBLICATIONS

1. 'Transmission and back-scattering of electrons and positrons by Rare Earth foils.
   T.S. Gill, P.S. Takhar,
   Proc. 14th Int. Rare Earth Res. Conf. North Dakota State Univ., Fargo (U.S.A.) 1979.

2. "Mirror properties of Materials by penetration of electrons and positrons'.
   P.S. Takhar, T.S. Gill and M.L. Sehgal
   Proc. 14th Int. Rare Earth Res. Conf. North Dakota State Univ., Fargo (U.S.A.) 1979.

3. "Ionization Cross-sections for Rare Earths'.
   Takhar, P.S. and Gill, T.S.
   The Rare Earths in Modern Science and Technology, Edited by Gregory J. McCarthy and J.J. Rhyne. Plenum Publishing Corp., New York, pp. 355-58 (1978).

4. "A theoretical method for the determination of electron and positron range in rare earth metals'.
   Gill, T.S., Sehgal, M.L. and Takhar, P.S.
   The Rare Earths in Modern Science and Technology'.
   Edited by Gregory J. McCarthy and J.J. Rhyne.
   Plenum Publishing Corp., New York, pp. 367-73 (1978).

5. "Ionization Cross-sections for positrons and electrons'.
   Takhar, P.S. and Gill, T.S.
   Proc. Int. Conf. on electronic and atomic collisions (Held in Paris) (1977).

6. "Penetration of electrons and positrons in chemical compounds and alloys.'
   Gill, T.S., Sehgal, M.L. and Takhar, P.S.
   Proc. 4th Int. Conf. on positron Annihilation (Helsinger, Denmark) H4 18 (1976).

7. "Environments and radiation standards for ionizing radiation'.
   Takhar, P.S., Gill, T.S. and Sehgal, M.L,
   Proc. 1st Asian regional Conf. on radiation protection (B.A.R.C., Bombay) 1974.

8. "Penetration of electrons and positrons in Rare Earth metals'..
   Gill, T.S., Sehgal, M.L. and Takhar, P.S.
   Proc. 11th Inst. Rare Earth Res. Conf. (Traverse City, Michigan, U.S.A.) Vol. 1, 82-89 (1974).

C_O_N_T_E_N_T_S

CHAPTER - III

EXPERIMENTAL TECHNIQUE AND MEASUREMENTS OF POSITRON AND ELECTRON PENETRATION, IN DIFFERENT MATERIALS

CHAPTER - IV

THEORETICAL METHOD TO BUILD-UP TRANSMISSION CURVES OF POSITRONS AND ELECTRONS

CHAPTER - V

CALCULATIONS OF STRAGGLING FREE PRACTICAL RANGES, $R^{\pm}_{sfp}$ OF POSITRONS AND ELECTRONS

- oOo -

CHAPTER - I

INTRODUCTION AND REVIEW OF THE PROBLEM

1.1 INTRODUCTION

The knowledge of the features of the transmission and absorption of low and intermediate energy electrons and positrons in elemental materials is of great importance for the experimental methods in nuclear, atomic and solid state physics. It is also useful in understanding the various interactions of these particles with matter. In the field of nuclear spectroscopy, for work with internal-conversion electrons, β-rays, Auger electrons and photo electrons etc., one needs to know the exact fraction of the incident electrons transmitted through an absorber. The knowledge of the ranges of these particles in matter has useful applications for the study of biological effects, radiation damage, dosage-rates and energy dissipation at various depths of an absorber. It has also useful applications in the design of detection systems, radiation technology, semi-conductor detectors, shielding and choosing the proper thickness of the targets.

Inspite of these important applications, the concept of ranges of electrons and positrons in matter is still ambiguous. The penetration of positrons through matter and their corresponding differences from electrons has been a subject of very little investigation both theoretically as well as experimentally. The ambiguous concept of the ranges, both from the experimental as well as theoretical point of view, is because of the fact that different experimentalists[1-11] have used different definitions

of range.

The transmission curves of electrons and positrons have a long straight portion down to fairly low transmission and then a considerable tail going into the back ground. At low transmissions, when the electrons have penetrated a certain fraction of their range, the beam becomes diffused and the phenomenon of diffusion sets in, with the result that transmission curves have nearly the same shape at the end. Several definitions have been employed to obtain ranges from the transmission curves. The various range definitions will be discussed in Chapter - III.

With the development of linear accelerators, some workers like Hereford and Swan[7], measured the absorption of monoenergetic electrons of few MeV. In their review article Katz and Penfold[12] gave a comprehensive summary of the earlier work of experimentally determined ranges of monoenergetic electrons and continuous beta-ray energies. They have pointed out that there is no distinct difference in range between monoenergetic electrons of energy E and beta-rays having the same end point energy.

1.2 SUMMARY OF THE EXPERIMENTAL WORK WITH ELECTRONS AND POSITRONS

The earlier experimental work was reviewed by Katz and Penfold[12] in 1952. The measurements were mostly in aluminium

absorber using electrons. The experimental geometries were given no consideration and the final percentage transmissions through absorbers in many cases were quite high and also different for different workers. The experimental work simply depicted the qualitative behaviour of electron transmission. In the early work on transmission experiments no attempt was made for the study of positron transmission. This was probably due to the non-availability of positron sources on the one hand and difficulty in their detection on account of back ground problems involved on the other hand. Seliger[8,9] and Gubernator[10,11] did some work on the transmission of positrons in the energy range of 180 KeV to 960 KeV, and 50 KeV to 160 KeV respectively. These measurements were made in limited absorbers and no considerations were given to the geometry of the detecting system. Nathu Ram et al.[13] have studied the mass absorption coefficients of electrons and positrons of 0.324 MeV and 0.544 MeV in Be, Al, Cu, Ag and Pb. However, they did not corelate their measurements with any theory.

The experimental work with electrons and positrons is represented in table 1.1, indicating the energies at which the measurements were made; the absorbing materials used and the geometry of the experimental set up used, where it is known.

1.3 THEORETICAL APPROACHES

(a) C.s.d.a. ranges:- The abbreviation C.s.d.a. stands for continuous-slowing-down-approximation. Berger and Seltzer[14]

TABLE - 1.1

Important Experimental Work on Electron and Positron Transmission Measurements

Authors with reference	Electron energy	Positron energy	Absorbing Materials used	Geometry of the Experimental Set up used and other details
Widdoson and Champion[27]	1.80 to 2.56 MeV	-	Al only	Geometry not mentioned.
Moore[26]	1.24 to 2.60 MeV	-	Al only	Geometry not mentioned.
Glendenin[23,30]	0.53 to 3.07 MeV	-	Al only	Geometry not mentioned.
Hereford and Swan[29]	3 to 12 MeV	-	Al and Cu	Magnetically analysed β-ray spectrum was used and absorption curves obtained with tripple coincidence counter train. No fixed Geometry used.
H.H. Seliger[8,9]	180 to 960 KeV	180 to 960 KeV	Al, Ag, Sn, Au and Pb	The angle of deflection of the spectrometer is $\Phi = 60^{\circ}$, the radius of curvature 4 cm, the solid angle used is 0.1% of 4π. The source is reflected on the counting tube in the approximate scale 1:1. The distance between the absorbing foils and the G.M. counter window is nearly 5 mm. Nothing has been mentioned about the suitability of this Geometry. The percentage transmission was very high in some cases.

Authors with reference	Electron energy	Positron energy	Absorbing Materials used	Geometry of the Experimental Set up used and other details
Trump et al[28]	2.00 MeV	-	Al only	No fixed Geometry used.
Katz and Penfold[12,24,25]	0.55 to 2.92 MeV	-	Al only	Geometry not defined. They have reviewed the measurements made upto 1952.
K.Gubernator[10,11]	50 to 167 KeV	50 to 167 KeV	Al,Ag,Au and Pb	The source at a considerable distance from the counter and absorber almost against the mica window. The results of any variation of Geometry are not discussed.
B.N.C. Agu et al[4]	0.25 to 0.75 MeV	-	Al,Cu,Ag and Au	No fixed Geometry used.
P.J. Ebert et al[5]	4 to 12 MeV	-	C,Al,Cu,Ag	No fixed Geometry used.
Patrick and Rupaal[33,34]	0.312 MeV	0.324 MeV	Al,Cu,Sn,Pb	Geometry not defined. Comparison of μ^+ and μ^- at unequal energies.
P.S. Takhar[35]	1.77 MeV	1.8 MeV	C,Al,Cu,Sn,Pb	Geometry is identical for positron and electron transmissions. $\mu(e^+)$ and $\mu(e^-)$ compared at unequal energies.

have tabulated these C.s.d.a. ranges taking into consideration the energy loss due to ionization and excitation[15] and also the bremsstrahlung process[16]. The C.s.d.a. range is the path length which a particle would travel in the course of slowing down, in an un-bounded homogeneous medium, from initial kinetic energy T to zero energy, if its rate of energy loss along the entire track were always equal to the mean rate of energy loss. C.s.d.a. range was calculated by integrating the reciprocal of the total stopping power:-

$$R^{\pm}_{C.s.d.a.}(T) = \int_{T_1}^{T} \left[-\frac{1}{\rho} \left(\frac{dE}{dx}\right)^{\pm}_{Total} \right]^{-1} dT + R^{\pm}(T_1) \quad .. \quad (1.1)$$

where T_1 is some lower limit of energy below which the calculations can not be performed because of the poor knowledge of the stopping power and also $\left(\frac{dE}{dx}\right)^{\pm}$ becomes infinite as the energy becomes zero. T_1 is normally taken as 1 KeV. For intermediate and high energy electrons the contribution of $R^{\pm}(T_1)$ is negligible. Also

$$-\frac{1}{\rho}\left(\frac{dE}{dx}\right)^{\pm}_{Total} = -\frac{1}{\rho}\left(\frac{dE}{dx}\right)^{\pm}_{Coll.} - \frac{1}{\rho}\left(\frac{dE}{dx}\right)^{\pm}_{Rad.} \quad \ldots \quad (1.2)$$

where the positive sign corresponds to positron and the negative sign corresponds to electron. ρ is the density of the material.

Berger and Seltzer[17] have tables for the energy loss due to excitation and ionization as well as due to radiation in different materials.

The C.s.d.a. range pertains to a particle track that is 'typical' but not experimentally realizable. If we compare the C.s.d.a. ranges of electrons and positrons in any material with the corresponding experimental values, it is observed that C.s.d.a. ranges are always greater than the measured values. It is also observed that although the C.s.d.a. range is an increasing function of the incident energy of the particle, and this is consistance with the experimental observation, nevertheless if these C.s.d.a. ranges for different elements are plotted as a function of energy, then at a fixed energy the values of these ranges are higher in a high Z material and smaller in low Z material. This is in contradiction with the experimental observations where the values of range at a fixed energy is less in high Z materials as compared with low Z materials. This fact is clear from Fig. 1.1 and 1.2. Hence the C.s.d.a. ranges fail to explain the observed values both qualitatively as well as quantitatively.

(b) Multiple scattering studies:- C.s.d.a. range was based on purely inelastic considerations. Using multiple scattering[32] Rohrlich and Carlson[15] calculated Z_d^+/Z_d^-, where Z_d^+ and Z_d^- are called the average penetration depth for positrons and electrons respectively, which is defined as the amount of absorber thickness to be placed in the path of the beam of positrons or electrons, such that the particles lose completely the memory of their initial orientation.

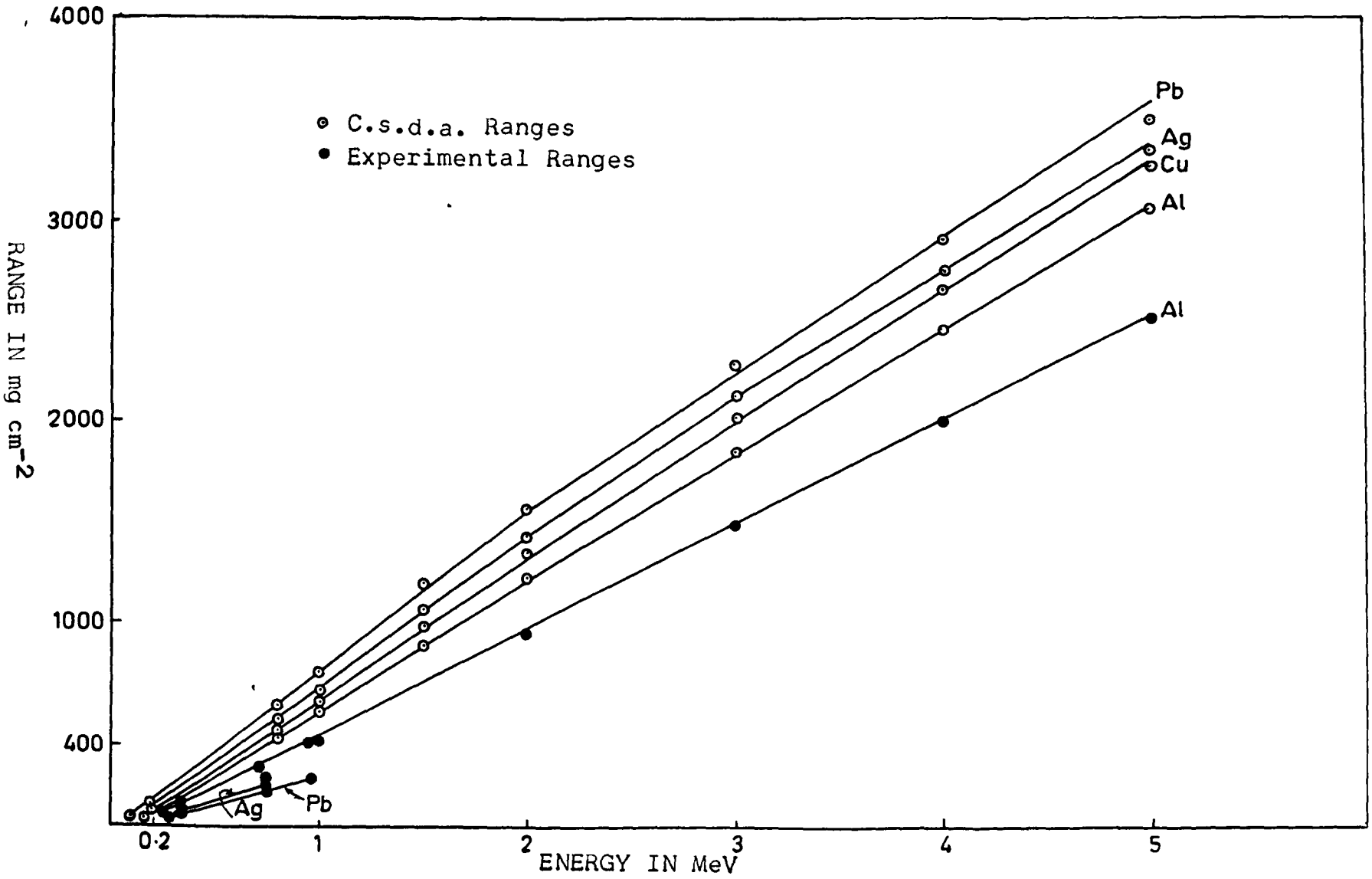

Fig. 1.1 Ranges of electrons as a function of energy.

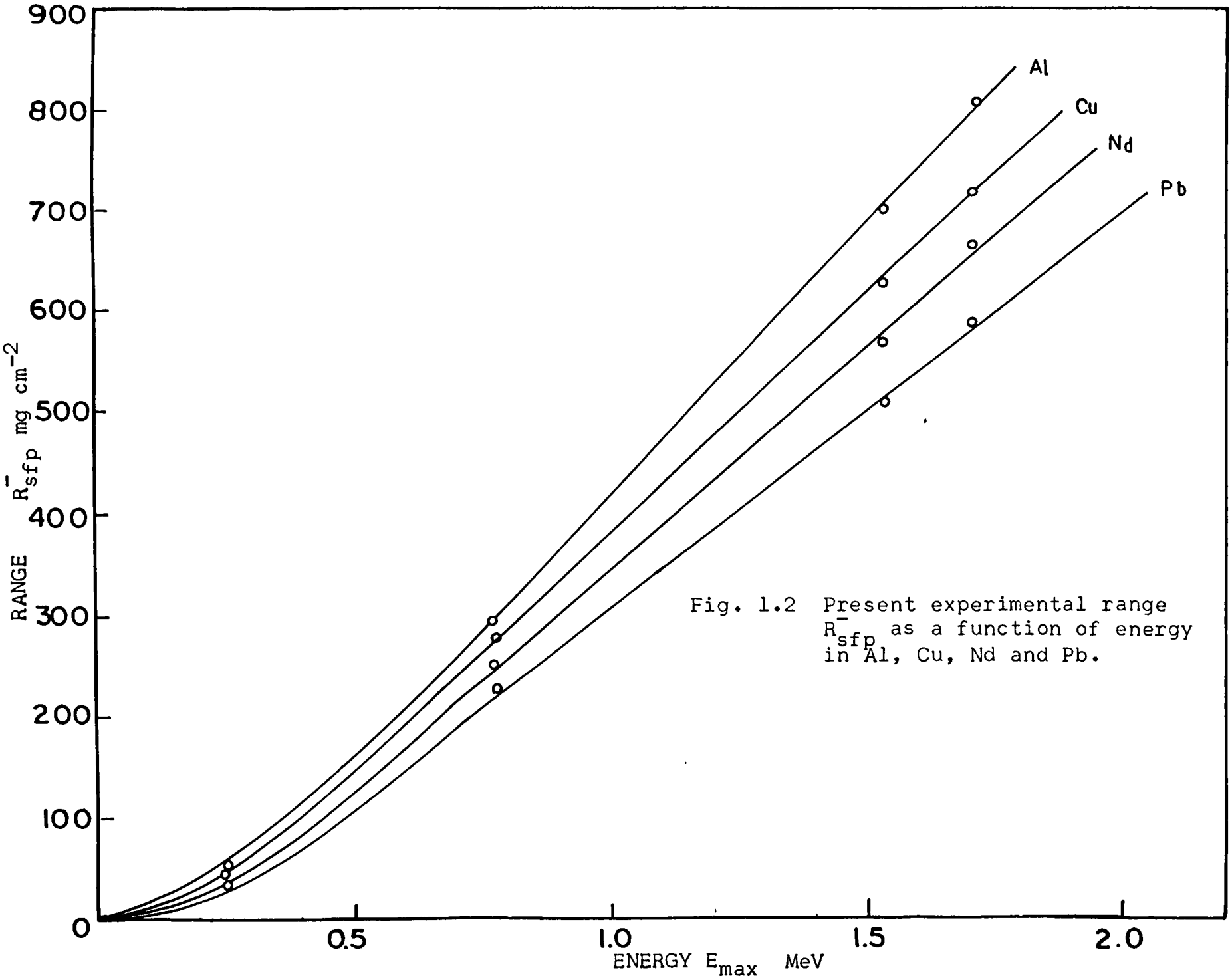

Fig. 1.2 Present experimental range $\bar{R}_{sfp}$ as a function of energy in Al, Cu, Nd and Pb.

The average energy $E_d = \gamma_d mc^2$ at which the particle losses its memory of initial direction is defined by the condition[31)]

$$\langle \text{Cos } \theta \rangle_{\text{average}} = 1/e \qquad \ldots \quad (1.3)$$

where θ is the angle of multiple scattering. They estimated approximately the values of $\gamma_d^{\pm}$ which correspond to the instant when the average cosine of the multiple scattering angle drops to 1/e, for any value of γ_o. The average penetration depth corresponding to $\gamma_d^{\pm}$ is given by:-

$$Z_d^{\pm} = \int_{\gamma_d^{\pm}}^{\gamma_o} k_1^{\pm} (\gamma_o, \gamma) \left| \left(\frac{d\gamma}{ds}\right)^{\pm} \right|^{-1} d\gamma \qquad \ldots \quad (1.4)$$

where

$$k_1^{\pm} (\gamma_o, \gamma) = \langle \text{Cos } \theta \rangle_{av}^{\pm} = \left[\frac{G(\gamma_o)}{G(\gamma)} \right]^{\pm} \qquad \ldots \quad (1.5)$$

and

$$G^{\pm} (\gamma) = \left(\frac{\gamma+1}{\gamma-1}\right)^{a^{\pm}Z} e^{b^{\pm}Z/\beta} \qquad \ldots \quad (1.6)$$

The constants $a^{\pm}$ and $b^{\pm}$ were assumed to be appreximately of the same order of magnitude for small and large values of atomic numbers.

Rohrlich and Carlson[15)] calculated the values of penetration depths in aluminium and lead for the energy range from 0.1 MeV to 2.04 MeV taking into account the energy loss due to

excitation and ionization only. Their values of Z_d^+/Z_d^- in aluminium increase with increasing energy upto about 1 MeV and after that this ratio decreases. In case of Pb, Z_d^+/Z_d^- first increases with energy upto 1 MeV and then becomes constant. No explanation has been given for this behaviour.

Further limitations of these calculations are as follows:

1. The average penetration depth Z_d^+ or Z_d^-, defined by the condition $\langle \text{Cos } \theta \rangle_{av} = 1/e$, has no physical significance and is not experimently realizable quantity, hence it can not be compared with range. The comparison of Z_d^+/Z_d^- with measured range ratio R^+/R^- does not seem to be justified. Z_d^+/Z_d^- at the most provides only the qualitative nature of the multiple scattering differences between electrons and positrons.

2. Rohrlich and Carlson[15] completely ignored the energy loss due to radiations and used only the energy loss due to collisions in their expressions for $\langle \text{Cos } \theta \rangle_{average}$ and $Z_d^{\pm}$. The contribution of radiation losses at 2 MeV for the case of Pb was reported[17] to be 21% of the total energy loss, hence their calculations are not at all reliable at these energies.

3. Due to the approximations used for the evaluation of the integrals in these calculations some percentage error is bound to appear in the final results, but no mention of this error has been made.

4. The values of Z_d^+/Z_d^- has been reported only for the case of

Al and Pb, and these calculations are not possible for other materials. This is because the constants like $a^{\pm}$ and $b^{\pm}$ have been tabulated only for lead and Aluminium.

(c) Theoretical projected ranges:- Rohrlich and Carlson[15] calculated $Z_d^{\pm}$ taking into account only the elastic scattering of electrons and positrons. Also the C.s.d.a. ranges[14] were based on purely inelastic considerations, and both of these approaches[14, 15] do not interpret the measured ranges. While penetrating an absorber the electrons and positrons undergo both elastic as well as inelastic interactions with the atoms of the absorber. Batra and Sehgal[18-21] have taken into account both these processes while calculating the projected ranges $R_p^{\pm}$ for positrons and electrons. The mean projected range is defined as the mean projection of the path of these particles on the direction of incidence in the absorber. They assume that the inelastic scattering is statistically independent of energy loss fluctuations. Near the end of the range of electrons and positrons the energy of the particle becomes small and therefore multiple scattering is large. When the multiple scattering angle becomes very large, the electrons thereafter diffuse randomly and this contributes to straggling. For simplification they assume that the electrons first undergo a straight motion and their interaction with matter is only through inelastic process. The effect of multiple scattering is incorporated afterwards.

In order to apply the multiple scattering correction, the

mean square angle of multiple scattering $\langle\theta^2\rangle_x^{\pm}$ (when electrons traverse a small thickness x of the absorber) is required. The total stopping power $-\frac{1}{\rho}\left(\frac{dE}{dx}\right)^{\pm}_{\text{Total}}$, (where ρ is the density of the material), is required as input parameter for calculating $\langle\theta^2\rangle_x^{\pm}$. Batra and Sehgal[18-21] found simple empirical relations of total stopping power, which are easily integrable. The situations of the random motion of electrons and positrons by multiple scattering have been visualized by them using the definition of transport mean free path λ_{tr}, i.e. the average distance a particle traverses before being scattered through an angle $\geq \pi/2$. This condition has been proved[18-21] to be $\langle\theta_r^2\rangle^{\pm} = 2$

If $T_r^{\pm}$ and $\langle\theta^2\rangle^{\pm}$ are the energy and the mean square projected angle respectively, corresponding to the instant when the motion of the particle becomes random, then the projected $R_p^{\pm}(T)$ is given as:-

$$R_p^{\pm}(T) = R^{\pm}_{\text{C.s.d.a.}}(T) - R^{\pm}_{\text{C.s.d.a.}}(T_r^{\pm}) \qquad \ldots \qquad (1.7)$$

The values or the projected ranges[18-21] are comparable with the present experimental values. The agreement for $6 \leq Z \leq 13$ materials is good. For intermediate and heavy elements these calculations[18-21] give lower values of range as compared to the experimental values. The difference is small for intermediate Z values but goes on increasing with increasing value of Z. At Z = 82 the theoretical values are off by 25% for particle energies of one MeV. The difference is more for still lower

energies. This difference in the theoretical and experimental values is probably because of two reasons.

(1) Batra and Sehgal[18-21] have used Mott's[22] expression for elastic scattering cross section, which is in the form of a power series in αZ, where $\alpha = 1/137$. They have used only the first term of this series, leaving the higher order terms. For small values of Z the higher order terms like $(\alpha Z)^2$ and $(\alpha Z)^3$ give negligible contribution, but for high values of Z, the contribution of these higher order terms may be appreciable.

(2) In these calculations[18-21] they have ignored the contribution to the range coming from the diffusion part. They considered diffusion to contribute to straggling only. From their reference - 21, Figs. 5 - 6, one observes that as the incident kinetic energy of electrons and positrons decreases and also with the increase of the atomic number Z of the absorber, the fraction of energy left with these particle increases. The contribution of the diffusion part of the ranges in the procedure based mainly on their[18-21] calculations, if taken into account makes these calculated values of straggling free practical ranges agree very well with the experimental data.

1.4 PRESENT INVESTIGATIONS

(i) The penetration of electrons of energy E_{max} = 0.25 MeV, 0.77 MeV, 1.53 MeV and 1.71 MeV through a large number of elemental materials, $6 \leqslant Z \leqslant 82$, has been studied experimentally.

Experimental measurements in the rare earth metals have been made for the first time. Simple empirical relations have been found for the straggling free range. Penetration of 1.88 MeV positrons in a number of materials including the rare earth metals has been experimentally investigated, and the comparison is made with the electron transmission.

(ii) An attempt has been made to build-up the transmission curves theoretically so as to get information about the practical ranges and absorption co-efficients of electrons and positrons for $6 \leqslant Z \leqslant 82$. The procedure used is to divide absorbing foils into a large number of thin slices. The scattering of the electrons and positrons in the backward direction in each slice has been taken into account to find the transmission through that particular slice. The energy loss in each slice has also been taken into account. This method is suitable for finding the absorption coefficients of different absorbers at different energies theoretically. The values of the absorption coefficients obtained from these theoretical transmission curves have been compared with the experimental values.

(iii) A simple method has been developed for calculating the straggling free practical ranges, $R^{\pm}_{sfp}$, of positrons and electrons of kinetic energy < 5.0 MeV in materials of any Z, taking into account the straggling part of the range and also accounting for higher order terms in the Mott's expression[22] for the elastic scattering cross section. The procedure is

mainly based on existing theoretical calculations[18-21] with the modification that the ranges of these particles are calculated by taking into account the contributions of both the parts of the range i.e. before and after the diffusion process starts. The ranges thus calculated would be of great use for better understanding of the present experimental data, and a meaningful comparison of the theoretical values with the experimental value:

REFERENCES

1. B.F. Schonland, Proc. Roy. Soc. (London) A135, 429-58(1925).
2. A. Flammersfield, Z. Nature - forsch 2a, 370 (1947).
3. R.W. Varder, Phil. Mag. 29, 725 (1915).
4. B.N.C. Agu, T.A. Burdett and E. Matsukawa,
   (i) Proc. Phys. Soc. (London) 71, 201-206 (1958).
   (ii) Proc. Phys. Soc. (London) 72, 727-732 (1958).
5. P.J. Ebert, A.F. Lauzon and E.M. Lent, Phys. Rev. 183, 422-30 (1969).
6. T. Tabata, R. Ito, S. Okabe and Y. Fujita, J. Appl. Phys. 42, 3361 (1971).
7. E.L. Hereford and C.P. Swan, Phys. Rev. 78, 727 (1950).
8. H.H. Seliger, Phys. Rev. 88, 408 (1952).
9. H.H. Seliger, Phys. Rev. 100, 1029 (1955).
10. K. Gubernator, Zeit Fur Physik, 152, 183 (1958).
11. K. Gubernator and A. Flammerfeld, Z. Phys. Vol. 156, No. 2 179 (1959).
12. L. Katz and A.S. Penfold, Rev. Mod. Phys. 24, 28-44 (1952).
13. Nathu Ram, I.S. Sundara Rao and M.K. Mehta, Phys. Rev. A, Vol. 23, No. 3, 1202 (1981).
14. M.J. Berger and S.M. Seltzer, 'Studies in penetration of charged particles through matter, 'National research council publication No. 1133 P. 205-268 (1964).
15. F. Rohrilish and B.C. Carlson, Phys. Rev. 93, 38 (1954).
16. W. Heither, the quantum theory of radiation (Oxford Univ. Press, London, 1954) Third edition, p. 242.
17. M.J. Berger and S.M. Seltzer, 'Tables of energy losses and Ranges of electrons and positrons, NASA SP-3012 (1964).
18. R.K. Batra and M.L. Sehgal, Nuclear Physics A156, 314-20 (1970).

19. R.K. Batra, Penetration of electrons and positrons in matter, Ph.D. thesis (Un-published) 1971.

20. R.K. Batra and M.L. Sehgal, Nucl. Inst. Methods 109, 565 (1973).

21. R.K. Batra and M.L. Sehgal, Phys. Rev. B, 23, No. 9, 4448 (1981).

22. N.F. Mott, Proc. Roy Soc. (London) A124, 425 (1929), and A135, 429 (1932).

23. L.E. Glendenin and C.D. Coryell, M.D.D.C. 19 (1946).

24. Haslam and Katz et al. Phys. Rev. 80, 318 (1950).

25. L. Katz and A.S. Penfold et al. Phys. Rev. 77, 289 (1950).

26. B.L. Moore, Phys. Rev. 57, 355 (1940).

27. E.E.W. Widdoson and F.C. Champion, Proc. Phil. Soc.(London) 50, 185 (1938).

28. Trump, Wright and Clarke, J. Appl. Phys. 21, 345 (1950).

29. F.L. Hereford and C.P. Swan, Phys. Rev. 78, 727 (1950).

30. L.E. Glendenin, Nucleonics 2, 12 (1948).

31. H.W. Lewis, Phys. Rev. 78, 526 (1950).

32. T. Scott. Williams, Rev. Mod. Phys. Vol. 32/2, 231 (1963).

33. J.R. Patrick and A.S. Rupaal, Physics Letters Vol. 35A, No. 4, 235 (1971).

34. A.S. Rupaal and J.R. Patrick, Physics Letters 38A, No. 6 387 (1972).

35. P.S. Takhar, Phys. Rev. Vol. 157, No. 2, 257 (1967).

CHAPTER - II

PENETRATION OF ELECTRONS AND POSITRONS THROUGH FOILS

2.1 INTRODUCTION

Like other moving charged particles, electrons and positrons, by virtue of their moving electric field create disturbances in the electronic structure of the atoms and molecules of the medium through which they move. The penetrating particles lose energy and are deflected from their origional course, i.e. scattering takes place. In the region of energy of the radio-active β-emitters, the deflection of the electrons is due almost entirely to the elastic collisions with the atomic nuclei, while the energy loss, except that due to the bremsstrahlung which is small, results from the interaction with the atomic electrons. Therefore, it is possible to treat the two phenomena separately, though of course they always occur together. For positrons the general behaviour is the same as that for electrons. A detailed review has been given by Bothe[1] and by Bethe and Ashkin[2]. The theoretical principles have also been discussed in detail by Sauter[3]. When electrons of definite energy pass through a foil of matter, they are slowed down and finally brought to rest by the combined action of these two processes. The total energy loss per unit path length is given by the sum:

$$\left[-\frac{1}{\rho}\frac{dE}{dx}\right]^{\pm}_{\text{Total}} = \left[-\frac{1}{\rho}\frac{dE}{dx}\right]^{\pm}_{\text{Collison}} + \left[-\frac{1}{\rho}\frac{dE}{dx}\right]^{\pm}_{\text{rad.}} \quad \ldots \quad (2.1)$$

2.2 ENERGY LOSS DUE TO COLLISIONS

The interaction of the incident electrons with the atomic electrons in the foil is characterized by the fact that the energy transferred to the atoms per collision is very small. Even for high primary energies (5 to 10 MeV), excitation is more probable than ionization, and the resulting secondary electrons have a mean kinetic energy of only a few ev. The total energy loss after passage through a foil of thickness 'X' is therefore the result of a very large number of small energy losses.

Rohrlich and Carlson[4] have given expressions of average energy loss due to collisions between positrons/electrons and the atomic electrons of the absorber. The well known Bethe - Bloch formula[5] for the average energy loss by collisions is derived for electrons under the assumption that above a certain fractional energy transfer E_1, the atomic electrons can be regarded as free, so that Moller's Cross-section[6] for the scattering of free electrons by free electrons at rest in Born approximation is applicable.

For small energy transfers i.e. $0<E<E_1$, an explicit summation over the various excitation probabilities of the atom must be carried out. The average collision loss per unit path length of electrons and positrons in a medium with N atoms per unit volume is:-

$$\left[-\frac{1}{\rho}\frac{dE}{dx}\right]^{\pm}_{\text{Collision}} = \frac{2\pi e^4 NZ}{Am_0c^2\beta^2}\left[\ln\left(\frac{T^2}{I^2}\cdot\frac{\gamma+1}{2}\right)+ f^{\pm}(\gamma)-\delta\right] \quad \ldots \quad (2.2)$$

where

$$f^{-}(\gamma) = 1 - \beta^2 - \frac{2\gamma-1}{\gamma^2} \ln 2 + \frac{1}{8}\left(\frac{\gamma-1}{\gamma}\right)^2 \text{ for electrons} \quad (2.3)$$

and

$$f^{+}(\gamma) = 2 \ln 2 - \frac{\beta^2}{12}\left[23 + \frac{14}{(\gamma+1)} + \frac{10}{(\gamma+1)^2} + \frac{4}{(\gamma+1)^3}\right]$$

for positrons ... (2.4)

e = Electronic charge, $m_o c^2$ = rest mass energy of an electron = 0.511 MeV.

Z = Atomic number of the scatterer.

β = Ratio of the particle velocity to the velocity of light in vacuum.

T = Kinetic energy of the electron in units of its rest mass energy.

I = Average ionization potential.

γ = Total energy expressed in units of the rest mass energy of the electron.

A = Atomic weight.

ρ = Density of the medium.

δ = Density effect correction factor.

The electron positron difference is collision loss is determined

by the function $f^{\pm}(\gamma)$. These functions which depend only on the incident energy and are independent of the atomic number were plotted by authors[4] as a function of the kinetic energy T of the incident particle in units of $m_o c^2$. From these curves one observes that positrons lose energy more rapidly than electrons below about 345 KeV, but less rapidly above that energy.

2.3 ENERGY LOSS DUE TO BREMSSTRAHLUNG

In addition to the energy loss due to excitation and ionization processes, the energy loss also takes place due to the emission of bremsstrahlung, which occurs when the electron is accelerated in the Coulomb field of the nucleus. A detailed discussion of bremsstrahlung process is given by Heitler[7] and Bethe[2]. When an electron traverses a foil of thickness dx, the everage energy loss due to radiation is given by:

$$\left(-\frac{1}{\rho}\frac{dE}{dx}\right)_{rad.} = N_o E \, \underline{\Phi}\, rad. \qquad \ldots \quad (2.5)$$

where

$$\underline{\Phi}\, rad. = \frac{1}{E}\int_o^T K \; d\sigma_k \qquad \ldots \quad (2.6)$$

where K is the energy of the emitted photon in units of $m_o c^2$, N_o is the number of nuclei per cm^3 and $d\sigma_k$, the differential form of the bremsstrahlung cross-section[8], and $E = \gamma m_o c^2$ is the total energy of the incident electron.

For relatively small energies, $E \ll m_0c^2$, the loss is nearly independent of the kinetic energy of the electrons, for energies very much greater than m_0c^2, it is proportional to E. Due to the use of Born approximation, the Bethe-Heitler theory becomes less reliable as the kinetic energy of the electron decreases. A detailed and comprehensive formulation of bremsstrahlung cross-sections have been reviewed by Koch and Motz[9].

2.4 EMPIRICAL RELATIONS OF TOTAL STOPPING POWER OF ELECTRONS AND POSITRONS:

Simple expressions corresponding to the total stopping power of electrons and positrons taking into account the energy loss both due to collisions and radiations has been given by Batra and Sehgal[10]. For the energy $T \leqslant 500$ KeV the expression for total stopping power is:-

$$\left[-\frac{1}{\rho}\frac{dE}{dx}\right]^{\pm}_{Total} = (mZ + C) \cdot F^{\pm}(\gamma) \qquad \ldots \quad (2.7)$$

where

$$\left.\begin{aligned} F^{+}(\gamma) &= \frac{\gamma^{2.4}}{\gamma^{1.9}-1} \\ F^{-}(\gamma) &= \frac{\gamma^{2.56}}{(\gamma^{2}-1)} \\ \gamma &= \frac{(T+m_0c^2)}{m_0c^2} \end{aligned}\right\} \qquad \ldots \quad (2.8)$$

whereas for energies lying within 0.5 MeV to 5.0 MeV it is given as:-

$$\left[-\frac{1}{\rho}\left(\frac{dE}{dx}\right)\right]^{\pm}_{\text{Total}} = (mZ + C)\left[\frac{\gamma^2}{\gamma(a^{\pm}Z + b^{\pm}) - 1}\right] \quad \ldots \quad (2.9)$$

γ-represents the total energy of positron and electron in units of the rest mass energy of the electron. m, C, $a^{\pm}$ and $b^{\pm}$ are constants and their values have been tabulated[10].

The approximate stopping power values[10] as compared with the theoretical predictions[11] agree within 4%, and they are very convenient to use.

2.5 MULTIPLE SCATTERING EFFECTS

The range estimation from the transmission curves becomes complicated because of the statistical fluctuations of path lengths of electrons on account of the energy loss due to large number of small angle successive deflections. A number of review papers[12-14] on small angle multiple scattering of fast charged particles are available giving the complete picture of the various theories developed from time to time with their merits and demerits.

An exact expression for the scattering of fast electrons by a bare nucleus has been derived by Mott[15]. The spin and the relativistic effects were taken care of by using the second order wave equation for Dirac electrons. Mott's[15]

formula is in the form of a series in Legendre polynomials and is valid when $Ze^2/\hbar v \ll 1$. An expression of this cross-section in powers of αZ ($\alpha = 1/137$) is equivalent to the solution in Born approximation. The resulting expression including only the first order term of the series in αZ is written as:-

$$\sigma^{\pm}(\theta,\gamma) = \frac{1}{4}(\gamma_o Z/\beta^2\gamma)^2 \left[1/\mathrm{Sin}^4(\theta/2)\right] \times$$

$$\left[1-\beta^2 \mathrm{Sin}^2 \theta/2 \mp (\alpha Z)\pi\beta \mathrm{Sin}\, \theta/2(1-\mathrm{Sin}\, \theta/2)\right] \quad \ldots \quad (2.10)$$

where

$$\gamma_o = \frac{e^2}{m_o c^2}, \quad \gamma = \frac{T+m_o c^2}{m_o c^2}, \quad \beta = v/c \quad \text{and} \quad m_o = \text{Electron}$$

rest mass. The upper sign stands for positrons and lower for electrons.

For heavy elements the power series in αZ converge too slowly, and one must resort to a numerical summation of the Mott solution. This was done at various energies by Barlett and Watson[16] for electrons and by Massey[17] for positrons. The last term in equation(2.10) gives the difference between positron and electron scattering and is an important term for heavy nuclei.

Williams[18-19] formulated the multiple scattering theory assuming that the small angle multiple scattering will yield a Gaussian distribution. The projection of the angular distribution of the scattering on a plane containing the incident beam

was also considered. The effects of the finite size of the nucleus and its shielding by orbital electrons were also taken into account. In order to derive the expression for the scattering cross-section[18-19] he used the potential:

$$V(r) = \frac{Ze^2}{r} e^{-r/a} \quad \ldots \quad (2.11)$$

where $a = a_o/Z^{1/3}$ and a_o = radius of the first Bohr orbit of the hydrogen atom.

The expression for the scattering cross-section is given by:

$$\sigma(\theta) = \frac{1}{4} \left(\frac{\gamma_o Z}{\beta\gamma}\right)^2 \frac{1}{\text{Sin}^4\theta/2} (1-\beta^2) \left[1+\left(\frac{\lambda\!\!\!^{-}}{2a \text{ Sin } \theta/2}\right)^2\right]^{-2} \ldots (2.12)$$

The shielding thus little affects the scattering for $\theta >> \theta_{min}$ where $\theta_{min} \backsim \lambda\!\!\!^{-}/a$, and greatly reduces it for $\theta << \theta_{min}$.

This of course is an immediate consequence of the use of Born approximation in which the scattering through an angle θ depends on the field at distances from the nucleus of the order of $\lambda\!\!\!^{-}/\theta$.

In order to incorporate the effect of the finite size of the nucleus Williams[18-19] used the potential:

$$V(r) = (Ze^2/r) (1 - e^{-2r/b}). \quad \ldots \quad (2.13)$$

where b represents the nuclear dimensions, and the scattering cross-section is given by:

$$\sigma(\theta) = \frac{Z^2 e^4}{4m^2v^2} (1-\beta^2)\left(\frac{1}{\text{Sin}^4\theta/2}\right) [1+(b \text{ Sin } \theta/2/\lambda)^2]^{-2} \quad ..(2.14)$$

It is seen that the nuclear size correction reduces the scattering, for θ of the order of and greater than λ/b, but the shielding reduces it for angles of the order and less than λ/a, where a represents atomic dimensions. The corrections thus apply to regions which do not overlap. Hence a general solution for $\sigma(\theta)$ is of the form

$$\sigma(\theta) = \frac{Z^2 e^4}{4m^2v^2} (1-\beta^2) \left(\frac{1}{\text{Sin}^4\theta/2}\right) [(1+ \lambda^2/4a^2 \text{ Sin}^2\theta/2)^{-1}$$

$$-(1+ \lambda^2(a^{-1} + 2b^{-1})^2/4 \text{ Sin}^2\theta/2)^{-1}]^{-2} \quad \ldots \quad (2.15)$$

A detailed evaluation of the effect of the finite size of the nucleus on the elastic scattering cross section has been reported by Elton[20].

Moliere[21] reported a useful fit to the Thomson-Fermi function for heavy atoms. Bethe[22] later on proved that multiple scattering of electrons[21] can be obtained from the exact theory of Goudsmit and Saunderson[23], by making some approximations. The problem of scattering through such angles for which Sin θ can not be replaced by θ was also studied by these authors[23].

An approximate solution of the integro-differential diffusion equation of the multiple scattering problem in an infinite

homogeneous medium without using small angle approximation was given by Lewis[24].

The root mean square (r.m.s.) angle of multiple scattering has been obtained experimentally[25, 26] by measuring the tracks of scattered electrons and positrons by cloud chamber technique and nuclear emulsions. It was reported that experimental curve between r.m.s. angle of the normal part of multiple scattering distribution versus energy agrees well with the theory of Williams[18, 19] and with Moliere's[21] theory.

For any systematic approach involved in the calculations regarding the penetration of electrons and positrons through matter, one needs to know the correct and convenient form of multiple scattering cross-section as input data. The experimental findings[25, 26] indicate that for electron energies above one MeV the agreement with the Moliere's[21] theory of multiple scattering is good, however below 1 MeV the comparison between various experiments and Moliere's theory on multiple scattering shows a disagreement which is more marked with decreasing energies. Also the experimental evidence for difference in multiple scattering of electrons and positrons is contradictory.

For our calculations (Chapter IV), we shall be making use of Mott's[15] scattering cross-section, modified to include the nuclear screening and inelastic scattering corrections. It also includes the relativistic and spin effects and clearly indicates the differences in the multiple scattering of electrons and

positrons.

2.6 EFFECTS OF STRAGGLING

In the case of a fast moving particle passing through thickness of matter the average energy loss may differ considerably from the actual amount lost in a particular case. The effect of straggling will be small only if the particle loses its energy in the form of a large number of small parts, which is true for heavy particles.

An electron however may lose a large fraction of its energy in a single collision. After having traversed a sheet of matter the electron will have emitted only few quanta of large energy and the fluctuations of the energy loss will be very large.

Bethe and Heitler[27] have studied this straggling by neglecting the collision loss. Eyges[28] studied the straggling of electrons caused by loss of energy by radiation as well as by collisions, and discussed the straggling of electrons with energy near the critical energy. Where the critical energy is defined as energy loss per radiation length. Straggling probability is found in the form of a series whose terms decrease rapidly for energies not too small and not too large thickness.

The straggling function $\pi(E,t)$ defined such that $\pi(E,t)\,dE$ is the probability that an electron has energy in the range E to E + dE at thickness t, satisfies the diffusion equation[29]

$$\frac{\partial \pi(E,t)}{\partial t} = - \int_o^1 [\pi(E,t) - \frac{1}{1-v} \pi(\frac{E}{1-v}, t)] \times$$

$$\Phi(E,v)\, dv + \beta \frac{\partial \pi(E,t)}{\partial E} . \qquad \ldots \qquad (2.16$$

Where $\Phi(v)\, dv\, dt$ is the probability that in the thickness dt the electron emits a photon which has a fraction between v and v+dv of the electron energy. The first term on the right hand side of (2.16) describes the decrease in $\pi(E,t)$ due to electrons initiall in the interval (E,dE) which leave it by radiation. The second term describes the increase in $\pi(E,t)$ due to electrons of energy greater then E which enter the interval (E,dE) by radiation and the last term takes account of the collision loss.

The main draw back of the treatment given by Eyges[28] is that no proof of the convergence of series of straggling probability is given. In fact for very small energies the terms increas and some higher order terms become infinite at zero energy.

Theories relating to the straggling of ionization losses by electrons in thin absorbing foils have been successively improved by Williams[30], Landau[31] and Blunck and Leisegang[32].

REFERENCES

1. W. Bothe, Hand buch der Physik 22/2 (Berlin, 1933) p. 1.
2. H.A. Bethe and J. Ashkin, Experimental nuclear physics I (ed. E. Segre; New York 1953).
3. F. Sauter, in: Kosmische stahlung (ed. W. Heisenberg, Berlin 1953).
4. F. Rohrlich and B.C. Carlson, Phys. Rev. 93, 38 (1954).
5. H.A. Bethe, Hand buch fur Physik (Julius springer, Berline 1933), Vol. 24/2, p. 273.
6. C. Moller, Ann. Physik, 14, 531 (1932).
7. W. Heitler, Quantum theory of radiations (Oxford 1948).
8. Rev. Mod. Phys. Vol. 31, No. 4, 924 (1959).
9. H.W. Koech and Motz, Rev. Mod. Phys. 31, 920 (1959).
10. R.K. Batra and M.L. Sehgal, Nuclear Inst. Meth. 109, 565 (1973).
11. M.J. Berger and S.M. Seltzer, NAS-NRC Publ. No. 1133 (1964) and NASA SP-3012 (1964).
12. R.D. Birkoff, 'Passage of fast electrons through matter, Hand buch der Physik Vol. 34, 115 (1958).
13. M.J. Berger, 'Monte Carlo Calculation of the penetration and diffusion of fast charged particles, 'Methods in computational Physics Vol. 1, 135, (1963) Academic Press.
14. T. Scott Williams, Rev. Mod. Phys. Vol. 35/2, 231 (1963).
15. N.F. Mott, Proc. Roy. Soc. (London) A124, 425 (1929) and A135, 429 (1932). N.F. Mott and H.S.W. Massey, 'The theory of Atomic collisions, Oxford University Press London,(1949).
16. J.H. Barlett and R.E. Watson, Proc. Am. Acad. Arts. Sci., 74, 53 (1940).
17. H.S.W. Massey, Proc. Roy. Soc. (London) A181, 14 (1942).
18. E.J. Williams, Proc. Roy. Soc. (London) A169, 531 (1939).

19. E.J. Williams, Phys. Rev. 58, 292 (1940).

20. L.R.B. Elton, Proc. Phy. Soc. A63, 1115 (1950).

21. G. Moliere, Z. Naturforsch 24, 133 (1947) and 34, 78 (1948).

22. H.A. Bethe, Phys. Rev. 89, 1256 (1953).

23. S. Goundsmit and J.L. Saunderson, Phys. Rev. 57, 24 (1940) and Phys. Rev. 58, 36 (1940).

24. H.W. Lewis, Phys. Rev. 78, 526 (1950).

25. G. Groetzinger, M.J. Berger and F.L. Ribe, Phys. Rev. 77, 584 (1950).

26. F.F. Heymann and W.F. Williams, Phil Mag, 1, 212 (1956).

27. H. Bethe and W. Heitler, Proc. Roy. Soc. (London) A126, 83, (1934).

28. L. Eyges, Phys. Rev. 76, 264 (1949) and Phys. Rev. 77, 81 (1950).

29. B. Rossi and K. Greisen, Rev. Mod. Phys. 13, 240 (1941).

30. E.J. Williams, Proc. Roy. Soc. (London) A125, 470 (1929).

31. L. Landau, J. Phys. (U.S.S.R.) 8, 201 (1944).

32. O. Blunck and S. Leisegang : Z. Physik 128, 500 (1950).

CHAPTER - III

EXPERIMENTAL TECHNIQUE AND MEASUREMENTS OF POSITRON AND ELECTRON PENETRATION IN DIFFERENT MATERIALS

3.1 INTRODUCTION

The absorption method is still widely used for determining electron energies of both monoenergetic electrons and β-rays from their range in aluminium. In the present measurements related to electrons and positrons, the absorption method has been used. This method has the advantage of simplicity, speed and above all sensitivity. It gives results of fair accuracy in the low energy region.

In the present measurements a new definition of the so called 'straggling free practical' range, $R^{\pm}_{sfp}$ is proposed, which includes the contribution of straggling of electrons and positrons. This range has been measured for β^- particles with E_{max} = 0.25 MeV (Ca^{45}), 0.77 MeV (Tl^{204}), 1.53 MeV (Y^{91}) and 1.71 MeV (P^{32}) in Carbon, Aluminium, Nickel, Copper, Yttrium, Zirconium, Silver, Cadmium, Indium, Neodymium, Holmium, Ytterbium, Gold and Lead absorbers. The transimission of β^+ (positrons) of 1.88 MeV has been studied through Carbon, Aluminium, Copper, Yttrium, Silver, Neodymium, Holmium, Ytterbium, Gold and Lead absorbers. The transmission measurements of β^+ and β^- in rare earth metals like Y, Nd, Ho and Yb have been carried out for the first time and it is found out that they behave exactly similar to other elemental materials studied at present. A new technique has been developed for the detection of the transmitted beam of positrons, which eliminates the problem of the gamma-ray back ground associated with the beam of positrons.

The present experimental measurements have been compared with the recent theoretical predictions of Batra and Sehgal[1-3]. This comparison points out the limitations of these theoretical calculations[1-3] and an improvement has been suggested. The details of the improvements have been discussed in Chapter V.

On the basis of the present experimental results a simple empirical relation between the straggling free practical range, $R^{\pm}_{sfp}$, energy E and the atomic number Z has been formulated with the help of least square fit method. The mass absorption coefficients $\mu_m(e^-)$ and $\mu_m(e^+)$ of electrons and positrons have been tabulated and a comparison of these coefficients is done at identical energies of electrons and positrons. This comparison of mass absorption coefficients indicates a small but finite difference, implying greater transmission of positrons than electrons.

3.2 RANGE DEFINITIONS

If the fraction of the incident betas which pass through the given thicknesses of the absorber are plotted against those thicknesses an absorption curve is obtained. For high thicknesses of the absorber the curve passes into the back-ground, which is due to cosmic rays and gamma rays when they are present. Encouraged by the similarity of the shape of the transmission curve. Schonland[4] and Flammersfield[5], defined the point at which the extension of the linear portion of the transmission curve meets

the back-ground as the practical range, whereas the point where the tail of the transmission curve meets the back-ground is known as the maximum range. The maximum range of electrons and positrons though a very useful quantity has not been explained theoretically, because of the complicated phenomenon of diffusion which sets in at the end of the transmission curve.

Varder[6] defined the extrapolation of the linear portion of the transmission curve of the monoenergetic electrons to the thickness axis as the 'practical maximum range'. Still some other workers like Agu et al.[7], Ebert et al.[8] and Tabata et al.[9] gave a similar definition of range as Varder[6] and they called it 'extrapolated range' R_{ex}, which is defined as the point where the tangent at the steepest point on the almost straight descending portion of the transmission curve meets the thickness axis.

The practical range[4,5], the practical maximum range[6] and the extrapolated range[7,9], as defined above, though useful experimental quantities, include the straggling effects and hence can not be compared with the theoretical straggling free ranges. Theoretically, range of electrons is defined[10] as the limiting thickness of the absorber beyond which essentially none of the originally incident electrons emerge. Such a thickness does not exist practically, because of the straggling effects. Therefore, even when the theories concerning the slowing down process[11] and multiple scattering[12,13] are available, it is

not possible to compare the experimental measurements, as defined above, with the theoretical ranges.

A new definition of the so called 'straggling free practical range' $R^{\pm}_{sfp}$, of electrons and positrons is proposed. It is defined as the point where the extrapolation of the linear portion of the transmission curve meets the straggling portion of the curve, when it is extrapolated in the backward direction. The range $R^{\pm}_{sfp}$ along with other ranges as explained above are shown in Fig. 3.1. The extrapolated range[7,9], R_{ex}, can not be shown on the semilog graph and hence it is not shown in Fig. 3.1. It has been experimentally verified that the range $R^{\pm}_{sfp}$ is not sensitive to the strength of the source used. However, range R_{ex} as defined in reference 7, 8 and 9 is very much sensitive to the strength of the source and also to the percentage of transmission reached.

For absorbers of light and medium atomic numbers the tail of the transmission curve which corresponds mostly to straggling can be approximately represented by a straight line and therefore the error involved in its extrapolation in the backward direction is negligibly small. For absorbers of high atomic number, the so called straggling part of the transmission curve can not be exactly approximated by a straight line and some subjective error is possibly introduced while extrapolating it in the backward direction to find $R^{\pm}_{sfp}$. In the present measurements this error has been found to be of the order of 2% for the case of Gold and Lead.

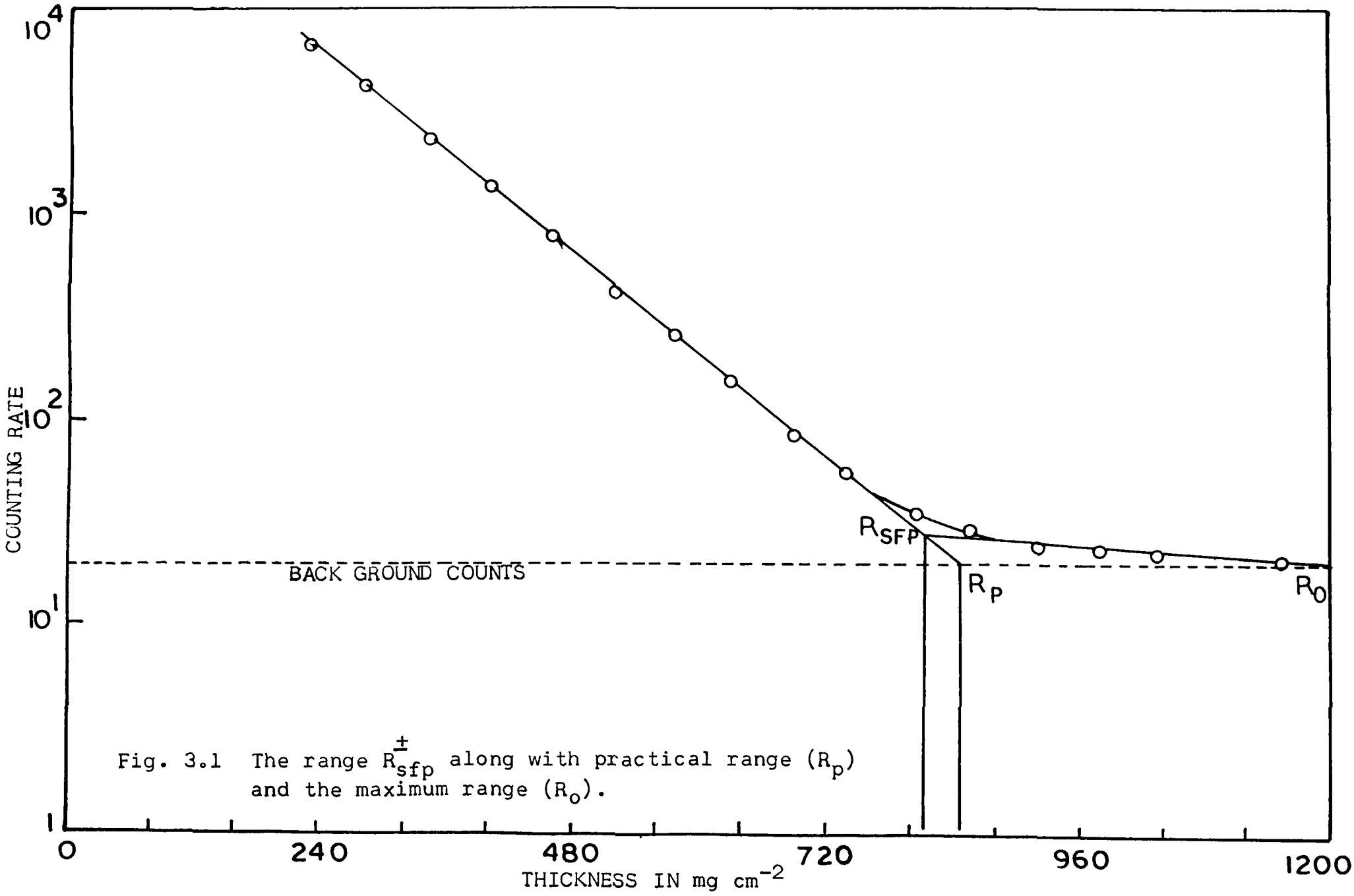

Fig. 3.1 The range $R^{\pm}_{sfp}$ along with practical range (R_p) and the maximum range (R_o).

3.3 GEOMETRY CONSIDERATION OF TRANSMISSION METHOD FOR MEASUREMENT OF RANGES OF ELECTRONS AND POSITRONS

Mostly in the experiments relating to the transmission of electrons and positrons the standard transmission method is used, in which absorbing foils are interposed in between the detector and the source. Different workers[4-9, 14-16] have choosen different positions of the absorbing foils with respect to the detector. Each of these different positions of the absorber corresponds to a different geometry of the detecting system. Apart from the importance of identical geometries in various measurements, it is also very essential to know as to which is the most suitable geometry, i.e. the position of the absorbing foils with respect to the detector, so that a meaningful comparison of the measured values of the ranges can be made with the available theoretical values[1-3].

The absorption of electrons and positrons means their removal from the incident beam due to multiple scattering or sometimes single scattering in the coulomb field of nuclei of the scatterer. When the absorber is held immediately above the detector and the electrons or positrons are incident perpendicularly on it, only those particles shall be absorbed i.e. removed from the incident beam, which get scattered through an angle $\geqslant \pi/2$. whereas when the detector is far away from the scattering foils, the electron will be removed from the beam even when the average angle of scattering is $\leqslant \pi/2$. Thus the

probability of an incident particle being removed is smaller for the case when the scatterer is very near to the detector than the case when the foil is kept away from the detector.

Batra and Sehgal[1-3] did some calculations for practical ranges of electrons and positrons taking into account the multiple scattering effects, which is important near the end of the electron's range. They used Wilson's[17] approach which is based on the approximation that the electrons proceed in the original direction till their energy is reduced to such a value for which the mean square projected angle becomes so large that electrons thereafter start diffusing randomly. The situation of the diffusion of the electrons by multiple scattering was visualized using the definition of transport mean free path, i.e. the average distance a particle travels before being scattered through an angle $\geq \pi/2$. In the light of these calculations[1-3], a suitable geometry of the detecting system is the one in which the foils are placed as near to the detector as possible. For relative transmission measurements of positrons and electrons to be meaningful, it is necessary that the experiments be performed under identical geometries.

The experimental verification of the effect of absorber position with respect to the detector on the range of electrons has been studied using the absorption method. It consists of an electron source placed at the centre of an evacuated brass metallic sphere with a thin mica window and a scintillation

detector. The experimental arrangement is shown in Fig. 3.2. β-particles with end point energies of 1.71 MeV and 0.77 MeV were used for recording the transmission in Aluminium absorber, corresponding to various positions of the absorber placed between the fixed positions of the source and the detector. The results of range measurements from these transmission curves are shown in table 3.1.

TABLE - 3.1

Distance of the absorber from the detector in cms	Range in mg cm^{-2} with E_{max}=1.71 MeV	Range in mg cm^{-2} with E_{max}=0.77 MeV
1	814 ± 24	296 ± 8
2	796 ± 23	278 ± 8
3	785 ± 23	272 ± 8
4	775 ± 23	264 ± 8
5	746 ± 22	254 ± 7

Table 3.1 shows that the value of the range in an absorber goes on increasing as the detector comes nearer to the absorber foil, and has a maximum value when the foil is placed just

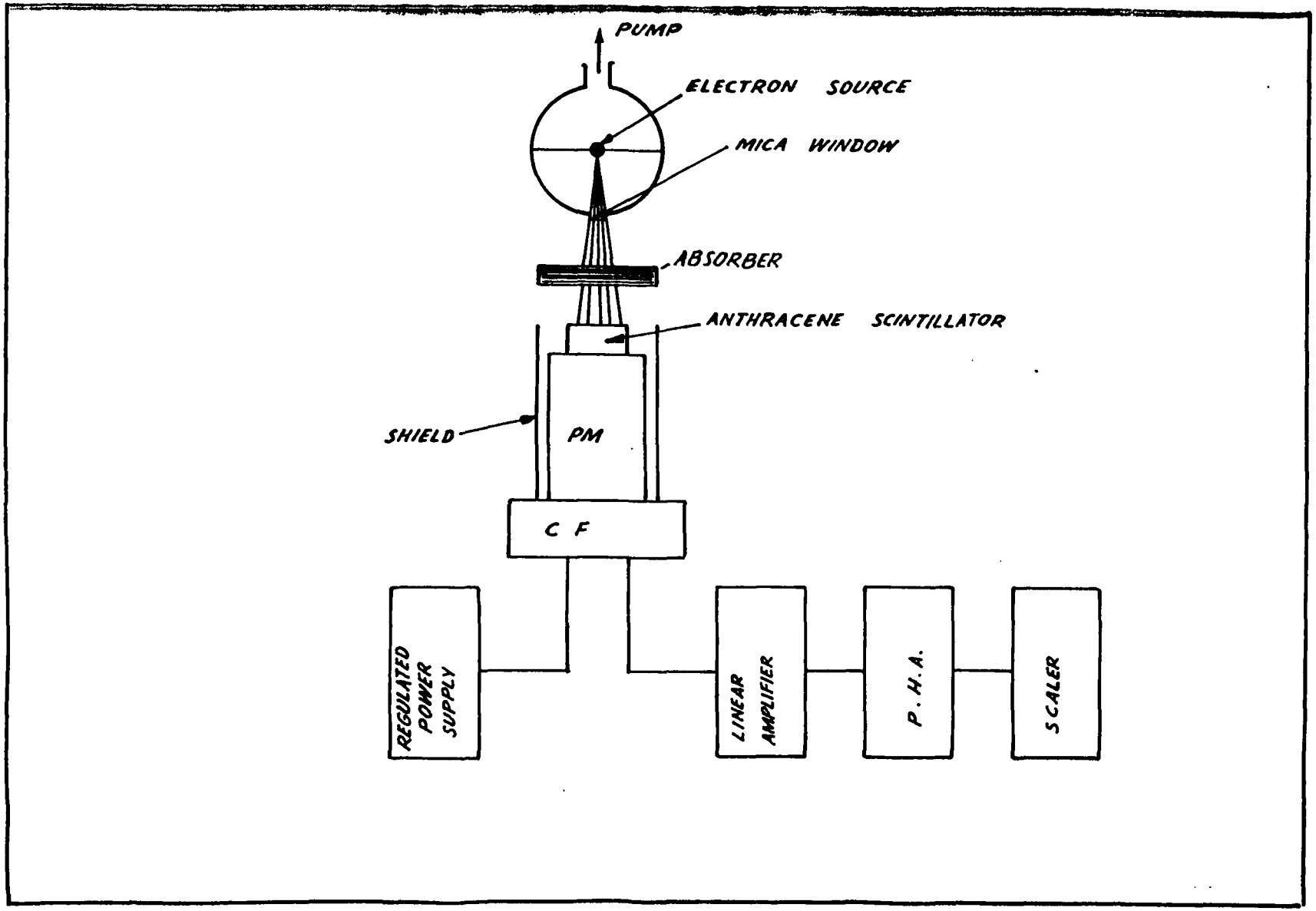

Fig. 3.2 Arrangement for electron transmission measurement. P.M., Photomultiplier, C.F., Cathode follower, P.H.A., Pulse Height Analyzer.

above the detector. The difference in range for two extreme positions is of the order of 14% which is beyond the limits of experimental uncertainties. These results are quite consistance with the qualitative interpretations given above.

3.4 EXPERIMENTAL METHOD AND MEASUREMENTS WITH POSITRONS

The earlier work on positron transmission was done by Seliger[14] and Gubernator[15,16]. They used 90° magnetic analyzers to eliminate the gamma-ray back-ground from the radioactive source. But no care was taken of the additional gamma-rays which are created by annihilation of positrons in the slit, walls, and the absorber itself. Hence there is a strong possibility that some gamma-rays always reach the detector inspite of direct shielding. Secondly the absorber in front of the detector in the presence of a gamma-ray acts as a radiator and this back-ground depends on the thickness of the absorber used and its atomic number. Therefore along with the positrons there may be some knock-on electrons going to the detector.

In the present experiments the positron transmission was measured very precisely using a slow-fast coincidence circuit[18-20]. This arrangement helps to eliminate the gamma-ray back-ground associated with the emission of positrons. Using his magnetic analyzer, Seliger[14] could detect the transmission intensity as low as 35% in the case of Pb absorber and positron energy of 960 KeV. For the same absorber the present lower limit of

transmission intensity is of the order of 2%.

The positron source Ge-Ga^{68} is placed at the centre of an evacuated brass sphere with a mica window (Fig. 3.3) of 4 mm diameter and thickness = 0.0006 inches. The brass sphere was shielded with a hemi-spherical well shaped enclosure. The pressure inside the brass-sphere was 10^{-5} Torr. The absorber in which the penetration of positrons is to be studied is placed below the window of the brass-sphere. The transmitted beam of positrons is then allowed to fall on an Aluminium block, where they annihilate giving rise to photons, each of 511 KeV. These photons are emitted at an angle of 180° to each other and they are detected by a pair of scintillation crystals, [NaI (Tl)], which are placed under a narrow geometry with three inches of Lead shielding. The pulses from two scintillation counters are mixed in a coincidence unit to give a coincidence count. The rate of chance coincidence is very low.

Annihilation Material

The thickness of the Aluminium block used for annihilation of positrons was varied slowly, starting from a very small thickness, till the count rate becomes maximum. Similar experiments were done with Copper, Nickel and Water as annihilation materials The water was contained in a liquid cell made with plexiglass. The empty container in the path of the beam corresponds to zero water thickness.

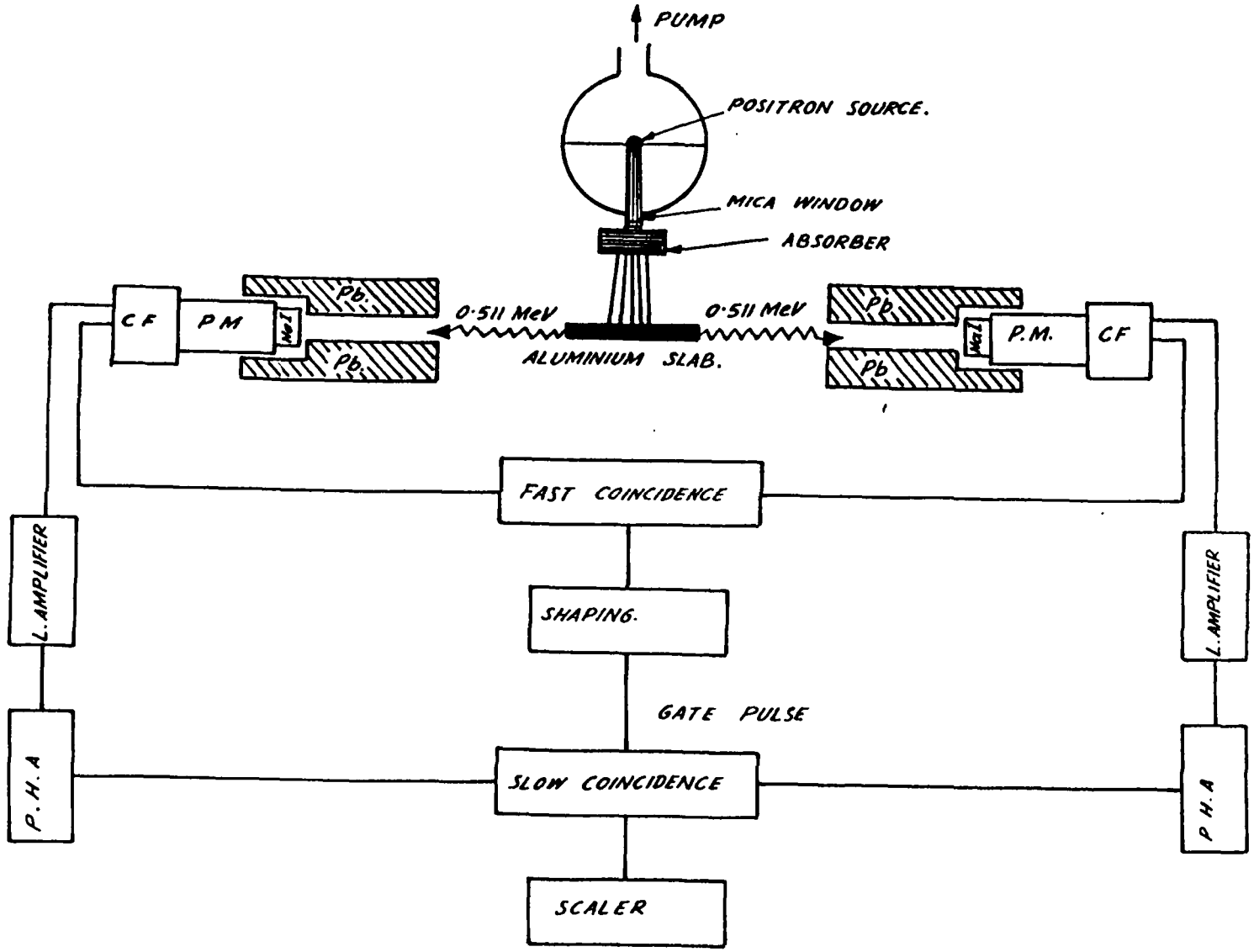

Fig. 3.3 Arrangement for positron transmission measurement. P.M., Photomultiplier, C.F., Cathode Follower, P.H.A., Pulse Height Analyzer.

The absorption of positrons in Al and Cu have been compared as shown in Fig. 3.4(i). The absorption curves for Ni and H_2O are given in Fig.3.4(ii) showing the logarithim of the observed annihilation rate N_t^+ as a function of absorber thickness in mg cm^{-2}. The thickness of the Aluminium block (4 mm) was adjusted to give the maximum number of counts Fig.3.4(iii)

3.5 EXPERIMENTAL SET-UP AND METHOD FOR ELECTRONS

The experimental arrangement for electrons is shown in Fig. 3.2. The electron source was mounted at the centre of the same hollow brass sphere as was used for positrons. The detector consists of an anthracene crystal mounted on a photomultiplier tube. The light pulses are fed to a linear amplifier through a cathode follower, and finally counted with the help of a scaler. The absorber through which the transmission is to be studied is placed in between the source and the detector. By using an anthracene crystal as a detector the dead time correction is reduced to almost zero value, whereas when window counters and ionization chambers are used, there will always be some dead time and recombination losses respectively. The minimum detectable energy in the anthracene crystal is approximately 5 KeV. The beta-sources used are carrier free which makes the measurements free of self absorption problems.

3.6 EXPERIMENTAL RESULTS AND DISCUSSION

(a) The percentage transmission of the beam intensity as a

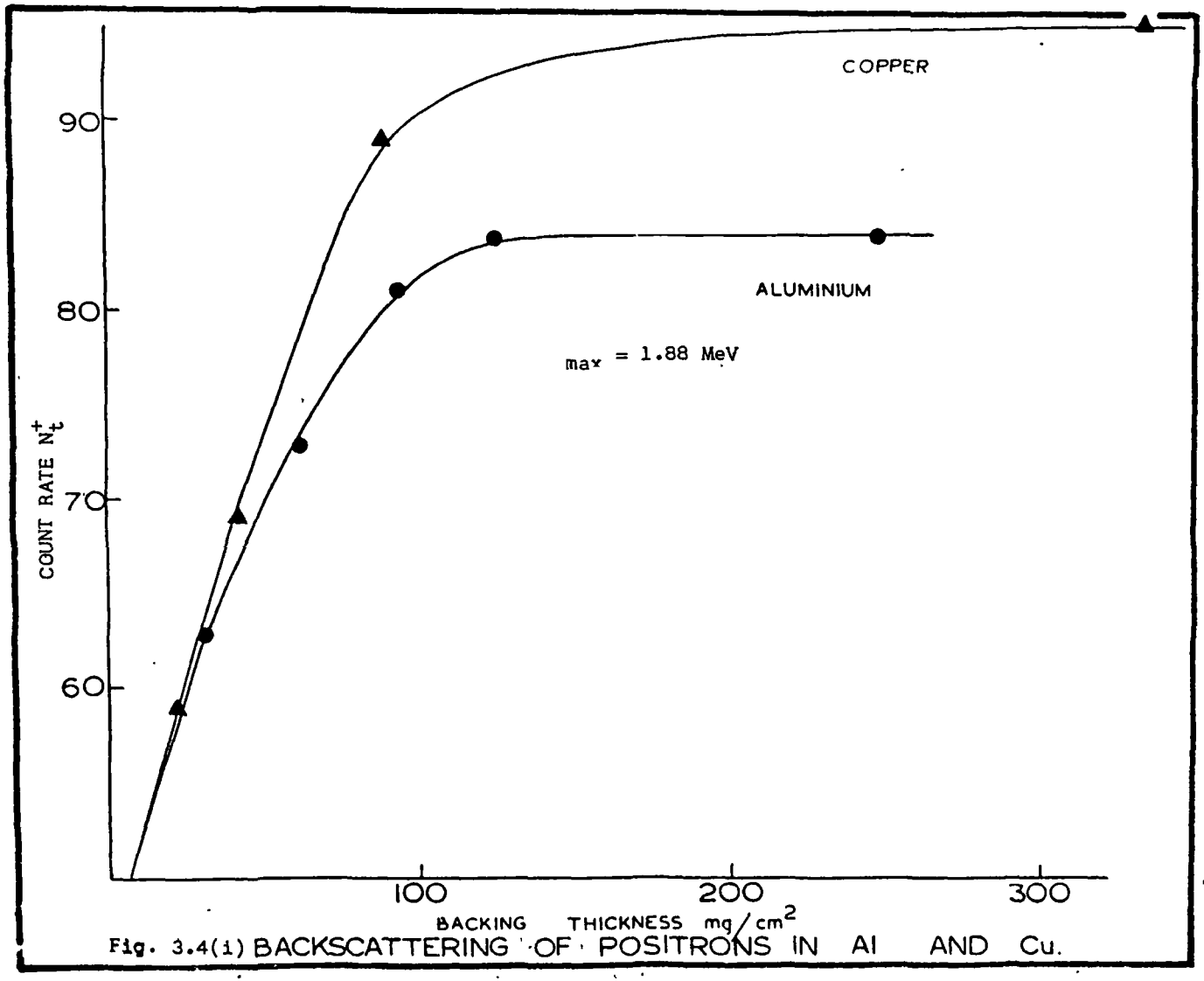

Fig. 3.4(i) BACKSCATTERING OF POSITRONS IN Al AND Cu.

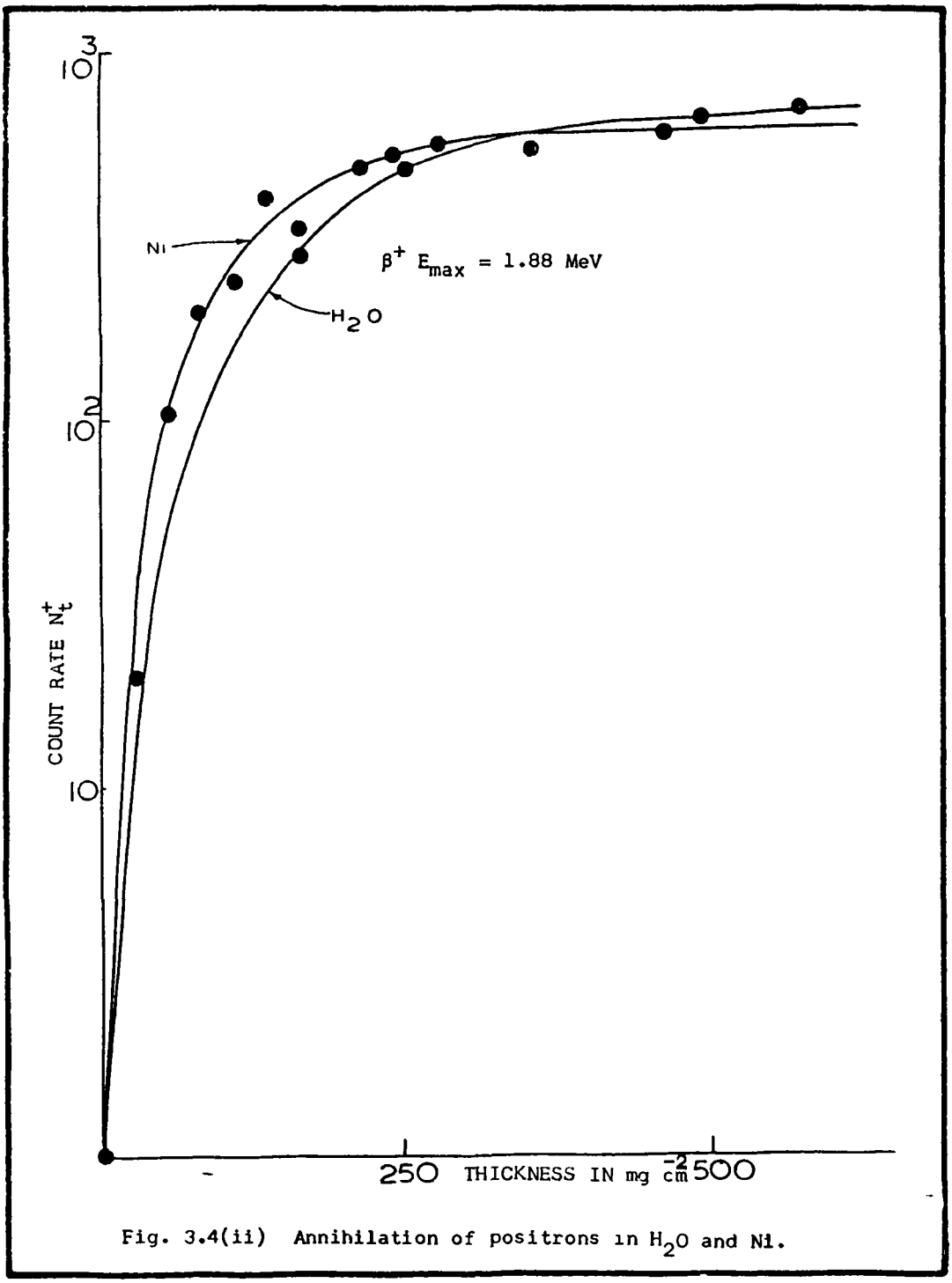

Fig. 3.4(ii) Annihilation of positrons in H_2O and Ni.

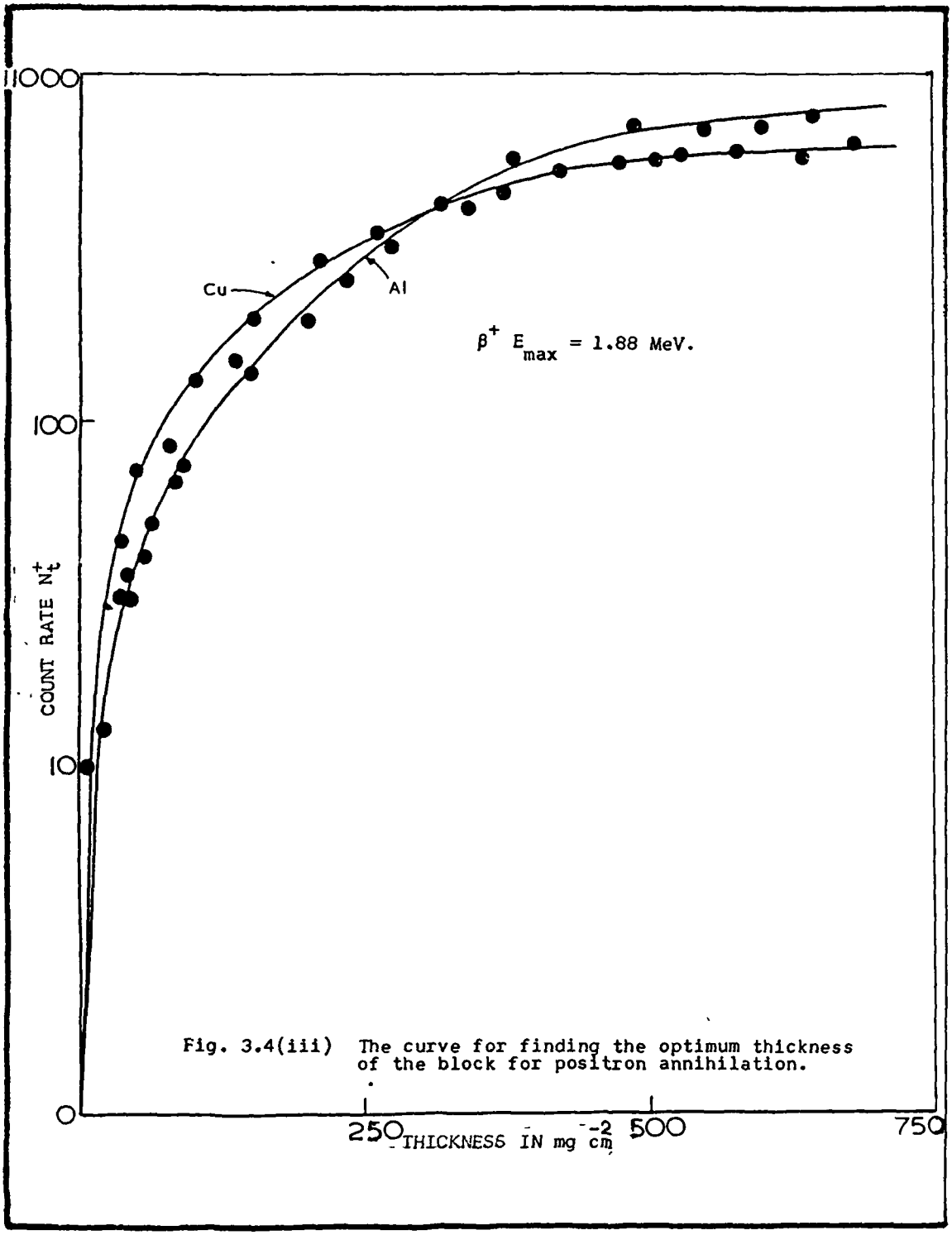

Fig. 3.4(iii) The curve for finding the optimum thickness of the block for positron annihilation.

function of the absorber thickness in mg cm^{-2} for some of the elemental materials is plotted in Figs. 3.5 - 3.10. The plots for other materials follow a similar trend, hence they are not shown. On a semilogarithmic graph these plots are linear. The experimental results on the transmission of positrons and electrons through some of the rare earth metals are shown in Figs. 3.11 - 3.14. The rest of the plots for rare earth metals also follow the similar trend.

The values of $\bar{R}_{sfp}$ for different absorbers are tabulated in table 3.2. The experimental uncertainties in the values of $\bar{R}_{sfp}$, which are of the order of 2 to 4% are also shown in table 3.2. The values of $\bar{R}_{sfp}$ of electrons with E_{max} = 0.25 MeV were not investigated for higher atomic numbers like Gold and Lead due to the non-availability of thin foils of these materials. The values of $\bar{R}_{sfp}$ for rare earth metals, i.e. Y, Nd, Ho and Yb are also shown in table 3.2 and they reveal similar trends as the other elemental materials.

(b) Empirical Relation for $\bar{R}_{sfp}$

In nuclear spectroscopy work the energy region of interest is upto 3 MeV or so. There is no simple relation between range, energy and the atomic number in this region of energy. Hence it was thought worthwhile to find some simple empirical relation between these three parameters in this energy region. On the basis of the present measurements for the straggling free

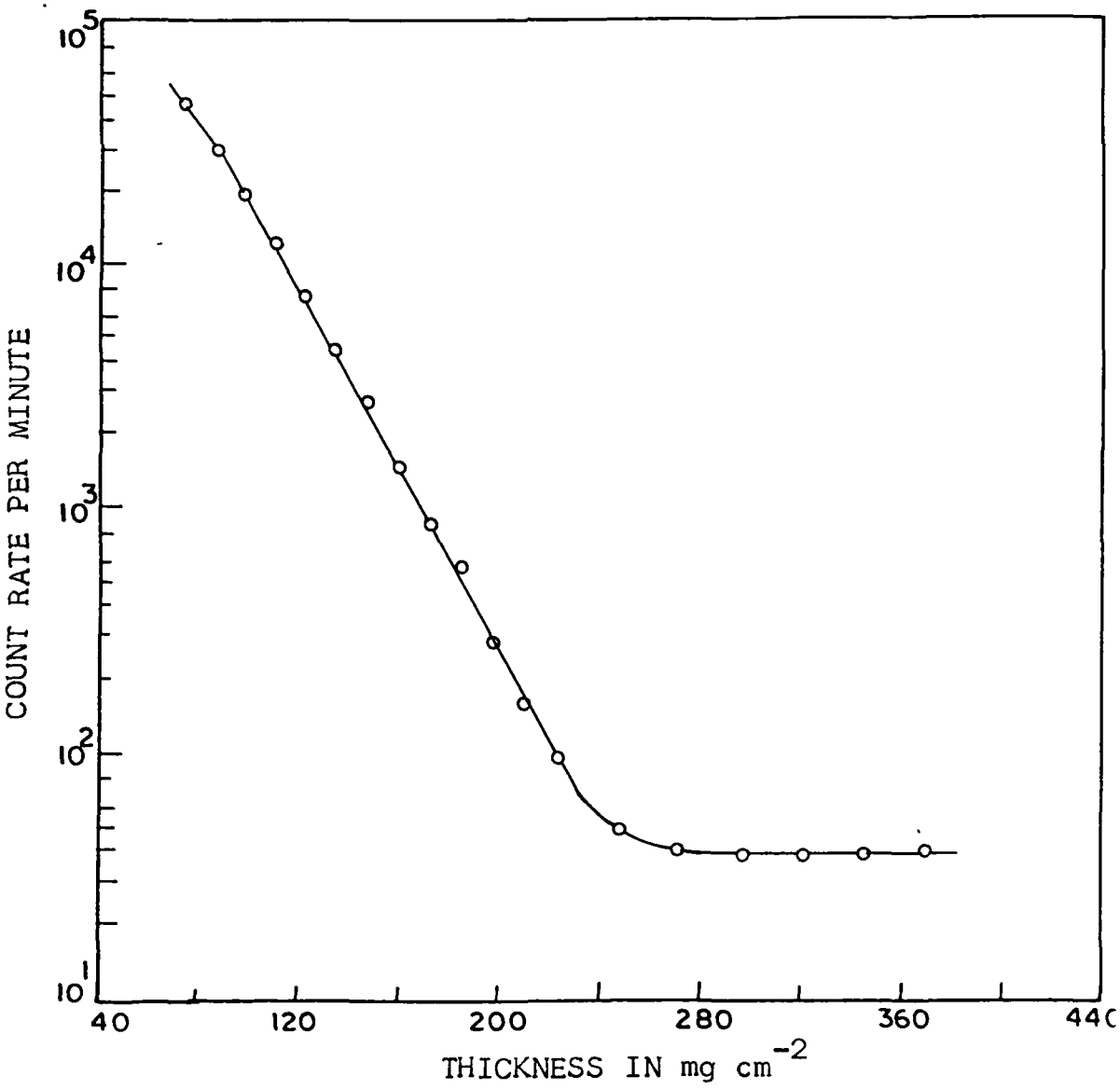

Fig. 3.5 Electron absorption curve in silver at energy E_{max} = 0.77 MeV.

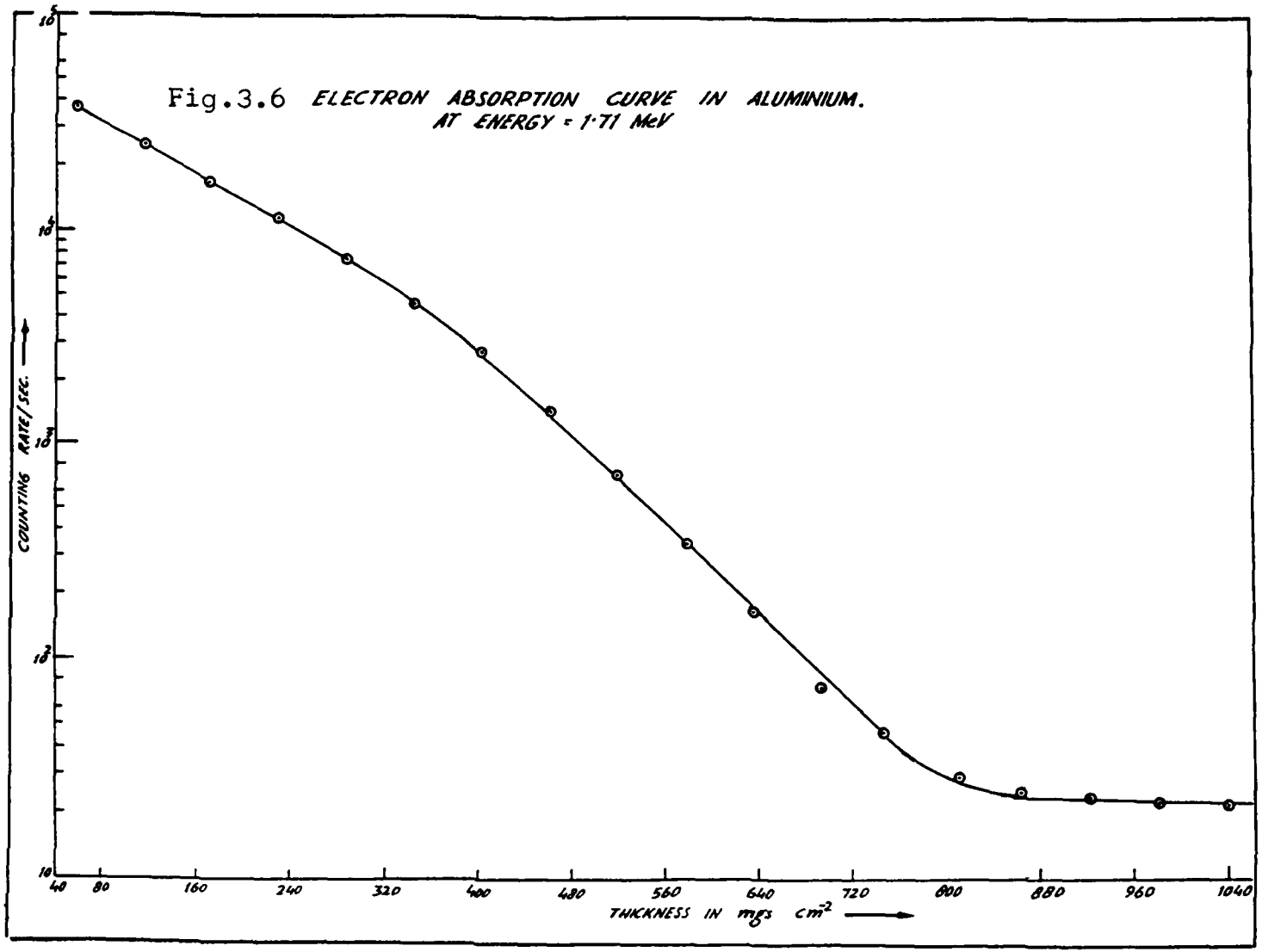

Fig.3.6 *ELECTRON ABSORPTION CURVE IN ALUMINIUM. AT ENERGY = 1·71 MeV*

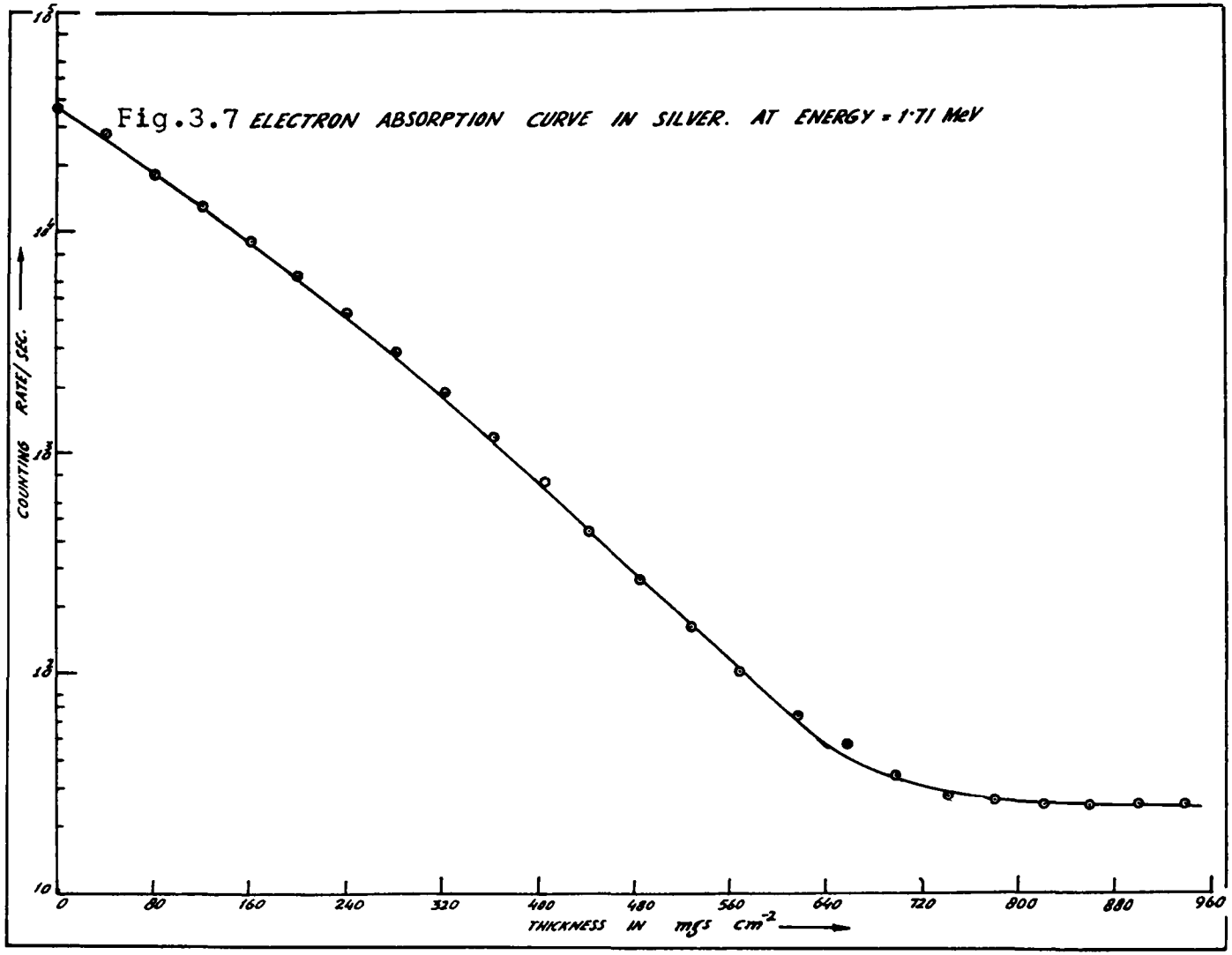
Fig.3.7 ELECTRON ABSORPTION CURVE IN SILVER. AT ENERGY = 1·71 MeV
COUNTING RATE/SEC.
10⁵
10⁴
10³
10²
10
0
80
160
240
320
400
480
560
640
720
800
880
960
THICKNESS IN mgs cm⁻²

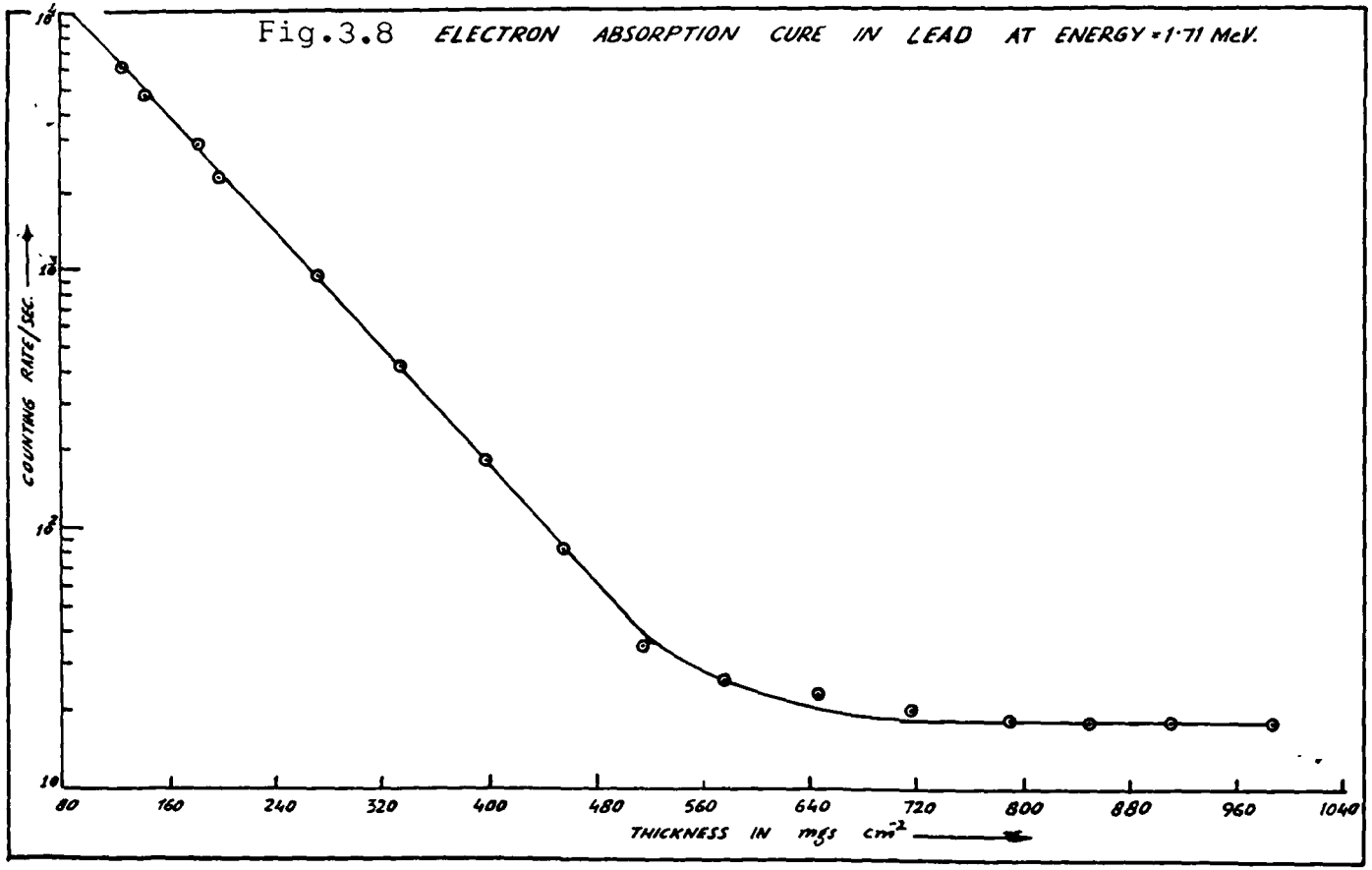

Fig.3.8 ELECTRON ABSORPTION CURE IN LEAD AT ENERGY = 1·71 McV.

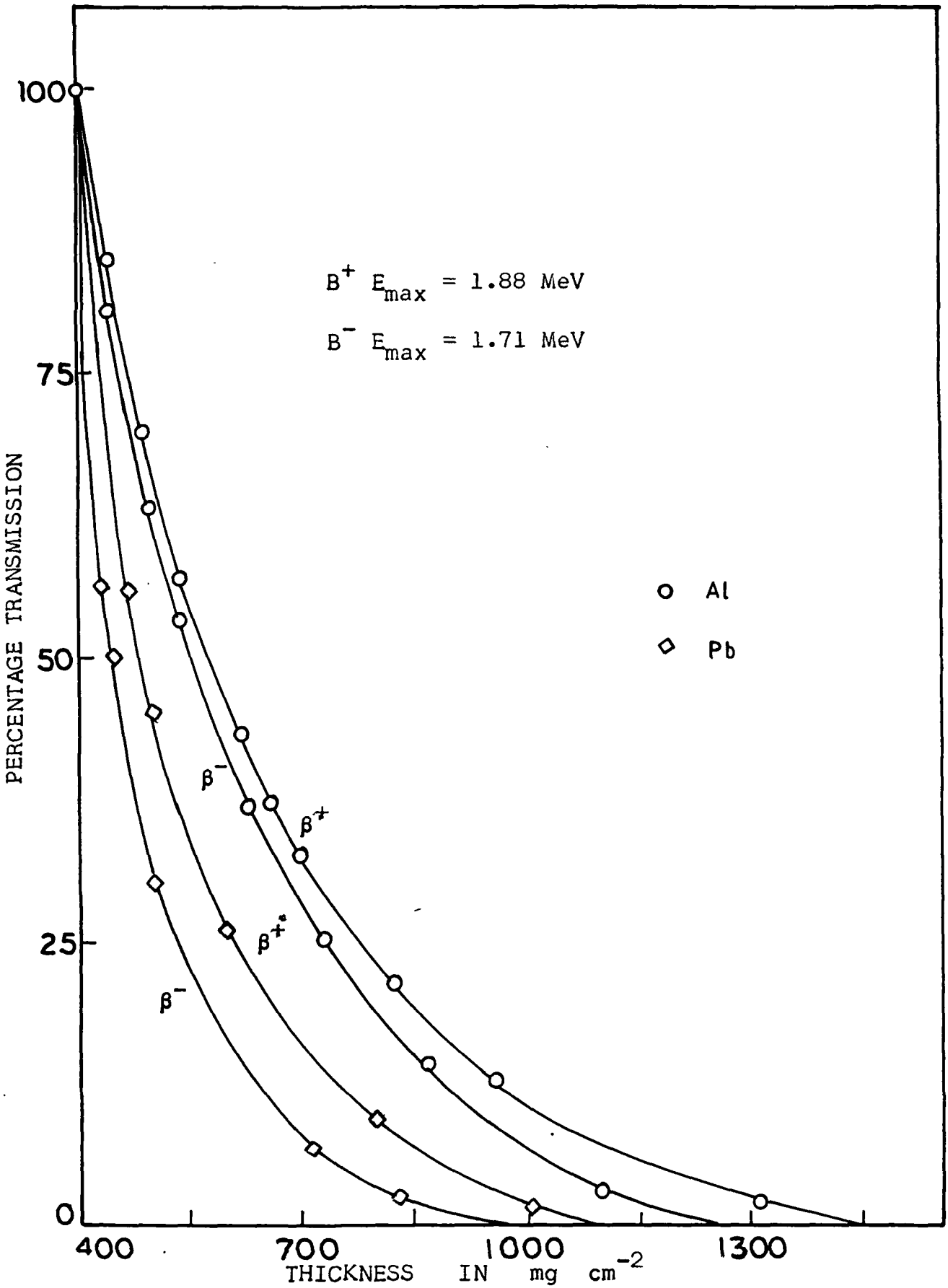

Fig. 3.9 Relative transmission of positrons and electrons in Al and Pb.

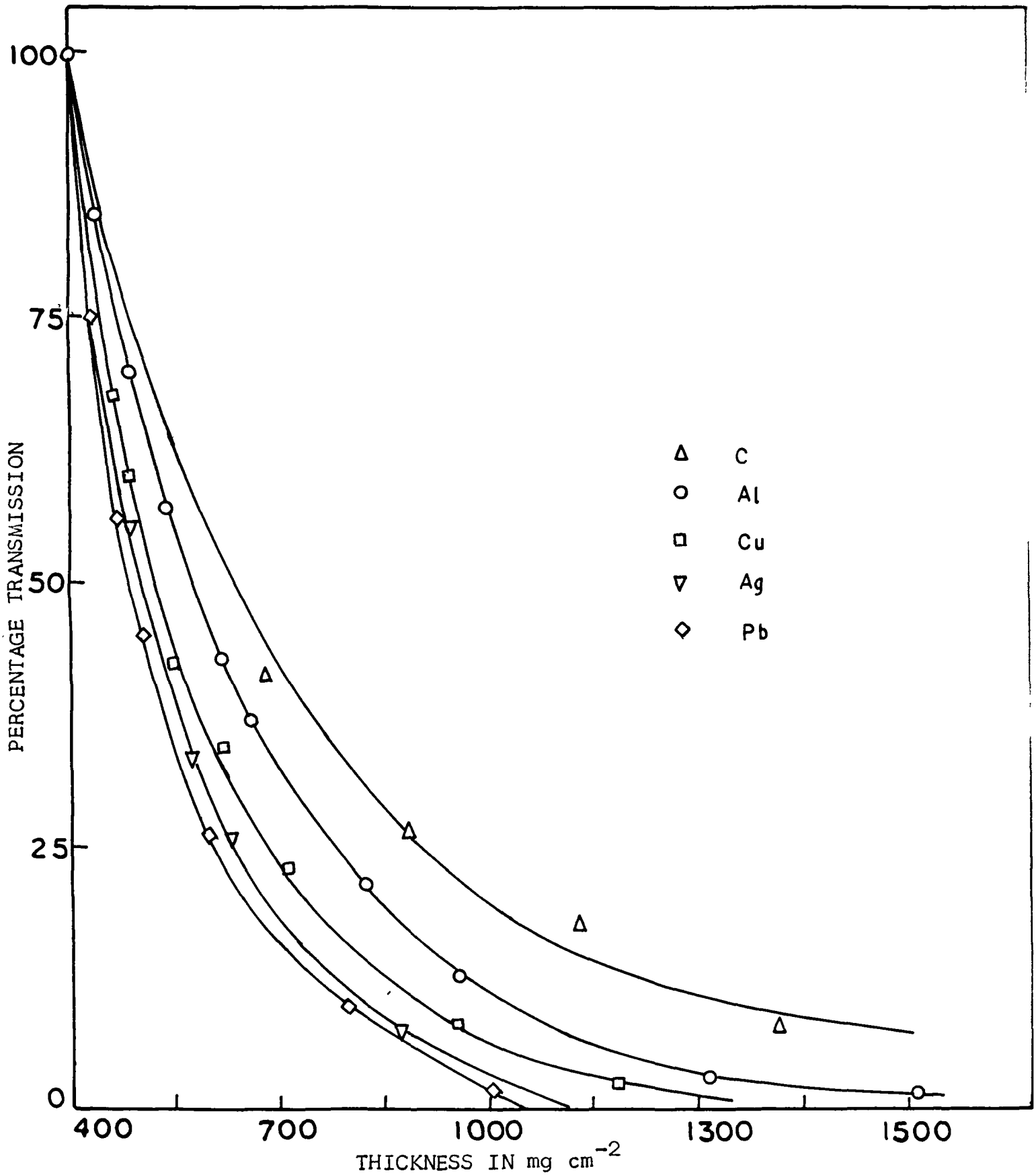

Fig. 3.10 Transmission of 1.88 MeV positrons in C, Al, Cu, Ag and Pb.

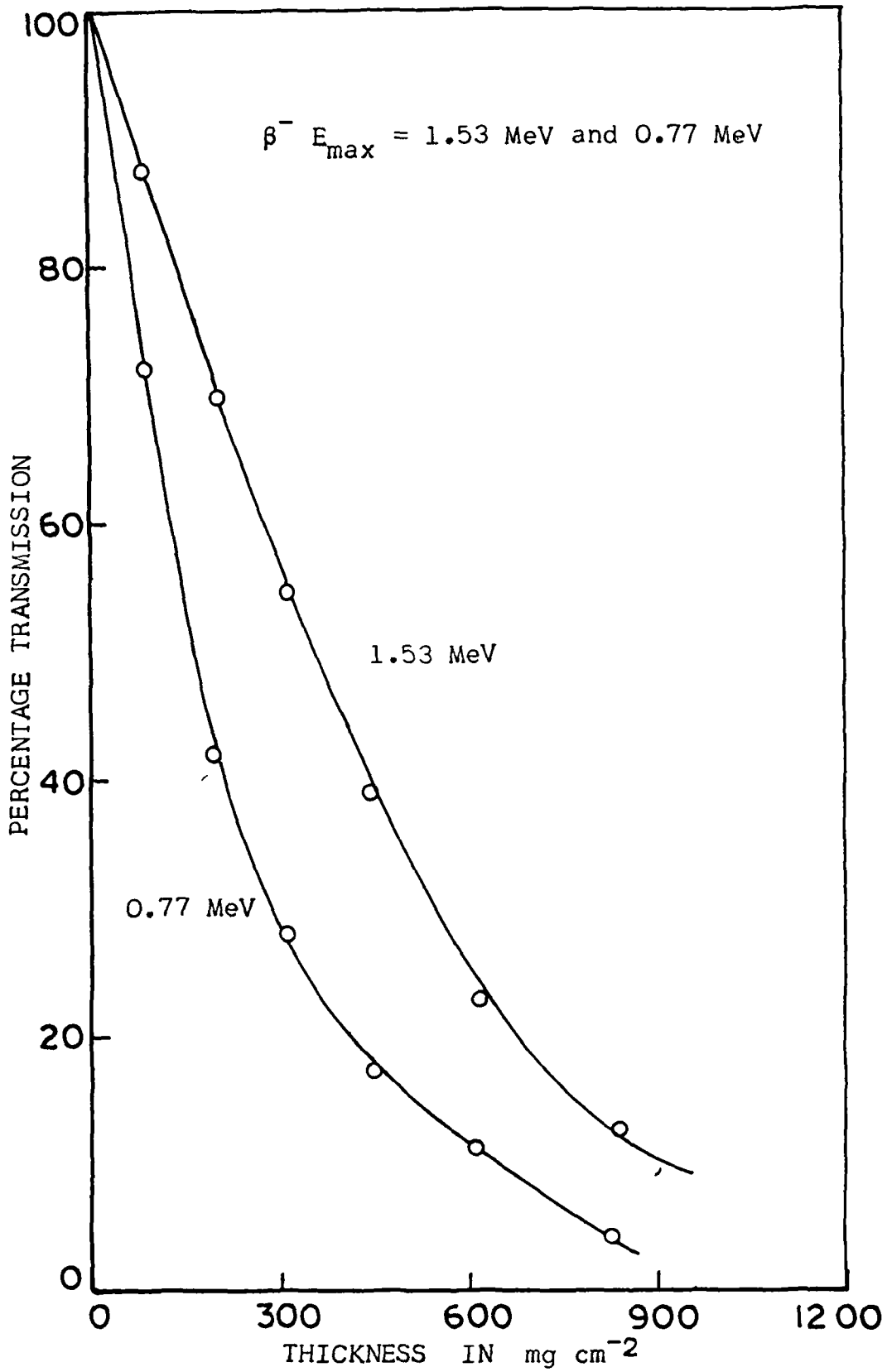

Fig. 3.11 Transmission curves of 1.53 MeV and 0.77 MeV electrons in Ytterbium.

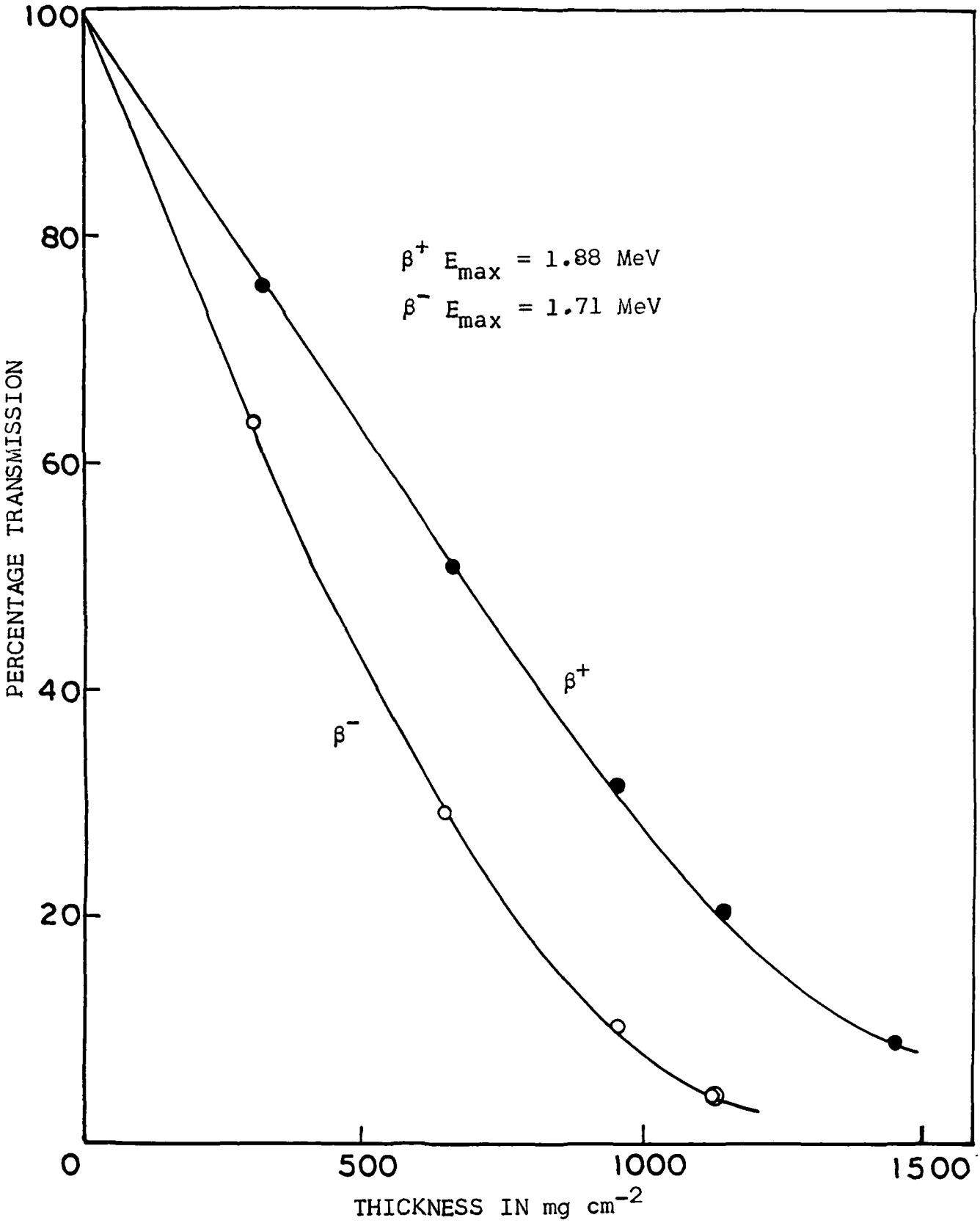

Fig. 3.12 Comparative transmission of positrons and electrons in Holmium.

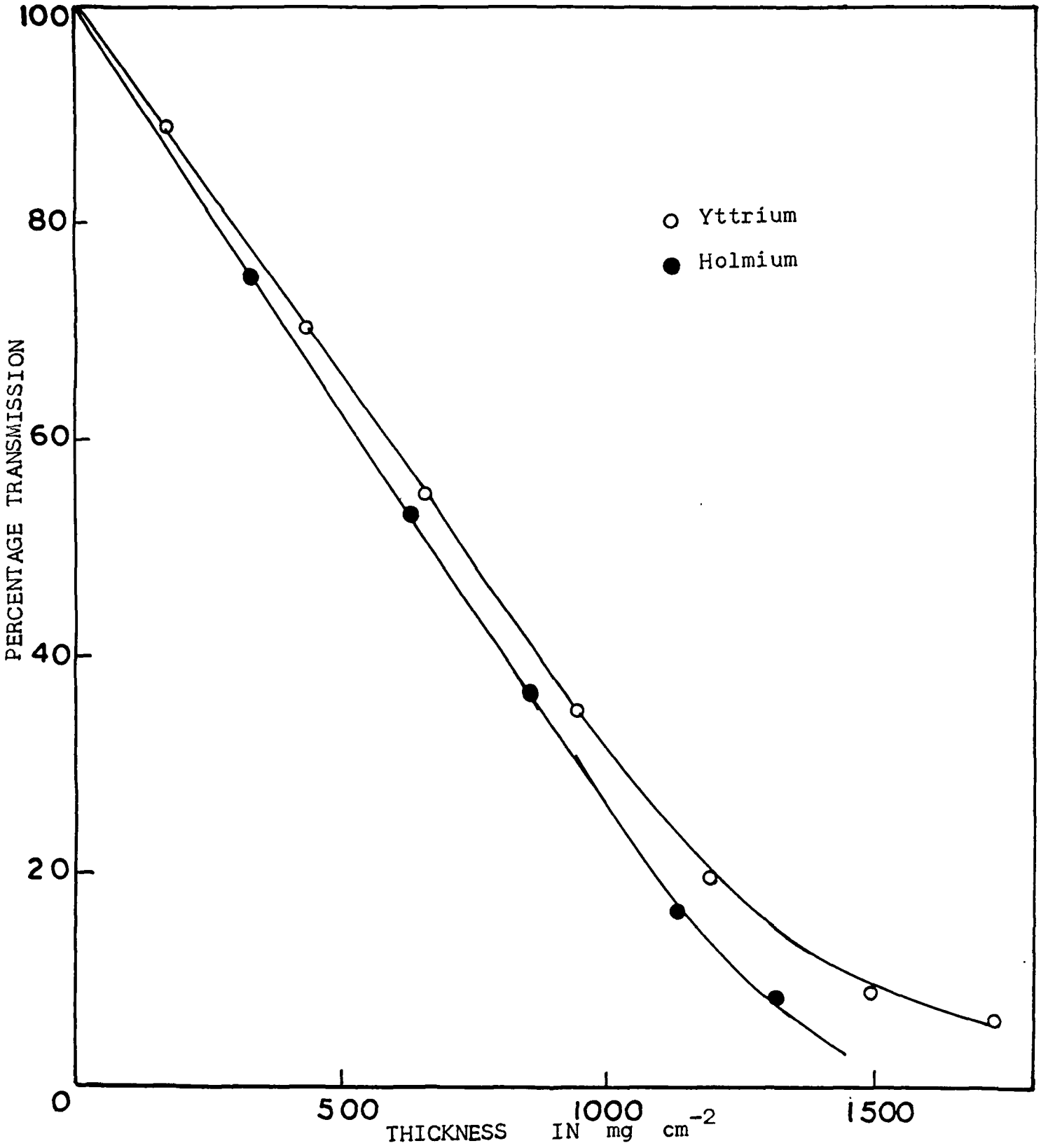

Fig. 3.13 Transmission of 1.88 MeV positrons through Yttrium and Holmium.

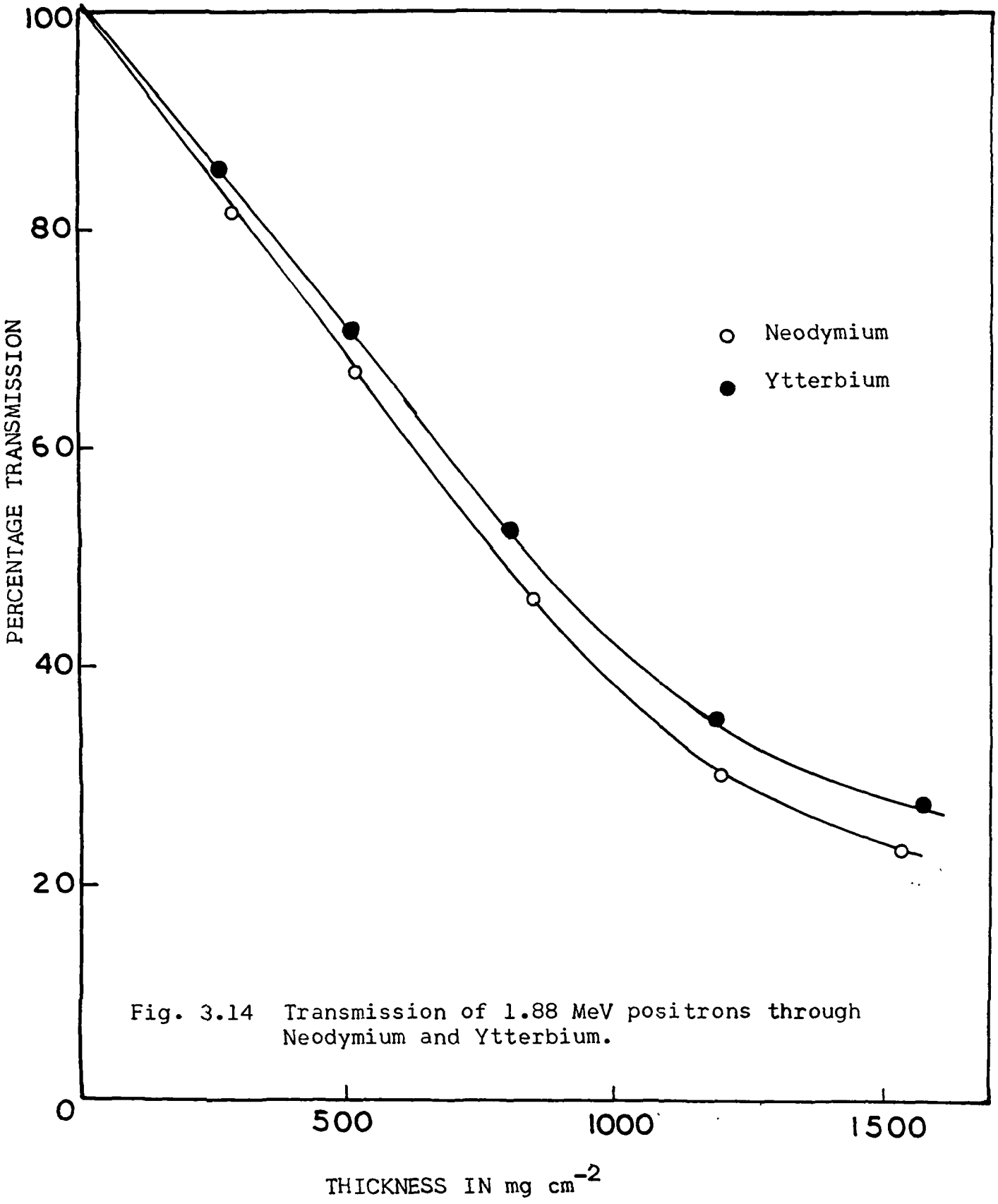

Fig. 3.14 Transmission of 1.88 MeV positrons through Neodymium and Ytterbium.

practical ranges in different absorbers, an empirical relation of the following form is determined:

$$\bar{R}_{sfp}(E,Z) = A + BZ + (\alpha + \beta Z)\, E \qquad \ldots \qquad (3.1)$$

where $\bar{R}_{sfp}$ is in units of mg cm^{-2}.

E = The incident kinetic energy of the electron in MeV.

Z = Atomic number of the absorber.

The constants A, B, α and β have the following values:

$A = -77.03$ mg cm^{-2} , $B = 0.1290$ mg cm^{-2},

$\alpha = 516.30$ mg cm^{-2} MeV and $\beta = -1.672$ mg cm^{-2} MeV.

The experimental data was subjected to the least squares fit method to determine the constants, A, B, α and β. The empirical values of $\bar{R}_{sfp}$ differ from the experimental values by about 4% and this discrepancy is of the same order as the error in the experimental values, table 3.2. The comparison of the empirical values and the experimental values at different energies is shown in table 3.3.

(c) Comparison of Experimental Values with the Theory:

The calculations made by Batra and Sehgal[1-3] regarding the practical ranges, $\bar{R}_p$, in matter, the basis of which has been discussed in Chapter I, are tabulated in table 3.4 and plotted in Figs. 3.15 - 3.18 along with the present experimental values

TABLE - 3.2

The values of the range R^{-}_{sfp} at different energies and in different absorbers, as measured in the present experiments.

Elements	Atomic No. Z	Range R^{-}_{sfp} in mg cm^{-2}			
		1.71 MeV	1.53 MeV	0.77 MeV	0.25 MeV
Carbon	6	826 ± 17	706 ± 14	306 ± 6	52 ± 2
Aluminium	13	814 ± 16	688 ± 13	296 ± 6	50 ± 2
Nickel	28	722 ± 15	624 ± 13	286 ± 6	45 ± 2
Copper	29	720 ± 14	622 ± 13	285 ± 6	44 ± 2
Yttrium	39	708 ± 14	596 ± 12	268 ± 6	41 ± 2
Zirconium	40	707 ± 14	594 ± 12	267 ± 6	41 ± 2
Silver	47	705 ± 14	580 ± 11	264 ± 8	40 ± 2
Cadmium	48	701 ± 14	576 ± 11	263 ± 8	38 ± 1
Indium	49	697 ± 13	574 ± 11	257 ± 8	35 ± 1
Neodymium	60	664 ± 13	553 ± 11	254 ± 8	33 ± 1
Holmium	67	652 ± 14	536 ± 20	242 ± 8	32 ± 1
Ytterbium	70	636 ± 23	526 ± 21	241 ± 8	30 ± 1
Gold	79	606 ± 22	514 ± 20	235 ± 8	-
Lead	82	590 ± 24	510 ± 22	231 ± 8	-

TABLE - 3.3

Comparison of experimental values of R^-_{sfp} with the empirical values, calculated with the help of relation (3.1).

Atomic No. Z	E = 1.71 MeV R^-_{sfp} in mg cm^{-2}			E = 1.53 MeV R^-_{sfp} in mg cm^{-2}		
	Experimental	Empirical	% Diff.	Experimental	Empirical	% Diff.
6	826	790	+4.4	706	698	+1.1
13	814	770	+4.2	688	681	+1.0
28	722	729	-1.0	624	645	-3.4
29	720	727	-1.0	622	643	-3.4
39	708	699	+1.3	596	618	-3.7
40	707	697	+1.4	594	616	-3.7
47	705	678	+3.8	580	599	-3.2
48	701	675	+3.7	576	596	-3.5
49	697	672	+3.6	574	594	-3.5
60	664	642	+3.3	552	567	-2.7
67	652	623	+4.4	536	550	-2.6
70	636	615	+3.3	526	543	-3.2
79	606	590	+2.6	514	521	-1.4
82	590	582	+1.4	510	513	-0.6

Contd.....

Contd..... (Table - 3.3)

Atomic No. Z	E = 0.77 MeV R^{-}_{sfp} in mg cm^{-2}			E = 0.25 MeV R^{-}_{sfp} in mg cm^{-2}		
	Experimental	Empirical	% Diff.	Experimental	Empirical	% Diff.
6	306	313	-2.3	52	50	+3.8
13	296	305	-3.0	50	48	+4.0
28	286	288	-0.7	45	44	+2.2
29	285	287	-0.7	44	44	0.0
39	268	275	-2.6	41	42	-2.4
40	267	274	-2.6	41	40	+2.4
47	264	266	-0.8	40	39	+2.5
48	263	265	-0.7	40	40	0.0
49	257	264	-2.7	38	39	-2.6
60	254	251	+1.2	38	37	+2.6
67	242	243	-0.4	35	36	-2.9
70	241	240	+0.4	32	34	-6.2
79	235	238	-1.2	-	-	-
82	231	226	+2.2	-	-	-

TABLE - 3.4

Comparison of experimental values of R^-_{sfp} and theoretical[1-3] values of R^-_p at different energies, in units mg cm^{-2}.

Material	1.71 MeV			1.53 MeV		
	R^-_{sfp}	R^-_p	% Diff.	R^-_{sfp}	R^-_p	% Diff.
Carbon	826	1028	-24.4	706	903	-27.9
Aluminium	814	797	+02.1	688	699	-01.6
Nickel	722	619	+14.3	624	543	+12.9
Copper	720	611	+15.1	622	537	+13.7
Yttrium	708	555	+21.6	596	487	+18.3
Zirconium	707	550	+22.2	594	483	+18.5
Silver	705	521	+26.1	580	458	+21.1
Cadmium	701	518	+26.1	576	454	+21.7
Indium	697	514	+26.2	574	451	+21.4
Neodymium	664	481	+27.5	552	422	+23.6
Holmium	652	464	+28.8	536	407	+24.1
Ytterbium	636	457	+28.1	526	401	+23.8
Gold	606	439	+27.5	514	386	+25.0
Lead	590	434	+26.4	510	381	+25.3

Contd.....

Contd..... (Table - 3.4)

Material	0.77 MeV			0.25 MeV		
	$\bar{R}_{sfp}$	$\bar{R}_{p}$	% Diff.	$\bar{R}_{sfp}$	$\bar{R}_{p}$	% Diff.
Carbon	306	383	-25.1	52	65	-25.0
Aluminium	296	297	-00.3	50	60	-20.0
Nickel	286	230	+19.5	45	47	-04.4
Copper	285	228	+20.0	44	46	-04.5
Yttrium	268	206	+23.1	41	43	-04.8
Zirconium	267	205	+23.2	41	40	+02.4
Silver	264	194	+26.5	40	39	+02.5
Cadmium	263	193	+26.6	38	26	+31.5
Indium	257	192	+25.3	38	24	+36.4
Neodymium	254	179	+29.5	35	25	+28.6
Holmium	242	173	+28.5	33	22	+33.3
Ytterbium	241	170	+29.0	32	23	+28.1
Gold	235	163	+30.6	-	-	-
Lead	231	161	+30.2	-	-	-

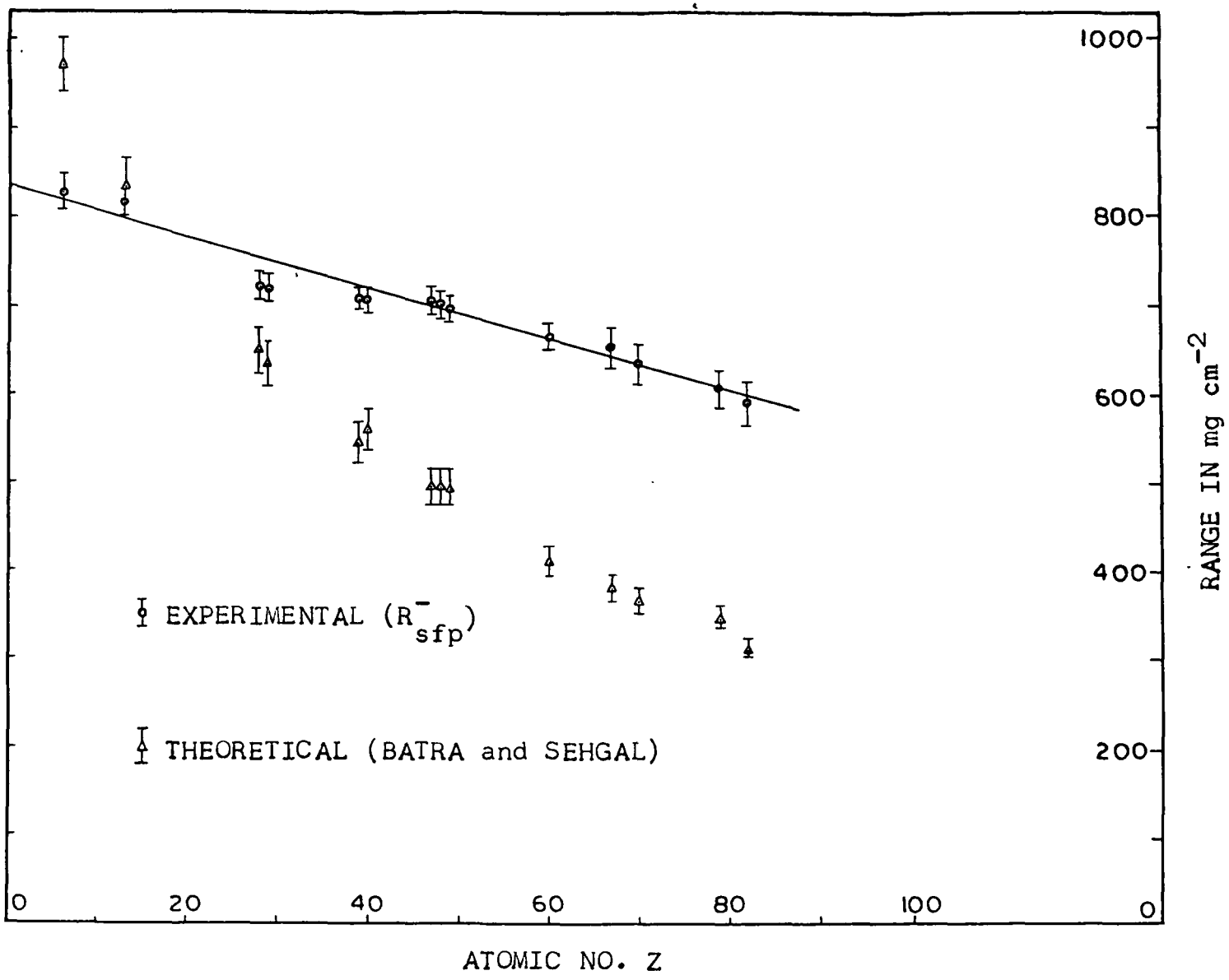

Fig. 3.15 Comparison of present experimental ranges with the theoretical values (Batra and Sehgal, Ref. 1-3) at E_{max} = 1.71 MeV.

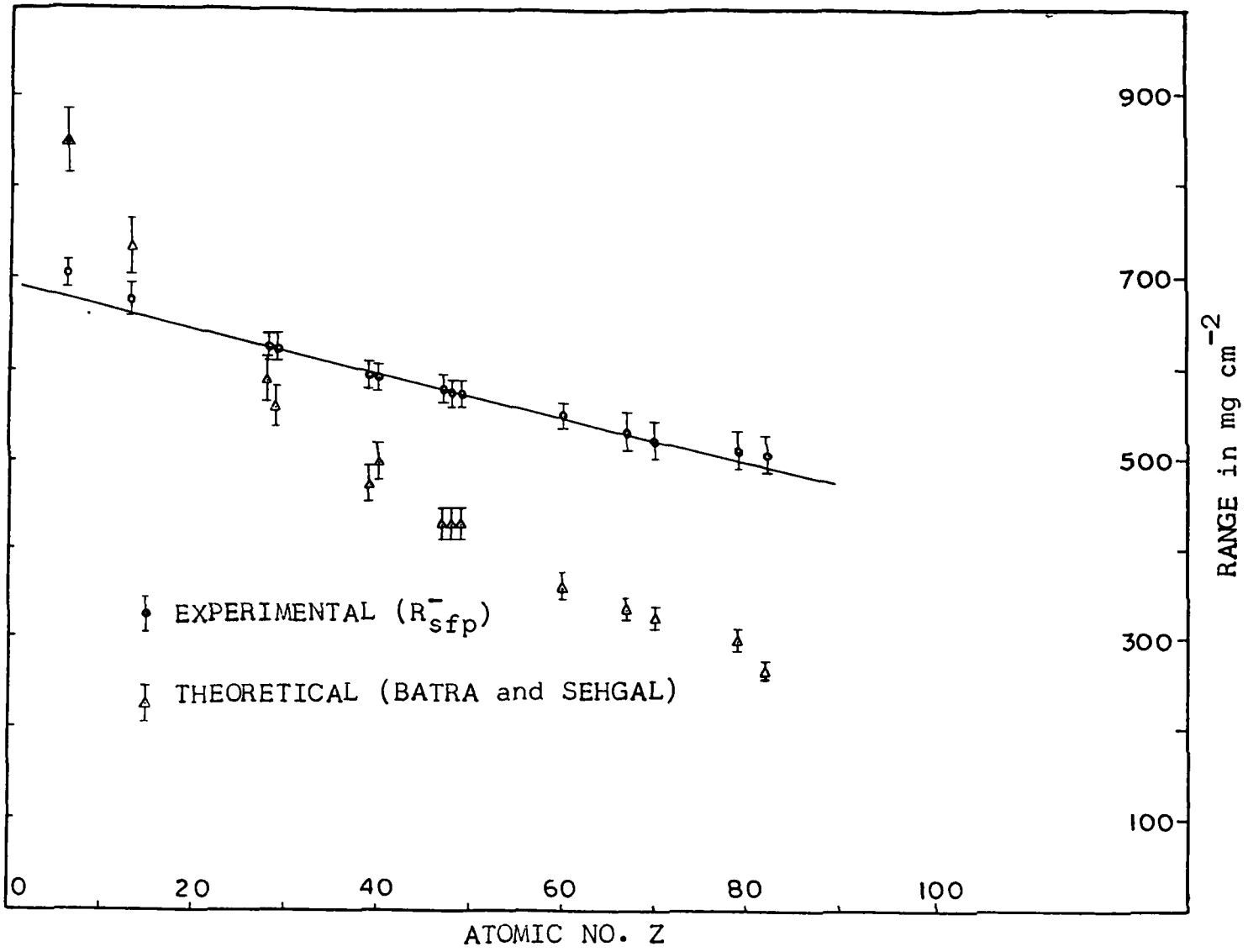

Fig. 3.16 Comparison of present experimental ranges with the theoretical values (Batra and Sehgal, Ref. 1-3) at E_{max} = 1.53 MeV

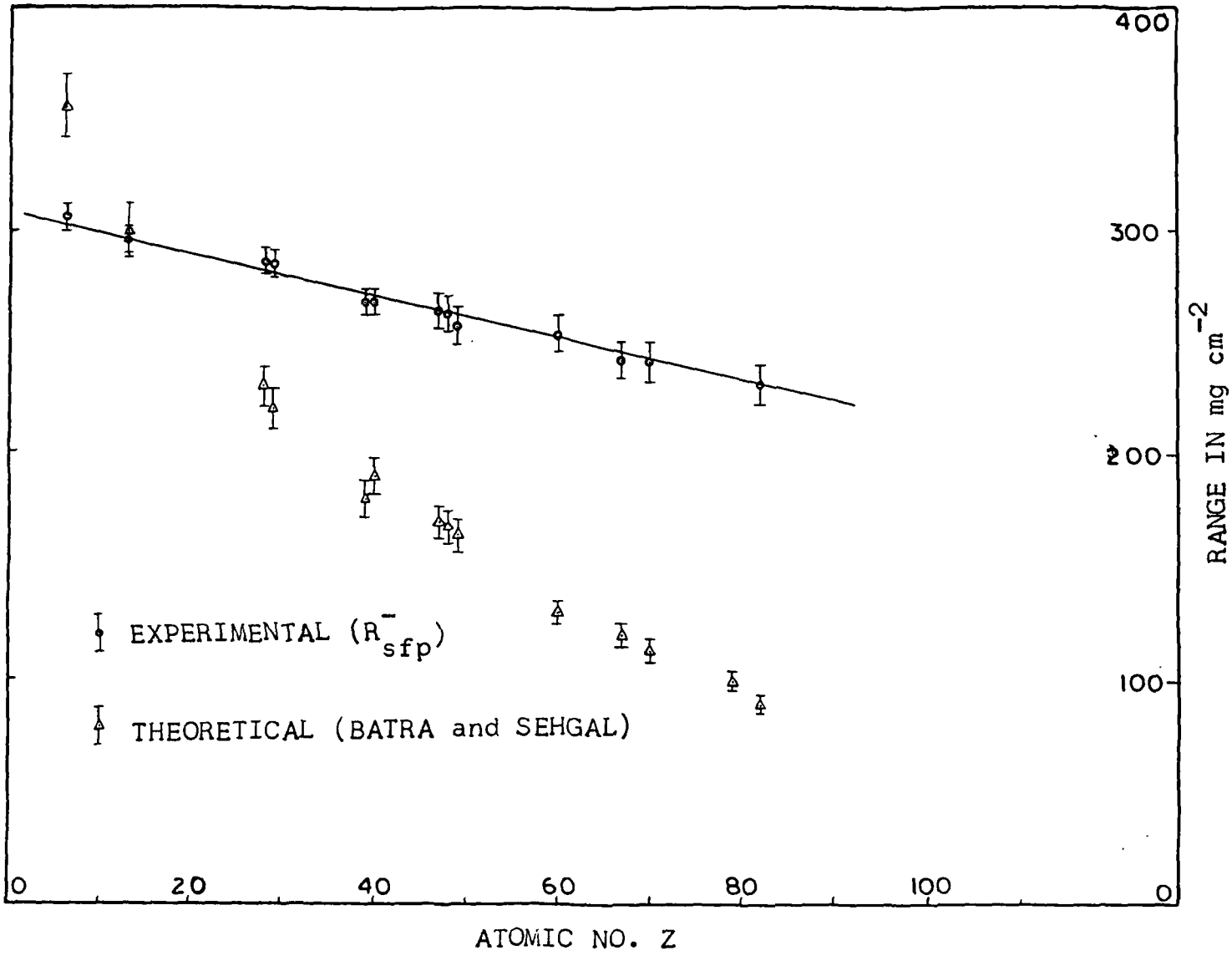

Fig. 3.17 Comparison of present experimental ranges with the theoretical values (Batra and Sehgal, Ref. 1-3) at E_{max} = 0.77 MeV.

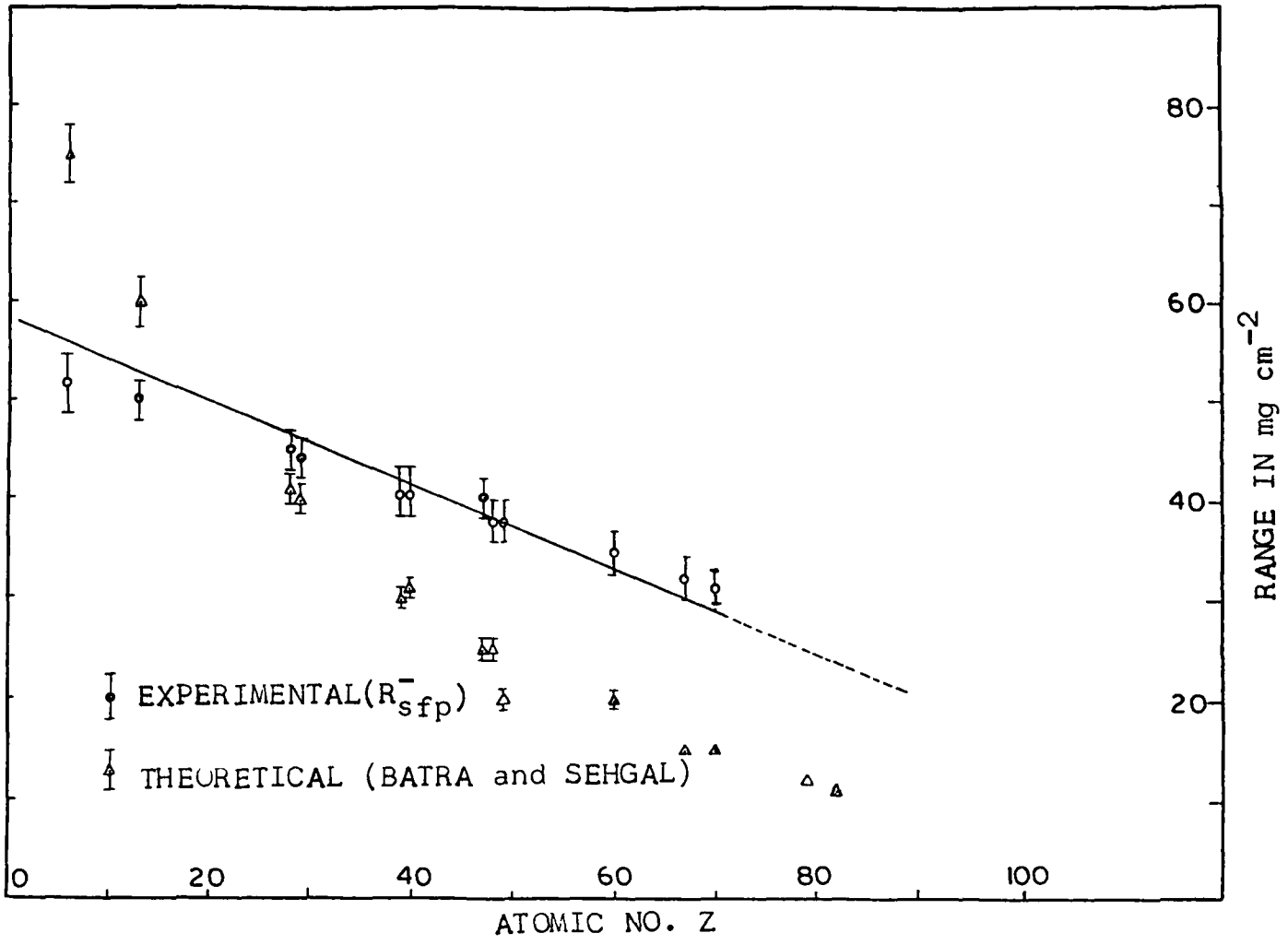

Fig. 3.18 Comparison of present experimental ranges with the theoretical values (Batra and Sehgal, Ref. 1-3) at E_{max} = 0.25 MeV.

order terms like $(\alpha Z)^2$ and $(\alpha Z)^3$ may be appreciable. In Chapter V theoretical calculations for the straggling free ranges have been carried out. The effect of higher order terms in the Mott[12] expression has also been investigated and discussed in Chapter V.

3.7 ABSORPTION COEFFICIENTS AND R^+_{sfp} TO R^-_{sfp} RATIO

The absorption coefficients in different materials have been calculated from the experimental transmission curves for electrons at different energies. Table 3.5 shows the mass absorption coefficients $\mu_m(e^-)$ for C, Al, Ni, Cu, Zr, Ag, Cd, In, Au and Pb. In table 3.6 the values of $\mu_m(e^-)$ for some rare earth metals are shown. It is observed that the qualitative as well as quantitative trend for absorption coefficients in rare earth metals is the same as for other materials in table 3.5. The experimental error in the absorption coefficients is the same as in R^-_{sfp}, i.e. about 4%.

Earlier workers[21-23] had measured the mass absorption coefficients for positrons and electrons and their results are at variance. The comparison of absorption coefficients of positrons and electrons by these worker[21-23] was done for non-identical end point energies of positrons and electrons. For example Patrick and Rupaal[21] used 0.324 MeV positrons and 0.312 MeV electrons to compare the absorption coefficients. Seliger[14] studied the transmission of monoenergetic positrons

TABLE - 3.5

Experimentally determined mass absorption coefficients $\mu_m(e^-)$ of electrons at different energies in units of gm^{-1} cm^2.

Energy (MeV)	Absorption coefficient, $\mu_m(e^-)$ in									
	Carbon	Aluminium	Nickel	Copper	Zirconium	Silver	Cadmium	Indium	Gold	Lead
0.25	144.51	157.80	178.53	181.97	188.00	190.55	192.05	192.00	201.55	207.03
0.77	21.04	25.71	34.52	35.11	36.55	35.95	37.03	37.31	41.54	43.38
1.53	7.50	9.12	12.02	11.98	13.01	13.49	13.50	13.45	15.93	16.47
1.71	5.52	6.92	8.65	8.71	10.34	10.47	10.45	10.52	11.70	11.75

TABLE - 3.6

Experimentally determined mass absorption coefficients, $\mu_m(e^-)$ of electrons at different energies in units gm^{-1} cm^2 in some rare earth elements.

Energy (MeV)	Absorption coefficients, $\mu_m(e^-)$ in			
	Yttrium	Neodymium	Holmium	Ytterbium
0.25	187.51	197.03	198.31	199.04
0.77	36.25	38.15	39.75	39.79
1.53	12.92	14.90	15.00	15.93
1.71	12.72	14.10	14.41	14.52

and electrons showing lesser penetration for positrons in low-Z and higher penetration in high-Z elements.

For a meaningful comparison of the absorption coefficients of positrons and electrons the values of E_{max} used should be equal. One needs a pair of radionuclides emitting either positrons or electrons of equal E_{max}. Such a pair of sources of positrons and electrons can not be obtained. Hence it was thought to use the data on $\mu_m(e^-)$ given in tables 3.5 and 3.6 at energies 0.25 MeV, 0.77 MeV, 1.53 MeV and 1.71 MeV. The values of mass absorption coefficients when plotted against energy (E_{max}) on a log-log graph for each element, represent a set of parallel lines. The values of mass absorption coefficients $\mu_m(e^-)$ for electrons of E_{max} = 1.88 MeV have been obtained for C, Al, Cu, Y, Ag, Na, Ho, Yb, Au and Pb from these lines by the extrapolation method. These values have been compared with the mass absorption coefficients $\mu_m(e^+)$ of 1.88 MeV positrons and shown in tables 3.7 and 3.8. The absorption coefficient for electrons is greater than that for positrons for each element, showing greater absorption of electrons than positrons. The range R^+_{sfp} and R^-_{sfp} for positrons and electrons at energy E_{max} = 1.88 MeV and the ratio R^+_{sfp}/R^-_{sfp} is shown in table 3.9. The ratio of the range R^+_{sfp} of positrons to the range R^-_{sfp} of electrons is always greater than one.

Seliger[14] had observed lesser penetration for positrons in low-Z materials, however, the present investigation shows

TABLE - 3.7

Comparison of experimental values of mass absorption coefficients, in units gm^{-1} cm^2, of positrons and electrons at energy E_{max} = 1.88 MeV.

Particles	Absorption coefficients, $\mu_m(e^+)$ and $\mu_m(e^-)$ in					
	Carbon	Aluminium	Copper	Silver	Gold	Lead
Positrons	3.92	6.03	6.61	7.08	8.42	8.71
Electrons	5.52	6.92	8.71	10.47	11.70	13.75
$\mu_m(e^-)/\mu_m(e^+)$	1.41	1.15	1.32	1.48	1.39	1.58

TABLE - 3.8

Comparison of experimental values of mass absorption coefficients, in unts gm^{-1} cm^2, of positrons and electrons in some rare earth elements at E_{max}=1.88 MeV.

Particles	Absorption coefficients, $\mu_m(e^+)$ and $\mu_m(e^-)$ in			
	Yttrium	Neodymium	Holmium	Ytterbium
Positrons	6.81	7.54	7.88	8.03
Electrons	10.25	11.13	11.45	11.55
$\mu_m(e^-)/\mu_m(e^+)$	1.51	1.48	1.46	1.44

TABLE - 3.9

Comparison of experimental values of R^{+}_{sfp} and R^{-}_{sfp} for positrons and electrons at energy E_{max} = 1.88 MeV

Particles	Range R^{+}_{sfp} and R^{-}_{sfp} in unit mg cm^{-2} in									
	Carbon	Aluminium	Copper	Yttrium	Silver	Neodymium	Holmium	Ytterbium	Gold	Lead
Positrons	1332	1240	1163	1230	1160	1142	1125	1106	1035	1026
Electrons	952	933	881	853	829	792	771	763	734	727
R^{+}_{sfp}/R^{-}_{sfp}	1.40	1.33	1.32	1.44	1.40	1.44	1.46	1.45	1.41	1.41

greater transmission of positrons than of electrons, even in low-Z materials.

Differences in scattering of positrons and electrons have been theoretically investigated by Rohrlich and Carlson[24]. Using correct values of elastic and inelastic scattering cross-sections, they[24] calculated the energy loss and multiple scattering of positrons and electrons in Aluminium and Lead. At very low energies the energy loss of positrons is faster than electrons and for low-Z the multiple scattering of electrons is only slightly greater than that of positrons. Therefore at very low energies and low-Z the transmission of positrons is to be lower than that of electrons. At higher-Z the excess multiple scattering of electrons over positrons overshadows the small energy loss differences. Therefore at energies of the order of the present values used, even for materials of low-Z, positrons should be transmitted to a greater extent than electrons. This is what actually is found in the present experiments for C, Al, Cu, Ag, Au and Pb and a number of rare earth metals where positrons are transmitted to a greater extent than electrons under similar geometrical conditions.

The dependence of the absorption coefficients $\mu_m(e^+)$ and $\mu_m(e^-)$ at energy E_{max} = 1.88 MeV, as a function of atomic number-Z of the absorber is shown in Fig. 3.19. It shows that as Z increases the absorption increases. It may go through a maximum, which needs to be looked into. The mass absorption

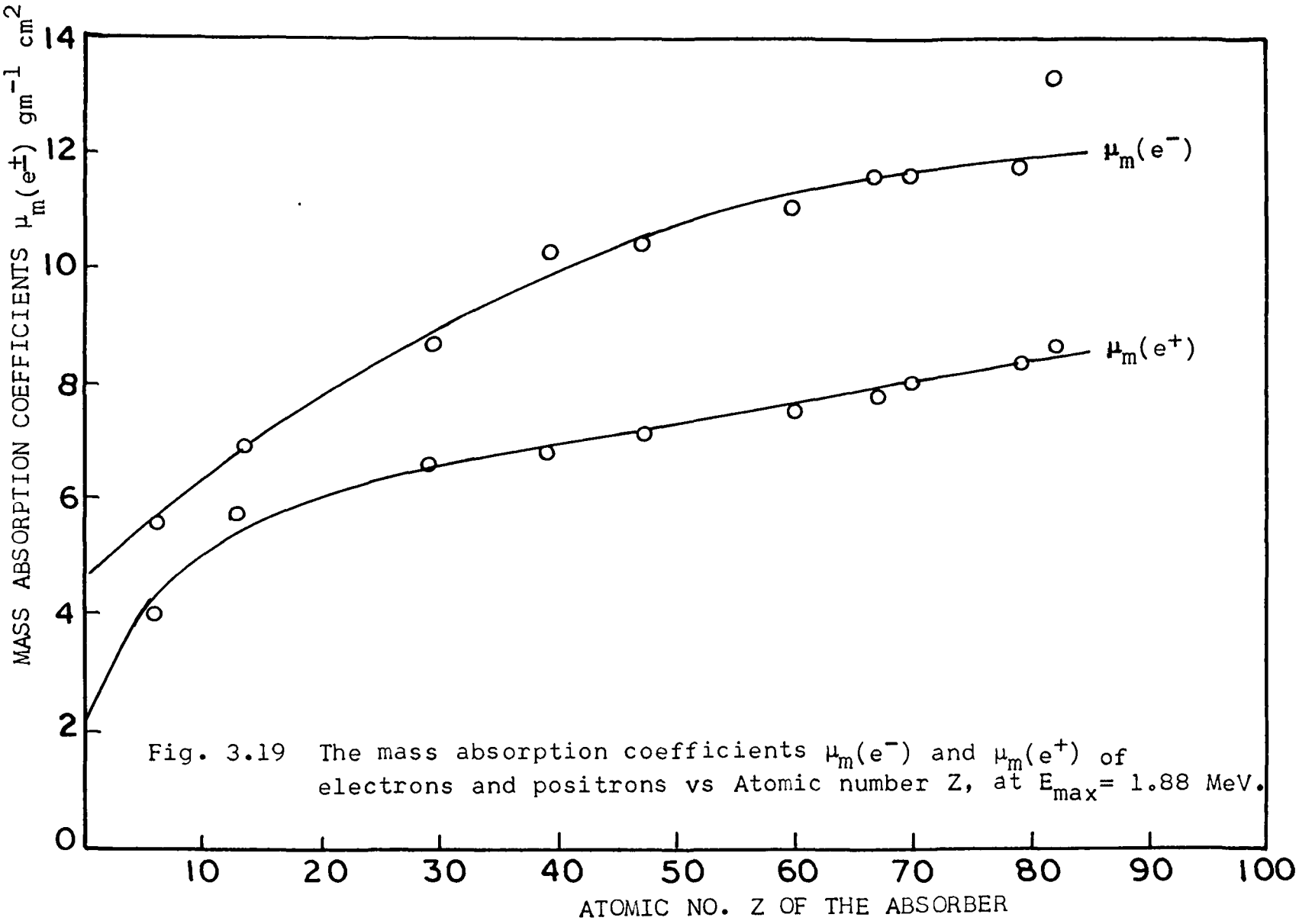

Fig. 3.19 The mass absorption coefficients $\mu_m(e^-)$ and $\mu_m(e^+)$ of electrons and positrons vs Atomic number Z, at E_{max}= 1.88 MeV.

coefficients, plotted as a function of energy on log-log scale for some elements are shown in Fig. 3.20 for comparison.

The process of positron annihilation during flight may effect the experimental transmission curves to some extent. Several workers[25-27] have reported that positronium formation is not possible in metals. However, positronium formation is possible in gaseous media, but the energy re ion for such a posssibility is around 10-20 eV. In the absence of positronium formation at energies 10-20 eV, what more distance the positrons could have traversed before coming to rest? This distance will not be more than a few micro gm. Thus the positronium formation does not have significant effect on the estimation of R^{+}_{sfp} of positrons from transmission curves.

It can be concluded that the results of the present investigations confirm that there is a difference between the transmission behaviour of positrons and electrons of the same initial energy and indicate that the differences observed by earlier workers[21-23] were not entirely due to the differences in their initial energies. The agreement of these investigations with theory[1-3] also becomes good when the theory[1-3] is improved by adding the straggling effect on the range. This part has been discussed in Chapter V.

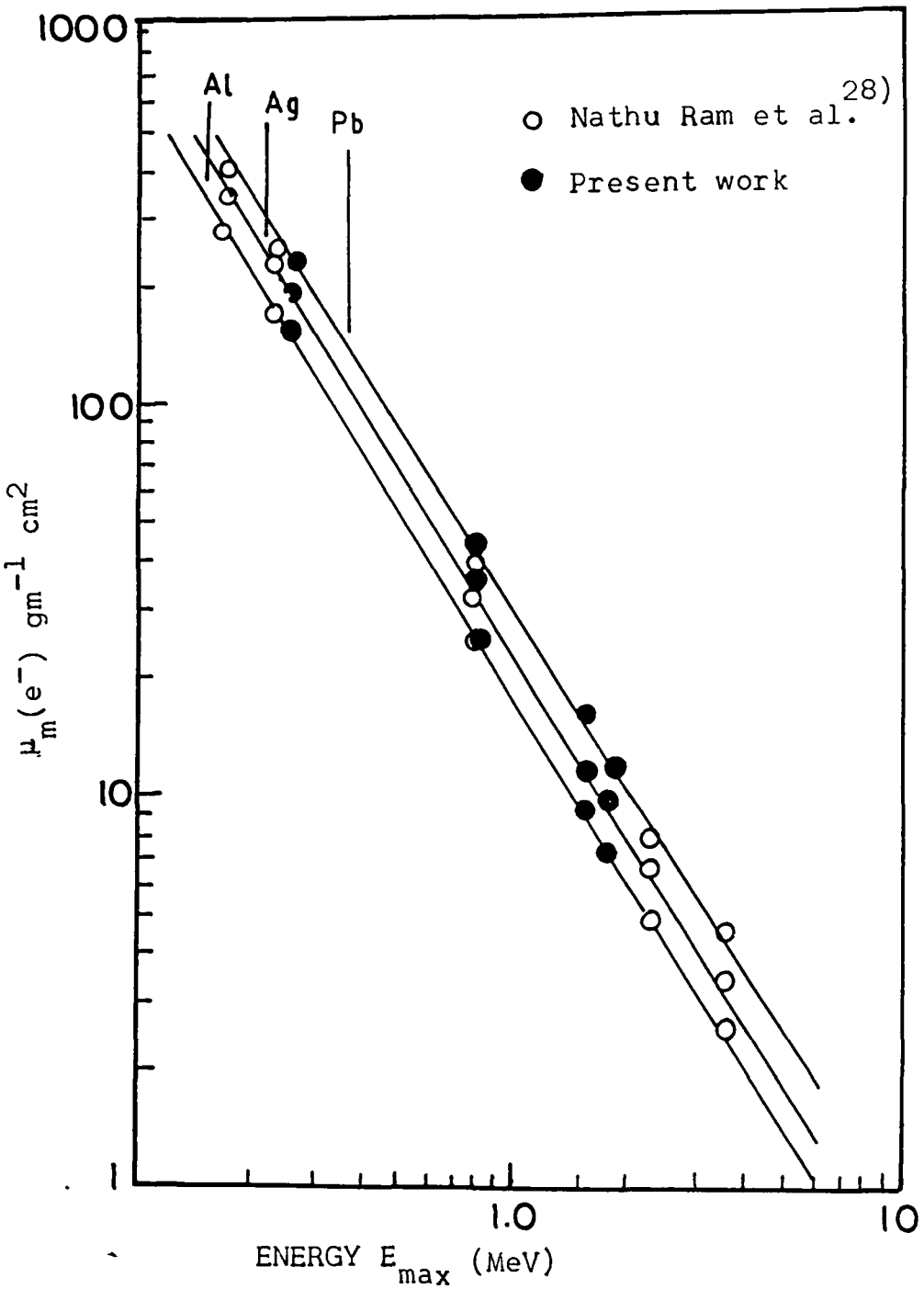

Fig. 3.20 Mass absorption coefficient of beta particles in Al, Ag and Pb vs Energy E_{max} (MeV) as compared with ref. 28.

REFERENCES

1. R.K. Batra and M.L. Sehgal, Nuclear Physics A156, 314-20 (1970).

2. R.K. Batra and M.L. Sehgal, Nucl. Inst. Methods 109, 565 (1973).

3. R.K. Batra and M.L. Sehgal, Phys. Rev. B23, No. 9, 4448 (1981).

4. B.F. Schonland, Proc. Roy. Soc. (London) A135, 429-58 (1925).

5. A. Flammersfield, Z. Nature-forsch 2a, 370 (1947).

6. R.W. Varder, Phil. Mag. 29, 725 (1915).

7. B.N.C. Agu, T.A. Burdett and E. Matsukawa,
   (i) Proc. Phy. Soc. (London) 71, 201-206 (1958).
   (ii) Proc. Phys. Soc. (London) 72, 727-732 (1958).

8. P.J. Ebert, A.F. Lauzon and E.M. Lent, Phys. Rev. 183, 422-30 (1969).

9. T. Tabata, R. Ito, S. Okabe and Y. Fujita, J. Appl. Phys. 42, 3361 (1971).

10. E. Segre, 'Experimental Nuclear Physics Vol. 1, 293 (1953).

11. M.J. Berger and S.M. Seltzer, Studies in Penetration of charged particles through matter. National research council publication No. 1133, 205-268 (1964).

12. N.F. Mott, Proc. Roy. Soc. (London), A124, 425-42 (1929) and Proc. Roy. Soc. (London) A135, 429-58 (1932).

13. H.S.W. Massey, Proc. Roy. Soc. (London) A181, 14-15 (1943).

14. H.H. Seliger, Phy. Rev. 88, 408 (1952) and Phys. Rev. 100, 1029 (1955).

15. K. Gubernator, Zeit Fur Physik 152, 183 (1958).

16. K. Gubernator and A. Flammersfield, Z. Phys. Vol. 156, No. 2, 179 (1959).

17. R.R. Wilson, Phys. Rev. 84, 100 (1951).

18. J.H. Green and G.J. Celitans, Proc. Phys. Soc. 82, 1002 (1963).

19. J. Fischer and J. Marshall, Rev. Sci. Instr. 23, 417 (1952).

20. R. Green and R. Bell, Nuclear Instruments 3, 127 (1955).

21. J.R. Patrick and A.S. Rupaal, Phys. Lett. 35A, No. 4, 235 (1971).

22. A.S. Rupaal and J.R. Patrick, Phys. Lett. 38A, No. 6, 387 (1972).

23. P.S. Takhar, Phys. Rev. 157, 257 (1967).

24. F. Rohrlich and B.C. Carlson, Phys. Rev. 93, 38 (1954).

25. R.E. Bell and H.N. Jorgensen, Can. J. Phys. 38, 652 (1960).

26. G. Jones and J.B. Warren, Can. J. Phys. 39, 1517 (1961).

27. H. Kanzawa, et al. Phys. Rev. A138, 1155 (1965).

28. Nathu Ram, I.S. Sundara Rao and V.K. Mehta, Pramana, Vol. 18, No. 2, 121-126 (1982).

CHAPTER - IV

THEORETICAL METHOD TO BUILD UP TRANSMISSION CURVES OF POSITRONS AND ELECTRONS

4.1 INTRODUCTION

It is impossible to build up the transmission curves and thus to get any useful information about the absorption coefficients etc., of positrons and electrons, on the basis of various theoretical developments[1-6], discussed in Chapter I. The relative differences in the transmission characteristics of positrons and electrons of same initial energies can not be accessed with the help of these theories[1-6], because no transmission curves can be produced from these calculations[1-6].

In order to get useful information about the ranges and absorption coefficients of these particles, their transmission curves in a large number of elemental materials, $6 \leqslant Z \leqslant 82$, including a number of rare earth metals like Yttrium, Neodymium, Holmium and Ytterbium, has been produced theoretically[7]. The physical properties of rare earth metals have been a subject of many recent investigations[8-9]. The study of the penetration of positrons and electrons through rare earth metals has received very little attention both experimentally and theoretically. It is interesting to reveal if any anomalies existed in the behaviour of rare earth metals from the rest of the elemental materials.

The present semi-theoretical approach is the first such attempt to reproduce the transmission curves of positrons and electrons almost in the same way as the experimental transmission curves. In this method the absorber is considered to consist

of a large number of extremely thin slices and Mott's[10-11] quantum mechanical expression for the scattering cross section has been used for computing the scattered flux at each individual slice of the absorber. Nuclear screening[12] and inelastic scattering corrections[13] have also been taken into account in the Mott's[10-11] formula.

For computing the transmission of electrons and positrons through a slice, the number of particles scattered through an angle $\geqslant 90^{o}$ have been considered to be removed from the incident beam for the successive slice. Also the energy loss of these particles at each slice has been taken into account. The agreement of these calculations with experimental values of ranges and absorption coefficients is satisfactory when the single scattering formula[10-11] used for these calculations is multiplied by an empirically determined correction factor. The energy dependence and Z-dependence of this correction factor has been evaluated.

4.2 THE METHOD OF CALCULATIONS

The electrons or positrons of the same initial energy are incident normally on the plane surface of an absorber. The absorber has been considered to consist of a large number of thin slices. The scattering, both elastic as well as inelastic of these particles occurs in each slice of the absorber. In order to compute the transmission of incident particles through

a slice, the number of particles scattered through an angle $\geqslant 90^{o}$ are considered to be removed from the incident beam for the successive slice. The energy loss in each slice is computed using the total stopping power expression[4]. For energies lying within 0.5 MeV to 5.0 MeV the following relation was used:

$$\left[-\frac{1}{\rho}\left(\frac{dE}{dx}\right)\right]^{\pm}_{\text{Total}} = (mz + C)\,\frac{\gamma^2}{\gamma\left(a^{\pm}Z + b^{\pm}\right)_{-1}}\,, \quad \ldots \qquad (4.1)$$

where the upper +ve sign stands for positrons and lower -ve sign for electrons. γ represents the total energy of e^{+} or e^{-} in units of the rest mass of electron. The constants $a^{\pm}$ and $b^{\pm}$ are as follows:-

$a^{+} = -0.0038, \qquad b^{+} = 1.8402$

$a^{-} = -0.0040, \qquad b^{-} = 1.8160$

The constants m and C for different Z values are given in table 4.1.

TABLE - 4.1

Atomic No.Z	m (MeV cm^2 g^{-1})	C (MeV cm^2 g^{-1})
$1 \leqslant Z \leqslant 10$	-0.0330	1.3230
$10 \leqslant Z \leqslant 36$	-0.0097	1.0911
$36 \leqslant Z \leqslant 92$	-0.0048	0.9156

For energies less than 0.5 MeV the following relation[4] for the total stopping power can be used.

$$\left[-\frac{1}{\rho}\frac{dE}{dx}\right]^{\pm}_{Total} = (mZ + C) \cdot F^{\pm}(\gamma) \qquad \ldots \quad (4.2)$$

where for positrons $F^{+}(\gamma) = \dfrac{\gamma^{2.4}}{\gamma^{1.9}-1}$

and for electrons $F^{-}(\gamma) = \dfrac{\gamma^{2.56}}{\gamma^{2}-1}$ $\qquad \ldots \quad (4.3)$

The incident energy on the next slice will be the incident energy on the preceeding slice, less the energy loss in that particular slice. Thus as the number of slices increases, the percentage transmission goes on falling. If the percentage transmission is plotted as a function of number of slices i.e. the absorber thickness, a transmission curve is constructed similar to the one obtained experimentally.

The following Mott's[10-11] expression for scattering cross section, modified to include the nuclear screening[12] and inelastic scattering corrections[13] is used:

$$d\sigma^{\mp} = N\pi Z(Z+1)(e^2/m_o c^2)^2 \frac{(Z+1)}{Z} (1-\beta^2/\beta^4) \operatorname{Sin}^{-4}(\theta/2)$$

$$\operatorname{Sin}(\theta/2) \operatorname{Cos}(\theta/2) [1-\beta^2 \operatorname{Sin}^2(\theta/2) \pm \pi\alpha\beta$$

$$(1 - \operatorname{Sin}\theta/2) \operatorname{Sin}\theta/2] d\theta \qquad \ldots \quad (4.4)$$

Where: The upper sign stands for electrons and lower for

positrons.

N = Total number of atoms/cm^2.

e = Electronic charge.

Z = Atomic number of the absorber.

$\alpha = Z/137$.

$\beta = (\gamma^2-1)/\gamma^2$.

Where γ is given in terms of the incident kinetic energy T by:

$$\gamma = \frac{(T + m_o c^2)}{m_o c^2}$$

and $m_o c^2$ = Rest energy of the electron.

In expression (4.4) the term Z(Z+1) replaces[12] the term Z^2 in the original Mott[10-11] formula, and is a satisfactory approximation to account for the screening of the nucleus by the orbital electrons. Also another term (Z+1)/Z in this expression (4.4) accounts for the inelastic deflections[13].

In order to compute the transmission curve by using expression (4.4), all the incident particles scattered through an angle $\geqslant 90^o$ have been considered to be removed or absorbed from the incident beam while traversing an individual slice of the absorber. The thickness of each slice is taken to be extremely small. Just for instance for particles of incident energy 0.77

MeV, the thickness of each slice for Al and Pb is taken to be $22 \times 10^{-5} \times \rho$ gm cm^{-2} and $11 \times 10^{-5} \times \rho$ gm cm^{-2} respectively. Where ρ is the density of the material. It is convenient to use more and more thin slices for energies of particles much smaller than above mentioned energy. For instance at energy 0.25 MeV we used tnickness of the slices to be ten times less than the one used for 0.77 MeV. The choice of the thickness of the slice though arbitrary, even with this approximation the computed transmission curves agree well with the experimental results.

The fraction of the incident particles scattered at an angle $\geqslant 90^{o}$ or considered to be removed from the incident beam is given by:

$$\text{Fraction of the scattered or removed beam flux} = \int_{\pi/2}^{\pi} d\sigma \Big/ \int_{o}^{\pi} d\sigma \qquad \ldots \qquad (4.5)$$

In the Mott's[10-11] expression used in (Eq. 4.4) the factor $\beta = (\gamma^2-1)/\gamma^2$ goes on changing at each subsequent slice. For computing the value of β at each subsequent slice the energy loss of the particles in each slice is computed by using the expression[4] for total stopping power (Eqs. 4.1 and 4.2) for different values of Z. For the first slice the total incident energy of the incident particles in terms of rest mass energy is given by $\gamma = (T + m_o c^2)/m_o c^2$, and for the subsequent slice the incident energy will be equal to the incident energy of the preceding slice, less the loss of energy in it.

Thus by incorporating the energy loss at each slice the fraction of the transmitted particles at each slice (thickness) can be computed and hence the transmission curve can be built.

4.3 CORRECTION FACTOR IN THE SCATTERING CROSS-SECTION EXPRESSION

The Mott[10-11] expression (Eq. 4.4) used for computing the scattered fraction of the incident flux is based on the assumption that all the particles which are scattered through an angle $\geqslant 90^{o}$ are removed from the incident beam. However, in actual situation the particles scattered at an angle $\geqslant 90^{o}$ may still remain in the incident beam due to back scattering of these particles. Also we are considering the scattering as well as the energy loss process by dividing the absorber into extremely small segments, i.e. the individual slices. In practice the scattering as well as the energy loss takes place in the bulk of the absorbing material. This introduces an error in the computation of the scattered or removed particle flux. Yet another error may arise from the fact that under the approximation that slice is so extremely thin to give rise to only single scattering events. The possibility of multiple scattering however can not be ruled out.

In order to account for the above mentioned errors an empirically determined correction factor has been introduced in the Mott[10-11] expression (Eq. 4.4). This correction factor is of the form:

$$A[1 - a + be^{-cZ}] \quad \ldots \quad (4.6)$$

where A = Atomic weight of the absorber. The constant a is energy dependent and is given by the expression:

$$a = (0.986 - 0.001586\ E) \quad \ldots \quad (4.7)$$

where E = Initial incident energy of the particle in MeV. The constants b and c for different values of Z and different values of E are tabulated in table 4.2.

TABLE - 4.2

Atomic No. Z	Energy E MeV	b	c
$6 \leqslant Z \leqslant 20$	$0.25 \leqslant E \leqslant 0.5$	4.446	0.1843
	$0.05 \leqslant E \leqslant 5.0$	4.446	0.1430
$21 \leqslant Z \leqslant 82$	$0.25 \leqslant E \leqslant 0.5$	1.117	0.0731
	$0.05 \leqslant E \leqslant 5.0$	1.7355	0.0712

4.4 RESULTS AND DISCUSSION

In this Chapter the attempt has been mainly to reproduce the transmission curves theoretically; i.e. to view the % of

transmitted beam intensity theoretically as a function of the thickness of the material through which the beam passage takes place. It may be outrightly said that the treatment of the method though not very rigorous, gives results of fairly good accuracy.

The transmission curves for a large number of absorbers including the rare earth metals were constructed. The shape of the transmission curves is precisely the same as that of an experimental curve. These curves have been used to determine the values of $R^{\pm}_{sfp}$ and the absorption coefficients in a similar manner as was done with the experimental transmission curves in Chapter III. These theoretically obtained transmission curves for few of the absorbers at different energies are shown in Figs. 4.1 - 4.9. The shape of these curves for rest of the absorbers at different energies is exactly the same.

Comparison of Absorption Coefficients and Range With Experimental Values

The mass absorption coefficients and the range have been realized from the theoretical transmission curves in different absorbers and at different energies of the incident particles. The comparison of the mass absorption coefficients realized from theoretical curves are compared with the present experimental values at energy E_{max} = 1.88 MeV in tables 4.3 and 4.4. The ratio of $\mu_m(e^-)$ to $\mu_m(e^+)$ as well as the actual values of $\mu_m(e^-)$ and $\mu_m(e^+)$ agree, both qualitatively as well as quantitatively,

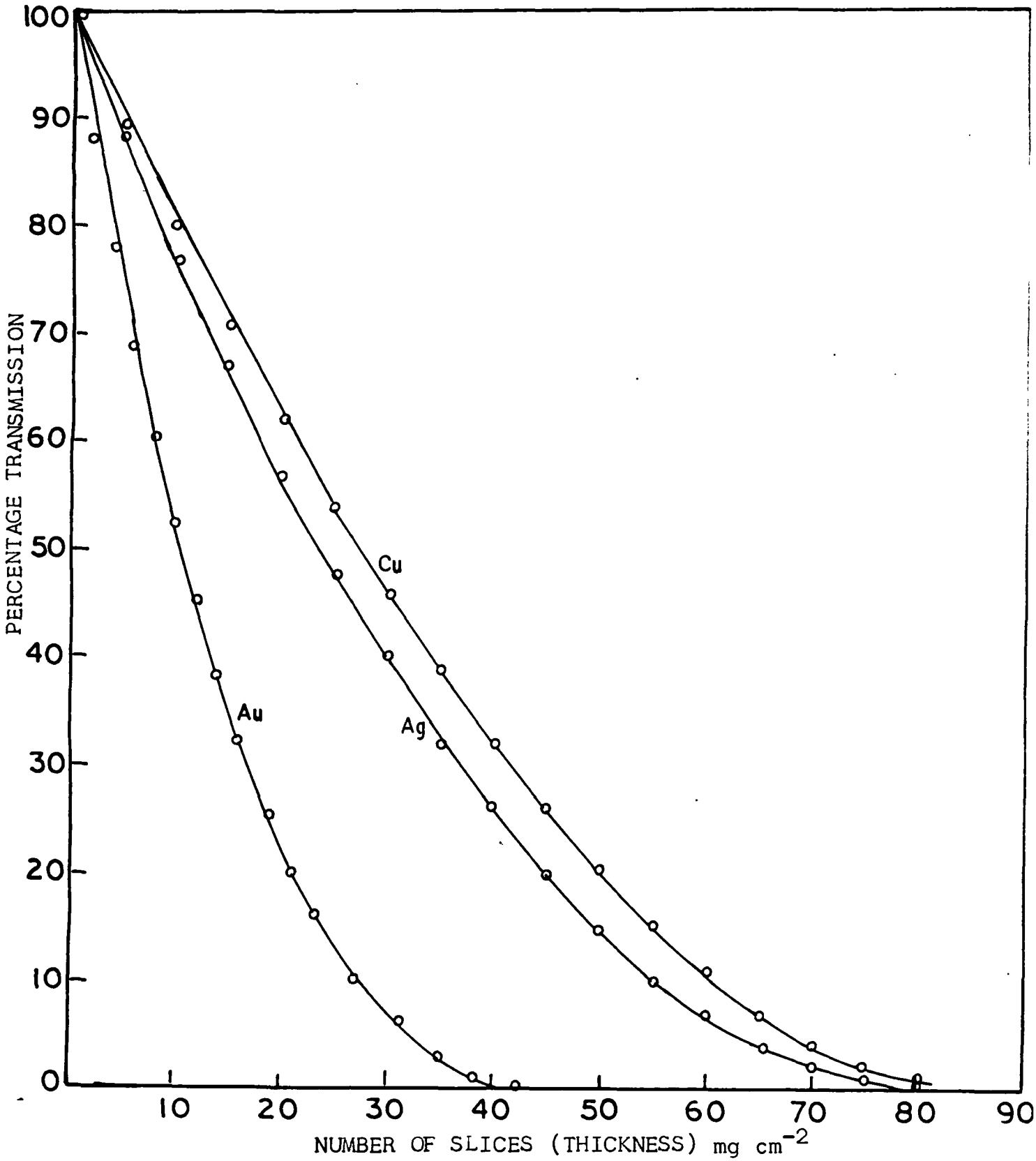

Fig. 4.1 Theoretical transmission curves for electrons of energy E_{max} = 0.25 MeV in Cu, Ag and Au.

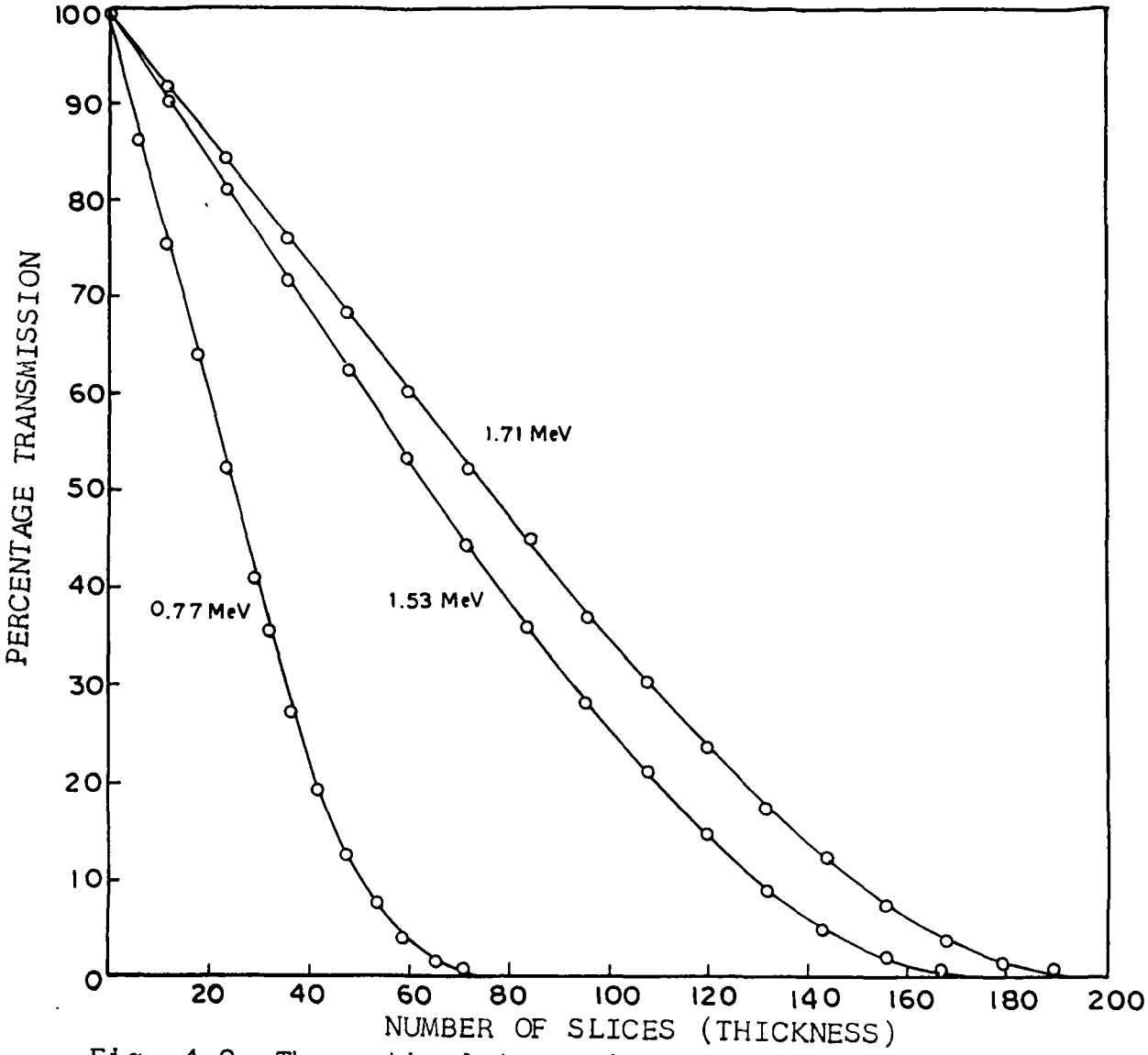

Fig. 4.2 Theoretical transmission curves at different energies of electrons for Yttrium absorber.

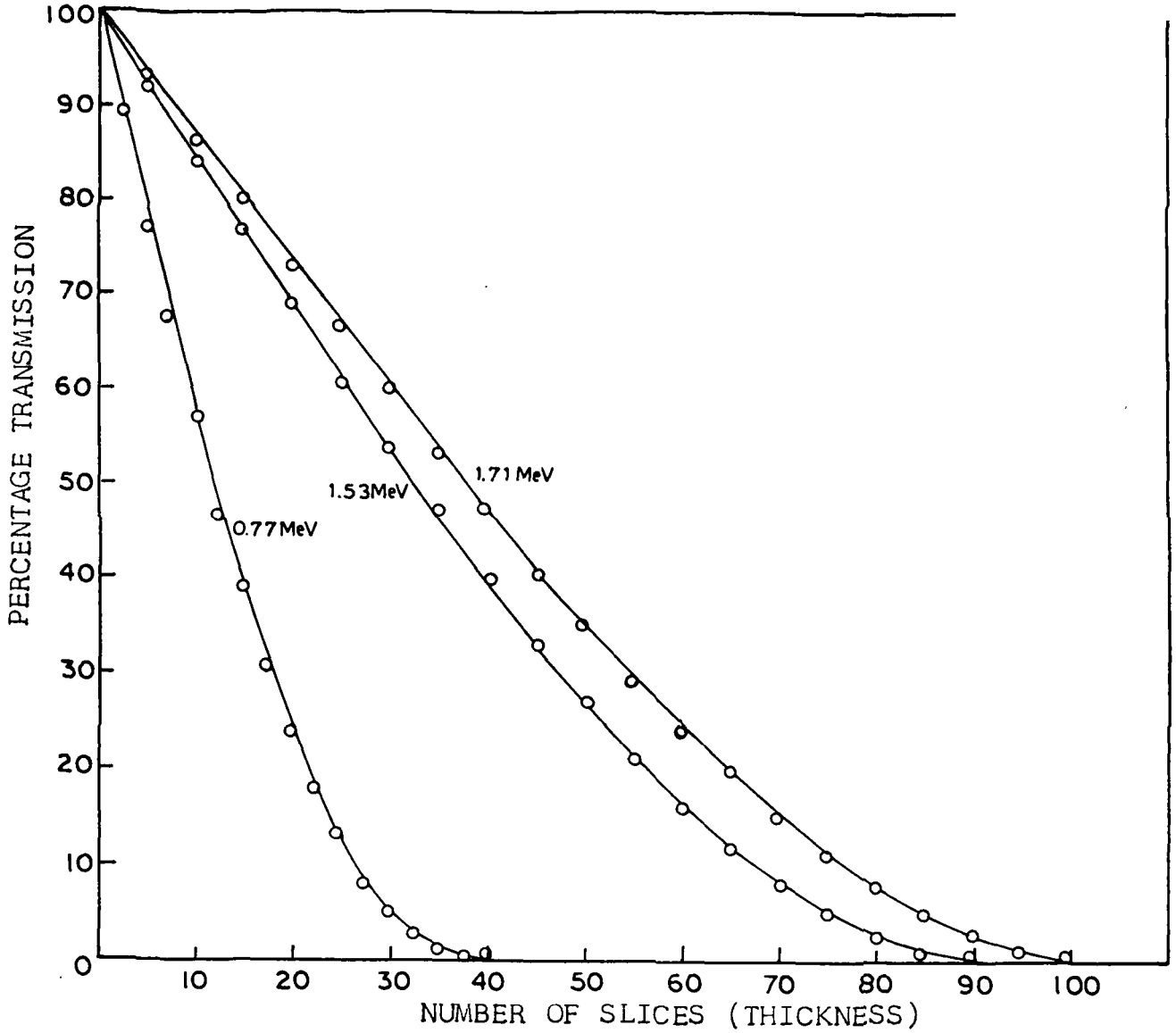

Fig. 4.3 Theoretical transmission curves at different energies of electrons for Silver Absorber.

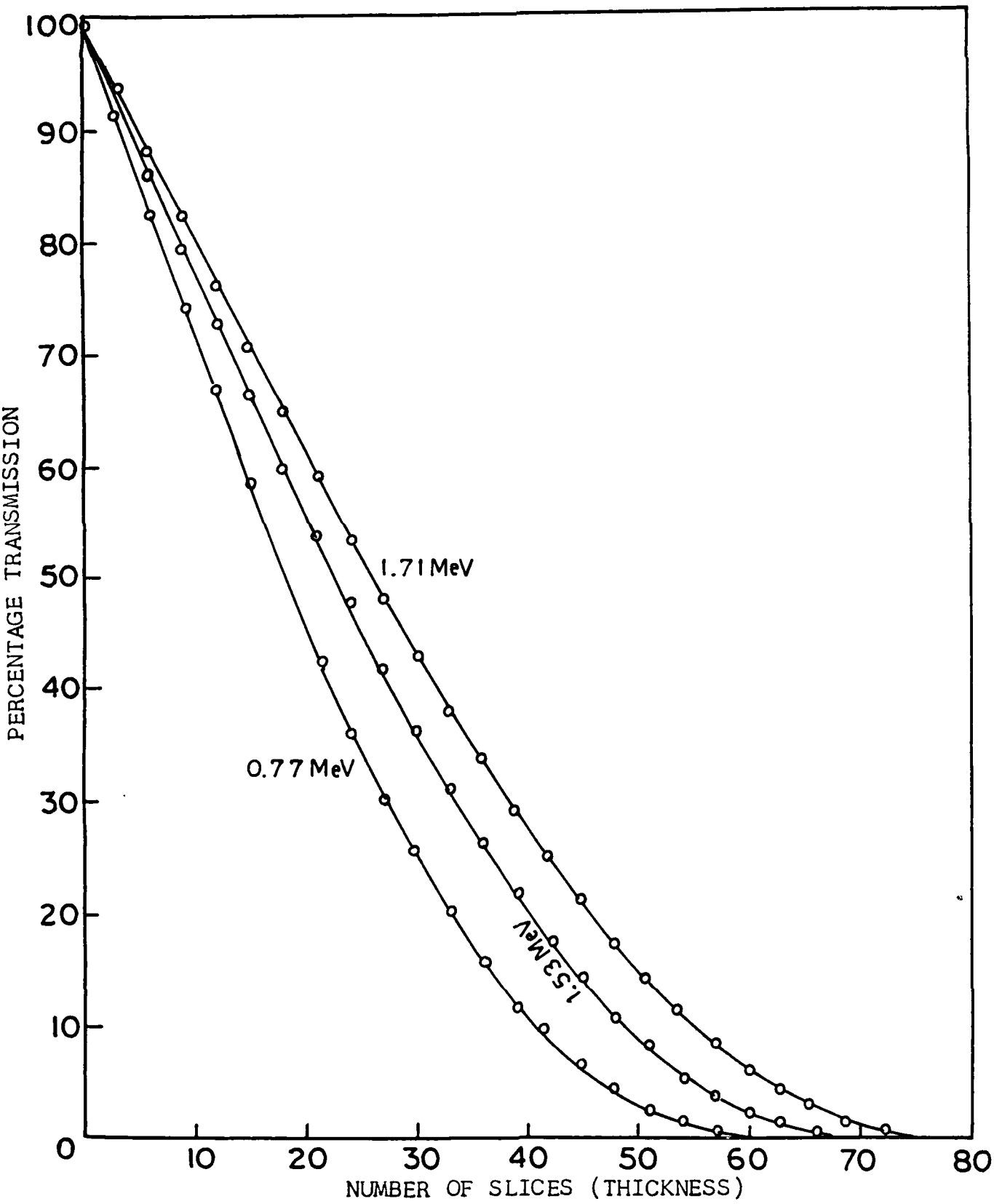

Fig. 4.4 Theoretical transmission curves at different energies of electrons for Neodymium absorber.

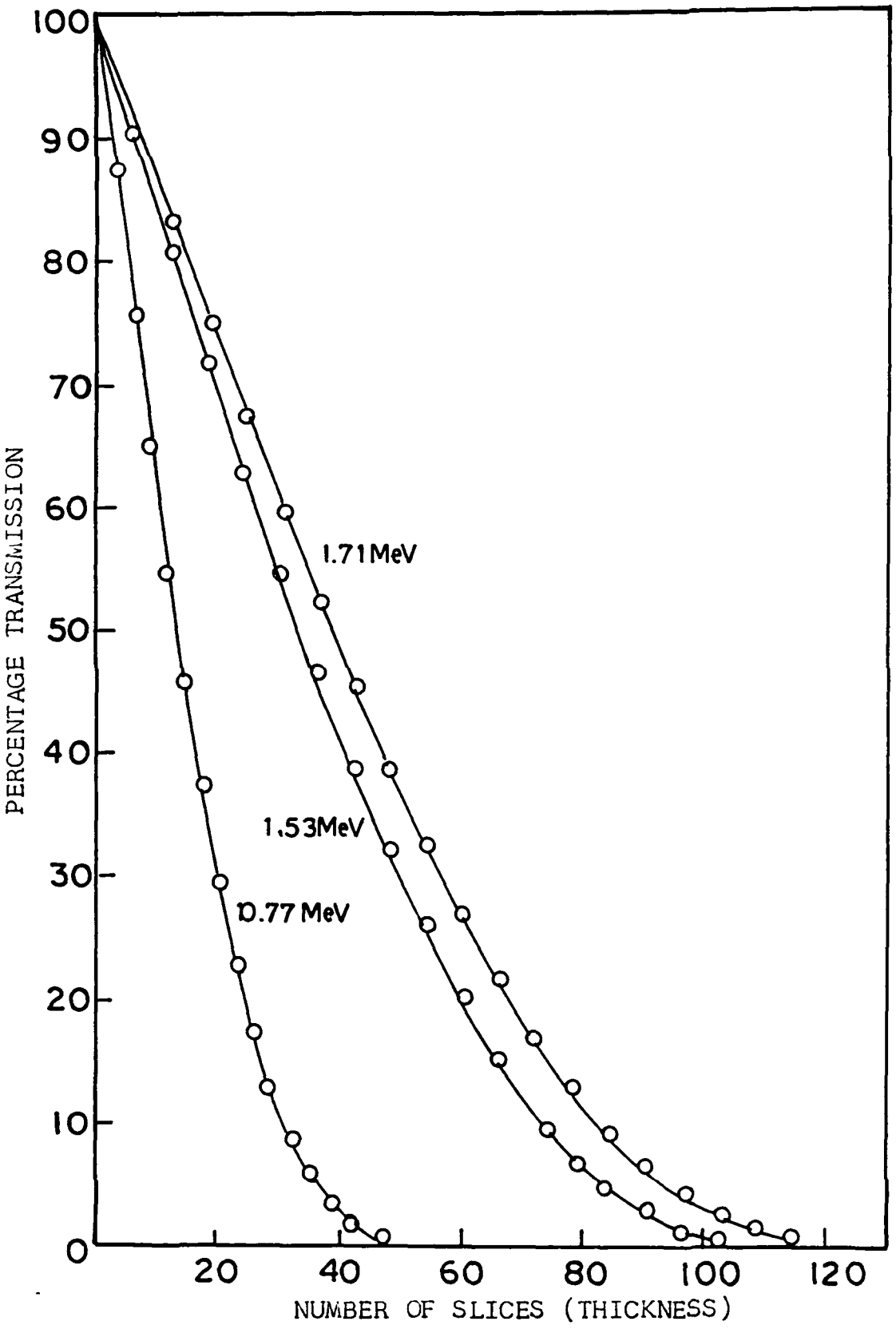

Fig. 4.5 Theoretical transmission curves at different energies of electrons for Holmium absorber.

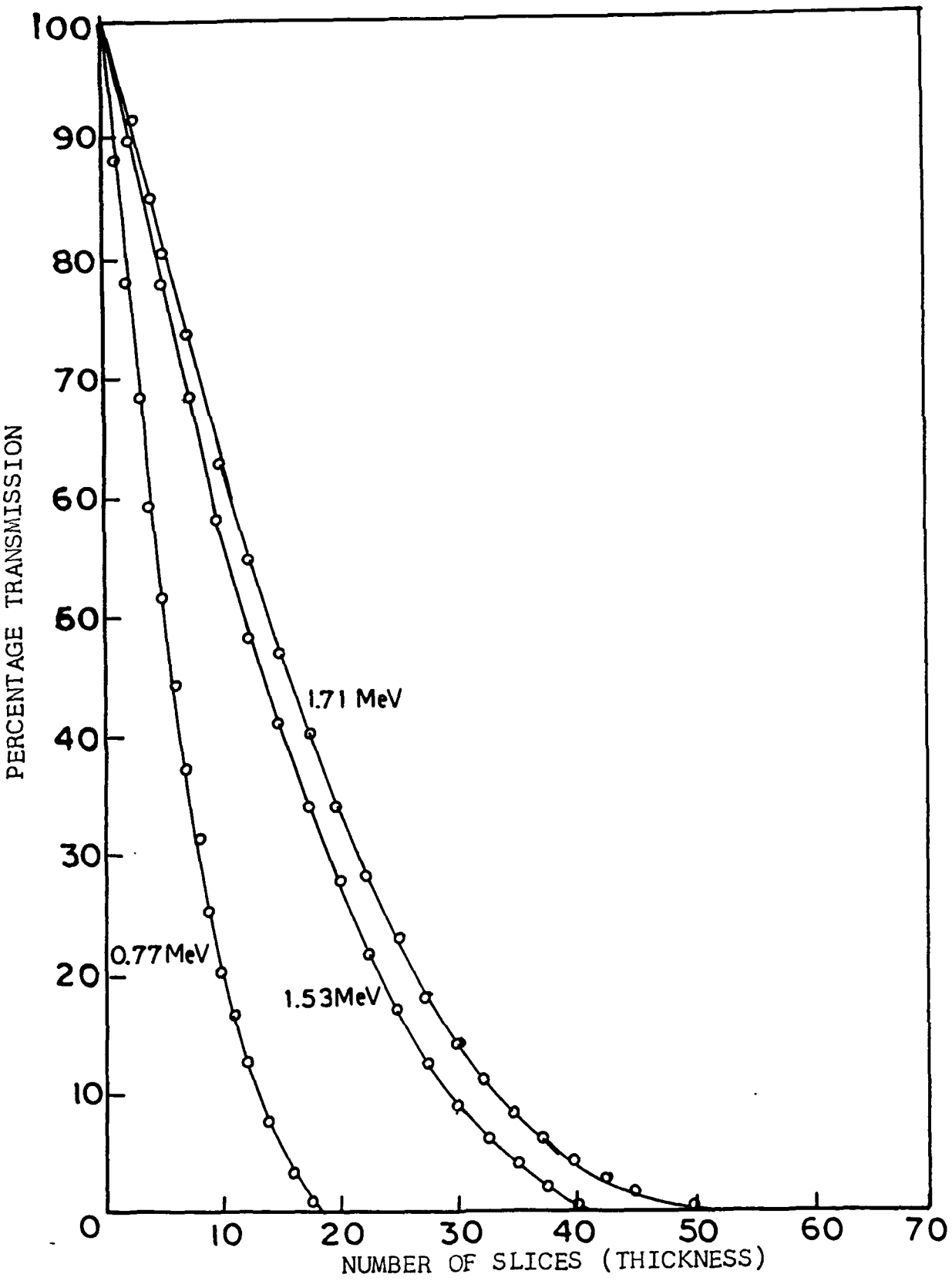

Fig. 4.6 Theoretical transmission curves at different energies of electrons for Gold absorber.

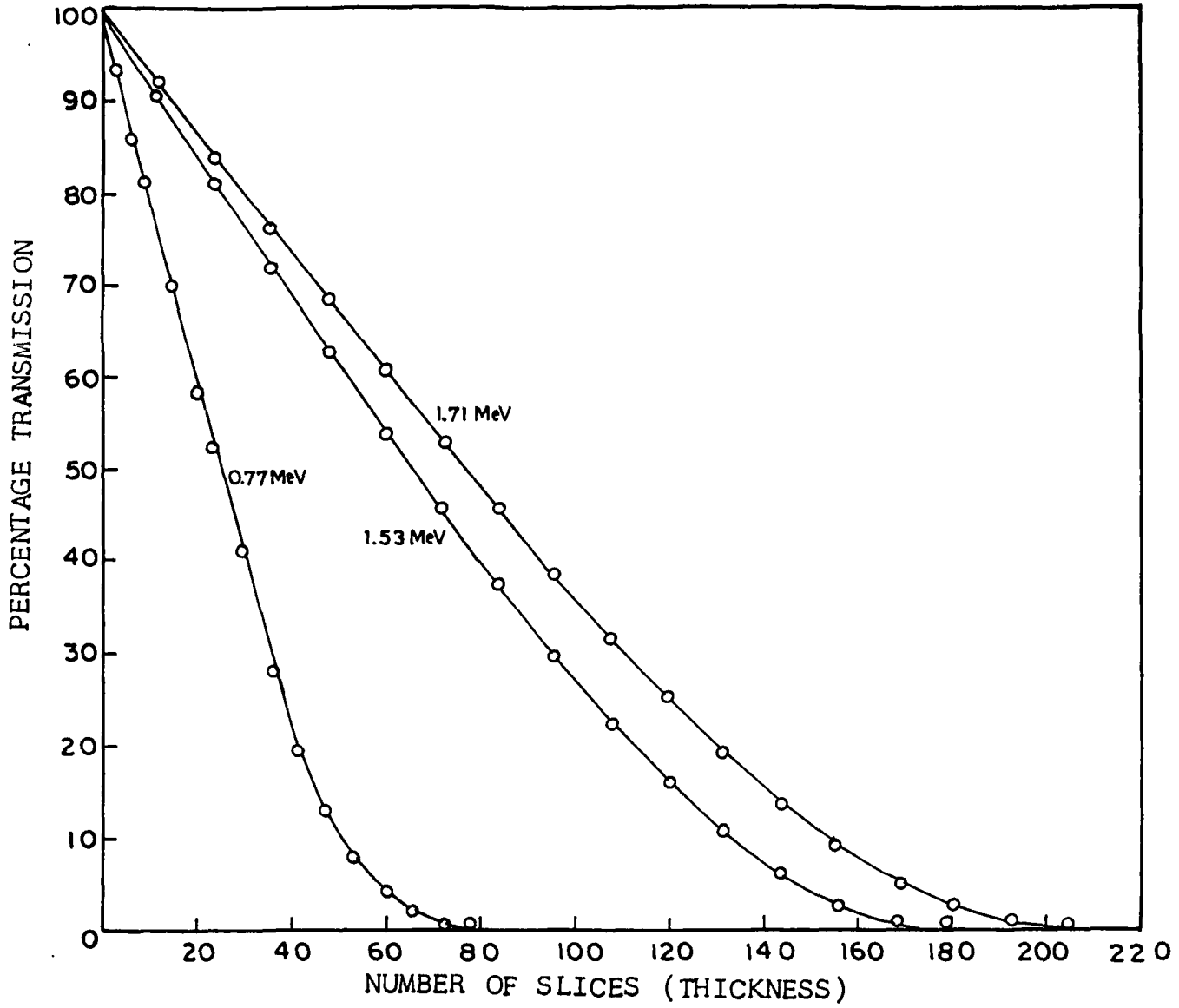

Fig. 4.7 Theoretical positron transmission curves at different energies in Yttrium.

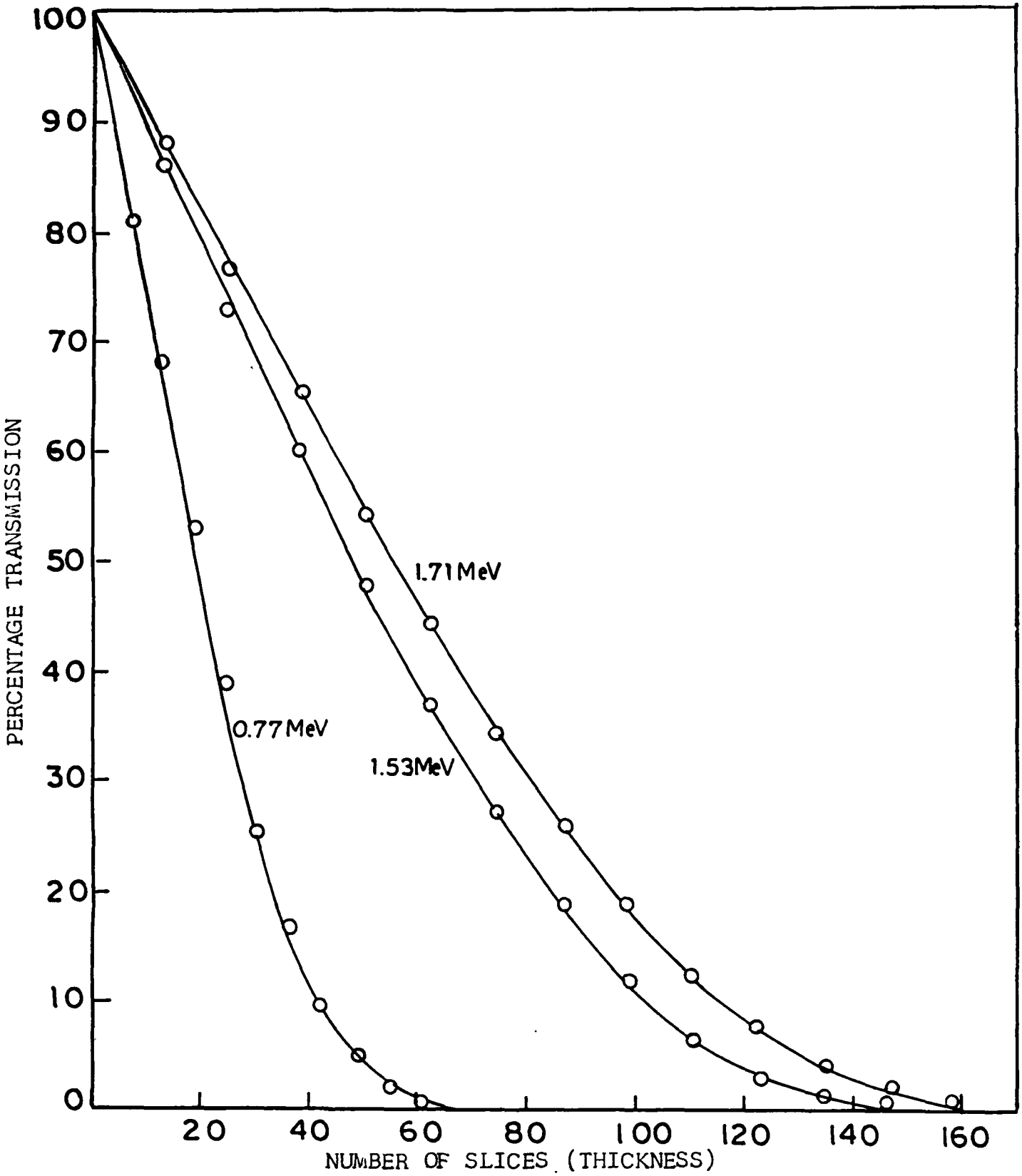

Fig. 4.8 Theoretical positron transmission curves at different energies in Neodymium.

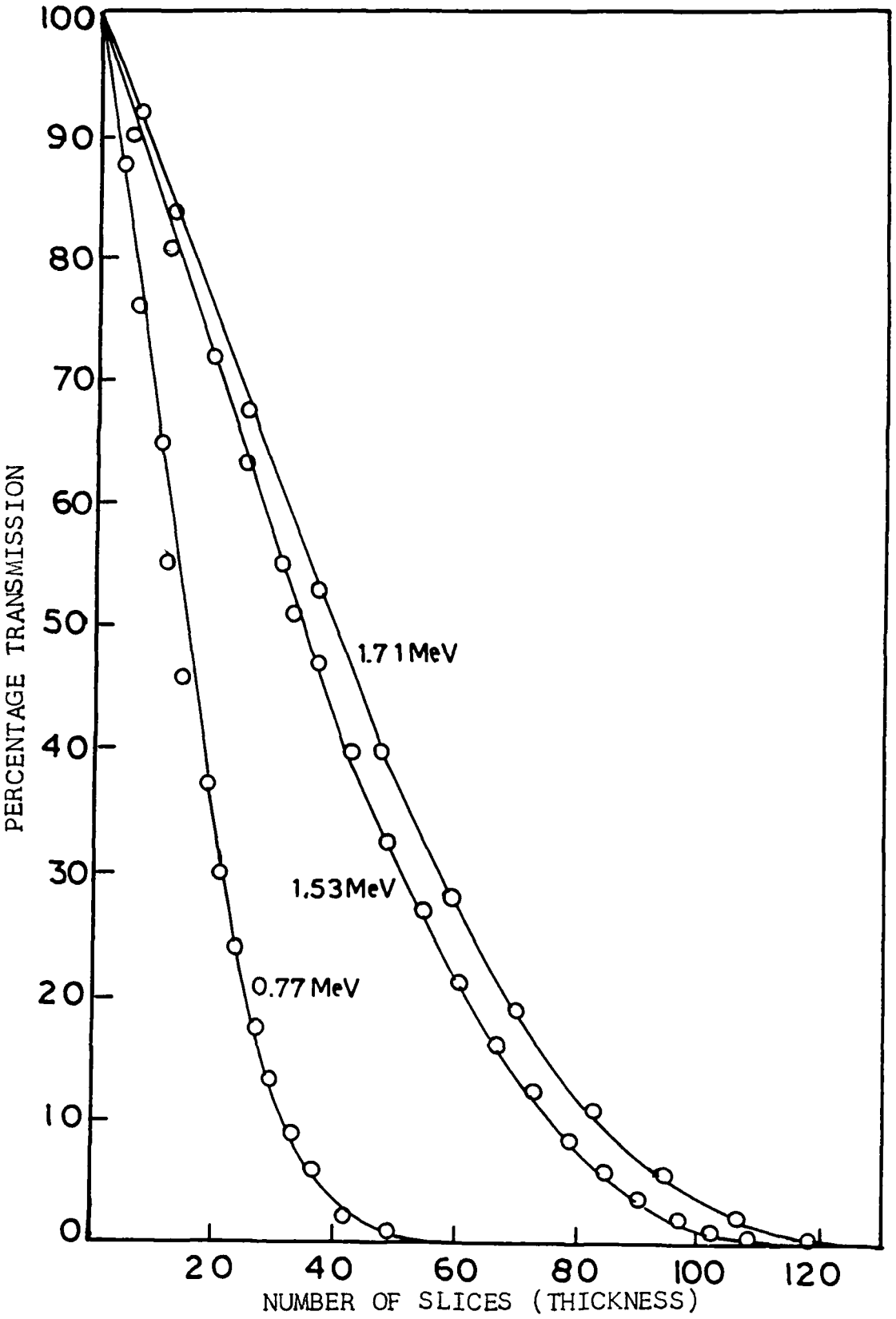

Fig. 4.9 Theoretical transmission curves at different energies of positrons for Holmium absorber.

TABLE - 4.3

Comparison of theoretically determined mass absorption coefficients (unit gm^{-1} cm^2) of positrons and electrons with present experimental values at E_{max} = 1.88 MeV.

Type	Particles	Absorption coefficients $\mu_m(e^+)$ and $\mu_m(e^-)$ in					
		Carbon	Aluminium	Copper	Silver	Gold	Lead
Theoretical	Positrons	4.27	6.07	7.29	7.76	9.98	9.49
	Electrons	6.02	7.64	9.09	11.47	12.15	14.98
	$\mu_m(e^-)/\mu_m(e^+)$	1.41	1.26	1.25	1.47	1.23	1.57
Experimental (present work)	Positrons	3.92	6.03	6.61	7.08	8.42	8.71
	Electrons	5.52	6.92	8.71	10.47	11.70	13.75
	$\mu_m(e^-)/\mu_m(e^+)$	1.41	1.15	1.32	1.48	1.39	1.58

TABLE - 4.4

Comparison of theoretically determined mass absorption coefficients (unit gm^{-1} cm^2) of positrons and electrons with present experimental values in some rare earth elements at energy E_{max} = 1.88 MeV

Type	Particles	Absorption coefficients $\mu_m(e^+)$ and $\mu_m(e^-)$ in			
		Yttrium	Neodymium	Holimium	Ytterbium
Theoretical	Positrons	7.22	8.02	0.04	8.70
	Electrons	11.13	12.10	12.08	12.39
	$\mu_m(e^-)/\mu_m(e^+)$	1.54	1.51	1.50	1.42
Experimental (Present work)	Positrons	6.81	7.54	7.83	8.03
	Electrons	10.25	11.13	11.45	11.55
	$\mu_m(e^-)/\mu_m(e^+)$	1.51	1.48	1.46	1.44

within an error of 4% to 8%. The difference is less in low-Z materials and is more for low energies and high-Z materials. The ratio $\mu_m(e^-)/\mu_m(e^+)$ slowly rises from low-Z materials to high-Z materials, with the exception of carbon and few other materials. This trend is identical for both theoretical and experimental values. The ratio $\mu_m(e^-)/\mu_m(e^+)$ for rare earth elements as shown in table 4.4 reveals almost constant values both for experimental as well as theoretical data.

It is of interest to examine these coefficients in the low energy region. The values of mass absorption coefficients for positrons and electrons as tabulated by Nathu Ram et al.[14-15] for Beryllium, Aluminium, Copper, Silver and Lead; at energies 0.324 MeV and 0.544 MeV, are compared with values realized from the theoretically constructed curves in table 4.5. The present ratio $\mu_m(e^-)/\mu_m(e^+)$ and μ_e-/μ_e+ are same, both of them are the mass absorption coefficient ratio for electrons and positrons. For Beryllium and Aluminium this ratio at energy 0.324 MeV is less than one for both, theoretical as well as experimental values. This is in agreement with the predictions of Seliger[16] and Rohrlich and Carlson[2], showing lesser penetration for positrons in low-Z materials at low energies. At energy E_{max} = 0.544 MeV, except for Beryllium the trend of theoretical and experimental values[14] is precisely the same; both sets of values show greater transmission of positrons than of electrons.

TABLE - 4.5

Comparison of theoretically determined mass absorption coefficients (unit gm^{-1} cm^2) of positrons and electrons with experimental[14] values at E_{max} = 0.324 MeV and 0.544 MeV.

Energy (MeV)	Type	Particles	Absorption coefficients $\mu_m(e^+)$ and $\mu_m(e^-)$ in				
			Beryllium	Aluminium	Copper	Silver	Lead
0.324	Theoretical	Positrons	85.28	95.68	112.53	118.56	127.83
		Electrons	84.05	94.33	114.40	125.84	136.56
		$\mu_m(e^-)/\mu_m(e^+)$	0.98	0.99	1.01	1.06	1.06
	Experimental (Ref. - 14)	Positrons	78.20	92.00	108.20	114.00	119.00
		Electrons	74.70	90.70	110.00	121.00	129.00
		μ_{e^-}/μ_{e^+}	0.96	0.99	1.02	1.06	1.08
0.544	Theoretical	Positrons	34.62	42.82	45.51	49.07	53.60
		Electrons	31.38	44.41	53.09	60.82	68.87
		$\mu_m(e^-)/\mu_m(e^+)$	0.91	1.03	1.17	1.22	1.28
	Experimental (Ref. - 14)	Positrons	26.80	41.10	43.90	44.40	47.60
		Electrons	32.90	42.70	51.00	57.90	62.90
		μ_{e^-}/μ_{e^+}	1.22	1.04	1.12	1.30	1.31

The ratio $\mu_m(e^-)/\mu_m(e^+)$ for Yttrium, Neodymium, Holmium, Ytterbium and Gold for energies 0.324 MeV and 0.544 MeV are shown in table 4.6. Except Yttrium at 0.324 MeV, the values of $\mu_m(e^-)/\mu_m(e^+)$ are more than one, showing more absorption of electrons than that of positrons.

In table 4.7 the comparison of the theoretically determined mass absorption coefficients with experimental values[15] for electrons of energy E_{max} = 1.71 MeV has been shown for Be, Al, Cu, Ag and Pb. The agreement is good within a difference of about 4 to 8%.

The comparison of values of the range for electrons as determined from the theoretically constructed curves and the experimental values R^-_{sfp} at different energies, in C, Al, Ni, Cu, Y, Zr, Ag, Cd, In, Nd, Ho, Yb, Au and Pb are shown in table 4.8. Also the values of experimental range R^+_{sfp} of positrons at energy 1.88 MeV is compared with theoretical values in table 4.9, for C, Al, Cu, Y, Ag, Nd, Ho, Yb, Au and Pb. The agreement of these values is good within a difference of 4 to 8%. The experimental and theoretical values of range for electrons and positrons at different energies as a function of atomic number Z of the absorber are shown in Fig. 4.10.

This difference in the range as well as the absorption coefficients in two sets of values is possibly due to the fact that Batra and Sehgal[4] had predicted an error of about 4% in their values of total stopping power, expression (Eq. 4.1).

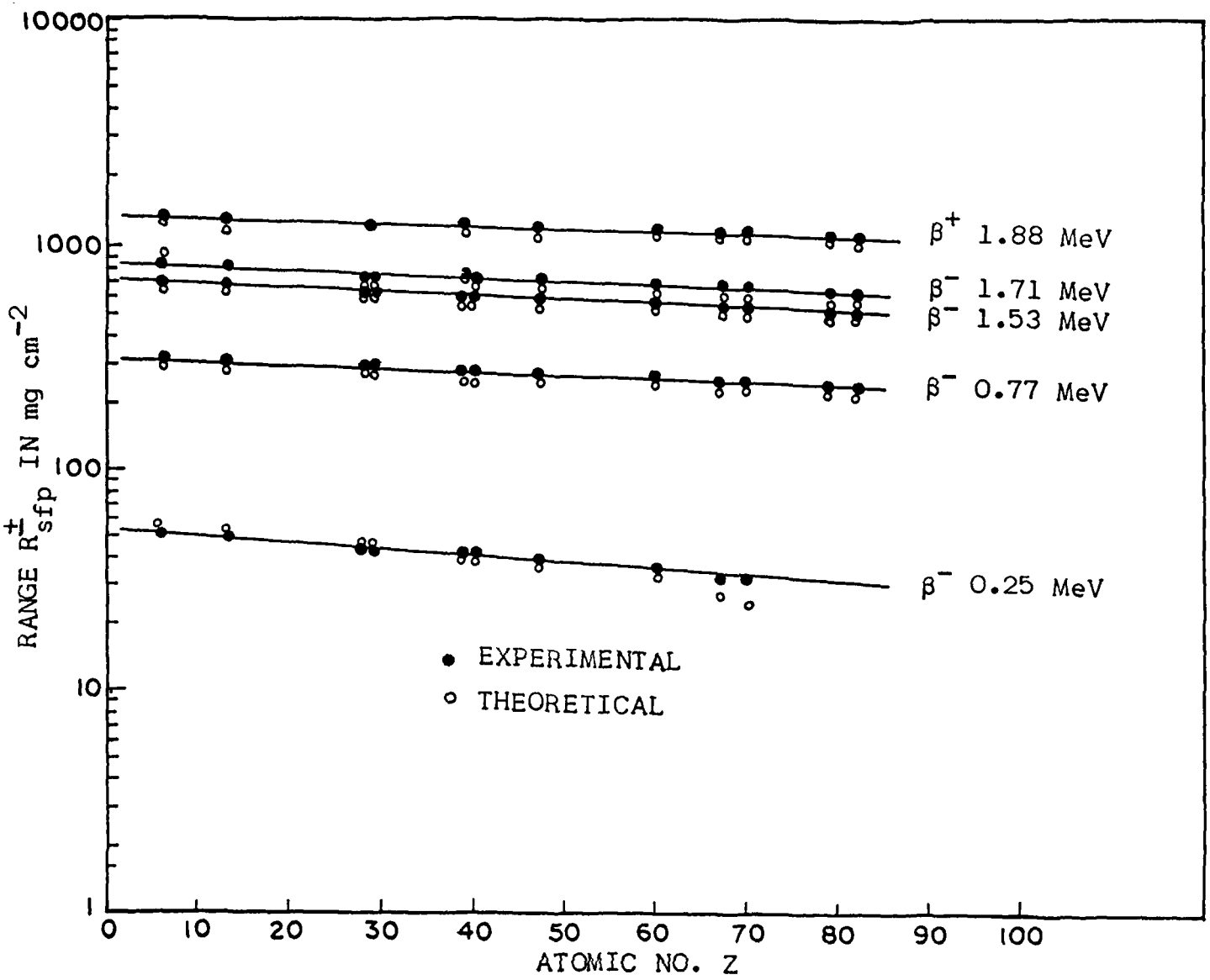

Fig. 4.10 Experimental and theoretical ranges of β^- and β^+ particles as a function of atomic number Z of the absorber.

TABLE - 4.6

Values of theoretical $\mu_m(e^+)$ and $\mu_m(e^-)$ (unit gm^{-1} cm^2) of positrons and electrons at energy E_{max} = 0.324 MeV and 0.544 MeV for elements for which no experimental data is available.

Energy (MeV)	Particles	Absorption coefficients in				
		Yttrium	Neodymium	Holmium	Ytterbium	Gold
0.324	Positrons	114.37	121.68	122.62	126.26	127.19
	Electrons	90.36	131.50	133.58	134.60	136.47
	$\mu_m(e^-)/\mu_m(e^+)$	0.79	1.08	1.09	1.07	1.07
0.544	Positrons	46.31	51.36	50.90	51.60	53.02
	Electrons	58.77	65.68	66.82	67.36	67.82
	$\mu_m(e^-)/\mu_m(e^+)$	1.27	1.28	1.31	1.31	1.28

TABLE - 4.7

Comparison of theoretically determined mass absorption coefficients (unit gm^{-1} cm^2) with experimental values[15] for electrons with E_{max} = 1.71 MeV.

Type	Absorption coefficients in				
	Beryllium	Aluminium	Copper	Silver	Gold
Theoretical (Present work)	7.01	9.12	12.57	13.32	15.98
Experimental (Ref. - 15)	6.60	8.40	11.60	12.30	14.80

TABLE - 4.8

Comparison of experimental values of range $\bar{R}_{sfp}$ and values of range determined from theoretically constructed curves at different energies in units mg cm^{-2}.

Material	1.71 MeV		1.53 MeV		0.77 MeV		0.25 MeV	
	Experimental	Theoretical	Experimental	Theoretical	Experimental	Theoretical	Experimental	Theoretical
Carbon	826	945	706	643	306	291	52	58
Aluminium	814	832	688	625	296	281	50	57
Nickel	722	650	624	570	286	270	45	47
Copper	720	635	622	568	285	269	44	49
Yttrium	708	720	596	542	268	250	41	39
Zirconium	707	690	594	540	267	251	41	38
Silver	705	695	580	526	264	249	40	37
Cadmium	701	652	576	522	263	248	38	33
Indium	697	647	574	520	257	249	38	32
Neodymium	664	660	552	502	254	240	35	30
Holmium	652	645	536	486	242	230	33	27
Ytterbium	636	630	526	481	241	231	32	25
Gold	606	530	514	470	235	228	-	-
Lead	590	520	510	455	231	219	-	-

TABLE - 4.9

Comparison of present experimental values of range R^{+}_{sfp} and values of range determined from present theoretically build up curves at energy E_{max} = 1.88 MeV.

Material	Range in mg cm^{-2}	
	Experimental	Theoretical
Carbon	1332	1232
Aluminium	1240	1138
Copper	1163	1195
Yttrium	1230	1190
Silver	1160	1100
Neodymium	1142	1087
Holmium	1125	1059
Ytterbium	1106	1051
Gold	1035	1005
Lead	1026	976

This value of the total stopping power has been used as input data for calculating the energy loss and finally the percentage transmission. On the other hand the present experimental data as well as the data of Nathu Ram et al.[14-15] also indicate an error of about 4% or so. Hence the compounded effect introduces an uncertainty of about 4% to 8%. This difference is possibly coming in all the present comparisons.

REFERENCES

1. M.J. Berger and S.M. Seltzer, 'Studies in penetration of charged particles through matter'
   (i) National research council publication No. 1133, p. 205-268 (1964).
   (ii) Tables of energy losses and ranges of electrons and positrons, NASA SP-3012 (1964).

2. F. Rohrlich and B.C. Carlson, Phys. Rev. 93, 38 (1954).

3. R.K. Batra and M.L. Sehgal, Nuclear Physics A156, 314-20 (1970).

4. R.K. Batra and M.L. Sehgal, Nucl. Inst. Methods, 109, 565 (1973).

5. P.S. Takhar and M.L. Sehgal, Nuovo Cimento (Italy) 47B, 31 (1978).

6. R.K. Batra and M.L. Sehgal, Phys. Rev. B, 23/9, 4448 (1981).

7. T.S. Gill, M.L. Sehgal and P.S. Takhar, 'The Rare earths in modern science and technology', Edited by Gregory J. McCarthy and J.J. Rhyne, (Plenum Publishing Corporation, New York), 367-373 (1978).

8. F.H. Spedding and A.H. Danne, The Rare Earths (John Wiley and Sons, Inc.) New York (1961).

9. K.A. Gschneider, Jr., Rare Earths, the Fraternal Fifteen, published by United States Atomic Energy Commission, Division of Technical Information (1966).

10. N.F. Mott, Proc. Roy. Soc. (London) A126, 259 (1930).

11. N.F. Mott and H.S.W. Massey, The theory of atomic collisions Oxford University Press, London (1949).

12. E.J. Williams, Phys. Rev. 58, 292 (1940).

13. L.V. Spencer, Phys. Rev. 98, 1597 (1955).

14. Nathu Ram, I.S. Sundara Rao and M.K. Mehta, Phys. Rev. 23, No. 3, 1202 (1981).

15. Nathu Ram I.S. Sundara Rao and M.K. Mehta, Pramana 18, No. 2, 121 (1982).

16. H.H. Seliger, Phys. Rev. 88, 408(1952) and Phys. Rev. 100, 1029 (1955).

CHAPTER - V

CALCULATIONS OF STRAGGLING FREE PRACTICAL RANGES, $R^{\pm}_{sfp}$ OF POSITRONS AND ELECTRONS

5.1 INTRODUCTION

The positrons and electrons while passing through matter have both the inelastic and elastic interactions with the atoms of the absorber. Their path gets distorted during slowing down due to multiple scattering, and with decreasing energy the process of distortion becomes more rapid. This is due to the fact that significance of multiple scattering is enhanced at low energies, until at some stage when the energy of these particles is decreased to such a level that their motion becomes random. This random motion results in diffusion of these particles in the absorber. The energy at which the diffusion sets-in depends upon the nature of the absorbing material as well as the initial kinetic energy of these particles. These randomly moving particles are left with substantial fraction of their incident kinetic energy. Hence, even after the diffusion process starts, the positrons and electrons can travel on an average, some distance. This distance is a substantial fraction of the practical range of these particles in the absorbing material. This fact is to be utilized for calculations of the straggling free practical ranges of these particles in the target materials. Both parts of the journey of these particles, i.e. before and after the diffusion process starts, must be taken into account. The approach for these calculations must be such that it can be

compared with the experimental results on transmission of positrons and electrons.

5.2 PRESENT METHOD FOR THEORETICAL CALCULATIONS OF STRAGGLING FREE PRACTICAL RANGES

The diffusion of electrons has been taken into account by Bethe et al.[1] in their theory of electron penetration. The assumptions used in this theory[1] not only bring this theory much nearer to the experimental situation, but also make the present approach of calculating the straggling free practical ranges simpler. These assumtions are extendable to positrons also. It is assumed that positrons and electrons while passing through absorbers in the beginning suffer energy loss but undergo very little multiple scattering, and travel almost along a straight path. With the decrease in the energy of these particles the multiple scattering process starts and finally when the motion of these particles becomes random the diffusion sets in. The process of multiple scattering of these particles during their slowing down in the absorbers is taken into account for finding the critical energy '$T_r^{\pm}$', at which the process of diffusion starts. However, both the multiple scattering and slowing down can not be easily treated simultaneously. Therefor to simplify, this situation is approximated by assuming a direct transition from a straight motion into diffusion.

This transition was visualized by Bethe et al.,[1] by using the definition of transport mean free path, to occur when

$$\langle \text{Cos } \theta \rangle_{\text{average}} = \frac{1}{e} \quad \ldots \quad (5.1)$$

where θ = Angle between the direction of motion of the particles in the target material and the direction of initial beam.

Therefore by knowing $\langle \text{Cos } \theta \rangle_{\text{average}}$, both the straight motion and diffusion of these particles can be treated to determine the desired range.

Batra and Sehgal[2-4] have evaluated the critical kinetic energy '$T_r^{\pm}$' for positrons and electrons and plotted against incident kinetic energy T for different absorbers. It can be noticed from graphs[2-4] that with decreasing value of T and increasing Z, the fraction $T_r^{\pm}/T$ of energy left with the positrons or electrons increases rapidly. Also for any absorber T_r^+ is smaller than T_r^-, except when T is <100 KeV, then $T_r^+ \simeq T_r^-$. Also the difference between T_r^+ and T_r^- increases with increasing value of T.

Once the critical kinetic energy $T_r^{\pm}$ for a particular initial kinetic energy is evaluated for some target material, the calculations of the part of range before and after diffusion process starts, can be done. The straight path traversed by positrons or electrons, i.e. the projected range is given[2-4]

in continuous slowing down approximation as:

$$R_p^{\pm}(T) = R^{\pm}_{C.s.d.a.}(T) - R^{\pm}_{C.s.d.a.}(T_r^{\pm}) \qquad \ldots \qquad (5.2)$$

where $R^{\pm}_{C.s.d.a.}(T)$ and $R^{\pm}_{C.s.d.a.}(T_r^{\pm})$ are the C.s.d.a. ranges of positrons and electrons for T and $T_r^{\pm}$, and can be obtained by using the Berger and Seltzer[5] tables.

(a) Inclusion of Higher order terms in Mott's[6] Expression as Used by Batra and Sehgal[2-4]

When the values of range $R_p^{\pm}$ obtained by Batra and Sehgal in the aforesaid manner are compared with the present experimental values in Chapter III, the discrepancies between the two sets of values are quite clear. The nature and extent of disagreement is discussed in Chapter I, 1.3(c) and then in Chapter III, table 3.4 and Figs. 3.15 to 3.18.

The disagreement between values due to Batra and Sehgal[2-4] and the present experimental data can be suspected due to the error involved in the empirical relations of total stopping power[3], used by Batra and Sehgal[2-4]. These empirical relations were modified by Rathi[7] for low energy region i.e. upto 500 KeV. For higher energies the empirical relation given by Batra and Sehgal[3] is valid. It has been verified that these empirical relations[3,7] for total stopping power give correct values of the energy loss within $\pm 4\%$ for all values of Z. The reason for this difference between the experimental values

and the values of $R_p^{\pm}$ due to Batra and Sehgal[2-4], have been spelled out in Chapter I, 1.3(c).

The Mott's[6] expression for elastic scattering cross-section as used by Batra and Sehgal[2-4] taking only the linear term in αZ is given by:

$$\sigma^{\pm}(\theta,\gamma) = \frac{1}{4}\left(\frac{\gamma_o Z}{\beta\gamma}\right)^2 \frac{1}{\sin^4(\theta/2)}\left[1 - \beta^2 \sin^2(\theta/2) \mp \pi\alpha\beta \sin(\theta/2)\,(1 - \sin(\theta/2))\right] \quad \ldots \quad (5.3)$$

where $\gamma_o = e^2/m_o c^2$ and other symbols have their usual meaning. The cross-section[6] having higher order terms is very complicated. R.M. Curr[8] has given the Mott's[6] cross-section upto the fifth power of (αZ) in the following form:

$$\sigma(\theta,\gamma) = Z^2\left(\frac{e^2}{2m_o c^2\beta^2}\right)\left(\frac{1-\beta^2}{\sin^4(\theta/2)}\right)\left[1 - \beta^2 \sin^2\theta/2 + \alpha\beta R_1 + \alpha^2 R_2 + \alpha^2\beta^2 R_2' + \frac{\alpha^3 R_3}{\beta} + \alpha^3\beta R_3' + \frac{\alpha^4 R_4}{\beta^2} + \alpha^4 R_4' + \alpha^4\beta^2 R_4'' + \frac{\alpha^5 R^5}{\beta^3} + \frac{\alpha^5 R_5'}{\beta} + \alpha^5\beta R_5''\right] \quad \ldots \quad (5.4)$$

where $\alpha = \frac{Z}{137}$, $\beta = v/c$ and θ = angle of scattering. This is for electrons and for positrons only the appropriate sign is

to be changed. The R's are complicated expressions and involve Γ functions of complex nature, and render $\sigma(\theta,\gamma)$ quite unintegrable. In order to have an idea about the extent of contribution due to higher order terms. One can compute the values of elastic scattering cross-section having only linear term in αZ and cross section having terms upto $(\alpha Z)^5$, calling them $\sigma_1(\theta,\gamma)$ and $\sigma_5(\theta,\gamma$ respectively. These values for different angles of scattering in Lead at energy 1 MeV, and different elements for scattering angle 30° at energy 1 MeV, are given in table (5.1) and (5.2) respectively.

TABLE - 5.1

Angle θ	$\sigma_1(\theta,\gamma)$ Barns	$\sigma_5(\theta,\gamma)$ Barns
30	24859.0	25273.0
45	5259.9	6505.8
60	1735.7	2612.8
80	560.5	1039.7
90	349.1	702.4
100	226.8	488.6
120	105.6	252.0
135	64.1	161.5
150	42.1	110.1
180	38.1	72.1

TABLE - 5.2

Elements	$\sigma_1(\theta,\gamma)$ Barns	$\sigma_5(\theta,\gamma)$ Barns
Aluminium	107.98	108.77
Silver	161.15	171.30
Gold	5083.20	5438.90
Lead	5530.30	5871.70

It is observed that the difference in $\sigma_1(\theta,\gamma)$ and $\sigma_5(\theta,\gamma)$ increases with increasing value of angle θ and the atomic number Z. By using the new expression for scattering cross section (Eq. 5.4) one can modify the terms $F^{\pm}(\gamma)^{2-4)}$ and hence $T_r^{\pm\ 2-4)}$ used by Batra and Sehgal. However, the expression (Eq. 5.4) is very tedious and values of R's can not be known in simple analytical form, the graphical method has been adopted to modify the various constants used by Batra and Sehgal[2-4].

(i) Modification of Constants D_1 and D_2

The mean square deflection, $\langle\theta^2\rangle$ of the particle[2-4] requires the knowledge of multiple scattering angle distribution:

$$\langle\theta^2\rangle = \frac{1}{\pi}\int \theta^2\ \sigma(\theta,\gamma)d\theta \qquad \ldots \qquad (5.5)$$

Because the real integration of $\sigma(\theta,\gamma)$ having terms upto 5 of

(αZ) is impossible, the cross-section $\sigma_5(\theta,\gamma)$ has been approximated in present calculations as:

$$\sigma_5(\theta,\gamma) = \eta_1 \sigma_1(\theta,\gamma) \quad \ldots \quad (5.6)$$

where constant η_1 is independent of θ. This constant η_1 is estimated in the following way:

The values of $\sigma_5(\theta,\gamma)$ and $\sigma_1(\theta,\gamma)$ as a function of θ are plotted on the same scale. The area covered under these curves between the screening angle $\theta_s^{2-4)}$ and $\theta_{max} = \pi$ is then estimate. This means the determination of:

$$\left.\begin{aligned} (\text{Area})_5 &= \int_{\theta_s}^{\pi} \sigma_5(\theta,\gamma)d\theta \\ \text{and} \\ (\text{Area})_1 &= \int_{\theta_s}^{\pi} \sigma_1(\theta,\gamma)d\theta \end{aligned}\right\} \quad \ldots \quad (5.7)$$

The constant η_1 is then estimated as:

$$\eta_1 = \frac{(\text{Area})_5}{(\text{Area})_1} \quad \ldots \quad (5.8)$$

The values of the constant η_1 for different elements and different energies are tabulated in table 5.3.

TABLE - 5.3

Elements	Constant η_1 at energy	
	0.77 MeV	1.53 MeV
Aluminium	1.0010	1.0010
Copper	1.0314	1.0226
Yttrium	1.0455	1.0330
Silver	1.0693	1.0434
Holmium	1.0778	1.0759
Gold	1.0990	1.0620
Lead	1.0959	1.0743

Thus solving (Eq. 5.5) in a similar way as done by Batra and Sehgal[2-4], the modified values of $\langle \Phi^2 \rangle^{\pm}_{\gamma_o - \gamma_r}$ for energy <0.5 MeV and energy between 0.5 to 5.0 MeV can be obtained. These values in terms of new values of D_1' and D_2' are given by:

$$\langle \Phi^2 \rangle^{\pm}_{\gamma_o - \gamma_r} = 1 = - D_1' [F_1^{\pm}(\gamma_o) - F_1^{\pm}(\gamma_r)]$$

for energy <0.5 MeV ... (5.9)

and

$$\langle \Phi^2 \rangle^{\pm}_{\gamma_o - \gamma_r} = 1 = - D_2' [F_2^{\pm}(\gamma_o) - F_2^{\pm}(\gamma_r)]$$

for energy >0.5 MeV. ... (5.10)

$$\left.\begin{aligned} \text{Hence} \quad F_1^{\pm}(\gamma_r) &= F_1^{\pm}(\gamma_o) + \frac{1}{D_1'} \\ \text{and} \quad F_2^{\pm}(\gamma_r) &= F_2^{\pm}(\gamma_o) + \frac{1}{D_2'} \end{aligned}\right] \quad \ldots \quad (5.11)$$

where γ_o corresponds to thickness dx = O of the absorber and γ_r corresponds to the thickness where the energy of the particle becomes equal to the critical energy. It is quite clear that the factors D_1' and D_2' will be η_1 times greater than the factors (D_1 and D_2)[2-4] respectively. This factor η_1 can be taken out of the integral and rest of the calculations are the same as carried by Batra and Sehgal[2-4]. The factors D_1 and D_2 are given by:

$$\left.\begin{aligned} D_1 &= 4\pi\, N\, r_e^2\, Z(Z+1)\, m_o c^2 / \rho (m_1 Z + C_1) \\ D_2 &= 4\pi\, N\, r_e^2\, Z(Z+1)\, m_o c^2 / \rho (m_2 Z + C_2) \end{aligned}\right] \quad \ldots \quad (5.12)$$

where r_e is the classical radius of the electron, ρ is the density of the scatterer, m_1, m_2, C_1 and C_2 are the constants listed in the papers of Batra and Sehgal[2-3]. The values of D_1 and D_2 have also been tabulated by them[2-3] for various elements.

(ii) Modification of the functions $F^{\pm}(\gamma_r)$

The functions $F_1^{\pm}(\gamma_r)$ and $F_2^{\pm}(\gamma_r)$ are given by Batra and Sehgal[2-4] in terms of large number of integrals. Few of them

can be integrated directly and the integrand for rest of them can be expanded in the form of convergent series. In the present case these series are integrated upto 200 terms with the help of an IBM 1130. The Mott's cross-section[6] is a function of γ, so for modification of the function $F^{\pm}(\gamma)$ we use the earlier method, $\sigma_5(\gamma) = \eta_2\ \sigma_1(\gamma)$ for some particular value of the scattering angle θ. The factor η_2 comes out to be more than one for different elements at an optimum angle $\theta \simeq 30^{\circ}$. Therefore, the modified values of the functions, $[F_1^{\pm}(\gamma_r)]_{mod.}$ and $[F_2^{\pm}(\gamma_r)]_{mod.}$ given by:

$$\left.\begin{aligned} F_1^{\pm}(\gamma_r)_{mod.} &= \eta_2\ [F_1^{\pm}(\gamma_r)] \\ \text{and} \qquad F_2^{\pm}(\gamma_r)_{mod.} &= \eta_2\ [F_2^{\pm}(\gamma_r)] \end{aligned}\right\} \quad \ldots \qquad (5.13)$$

are also increased.

By using the modified values of factors D_1, D_2, $F_1^{\pm}(\gamma_r)$ and $F_2^{\pm}(\gamma_r)$, the values of the range were computed in the same way as done by Batra and Sehgal[2-4] the values show improvement of about 6% in the low-Z region, 18% in the high-Z region and about 10% in the intermediate Z values.

(b) Effects of Diffusion on the Range of Positrons and Electrons

After evaluation of the projected range $R_p^{\pm}$, i.e. the straight path traversed by positrons and electrons, by

incarporating the modified values of D_1, D_2 and $F^{\pm}(\gamma_r)$ functions as discussed above in article 5.2(a) and using(Eq. 5.2) one can proceed to evaluate the effects of diffusion on the range of these particles, i.e. the contribution to range of these particles after the energy of these particles is reduced to the level of critical energy.

Assuming a uniform source of positrons and electrons at distances $= R_p^{\pm}$, the age equation of diffusion theory, i.e.

$$\frac{\partial F}{\partial s} + \frac{1}{3\chi^{\pm}(\gamma)} \nabla^2 F = 0 \qquad \ldots \qquad (5.14)$$

can be used to evaluate the distance traversed after the start of diffusion by these particles along their initial direction. Where $\chi^{\pm}(\gamma)$ is the reciprocal of the transport mean free path $\lambda^{\pm}(\gamma)$ and for positrons and electrons is given as:

$$\chi^{\pm}(\gamma) = \frac{1}{\lambda^{\pm}(\gamma)} = 2\pi N \int_{\theta_{min.}}^{\pi} \sigma^{\pm}(\theta,\gamma)\,(1-\cos\theta)\sin\theta\, d\theta \quad \ldots(5.15)$$

$\theta_{min.}$ is the non-zero lower limit of the integral which takes into account the atomic screening and has been taken in the present calculation, according to William[9] i.e. $\theta_{min.} = \alpha Z^{1/3}(\gamma^2-1)^{-1/2}$, where α is the fine structure constant. The upper limit $\theta_{max.}$ is taken as π, its natural value for a point nucleus, so long as the energy remains below 5.0 MeV[10], which

is the region of energy of the present investigations. $\sigma^{\pm}(\theta,\gamma)$ is the elastic single scattering cross-section[6,11] for positrons and electrons:

$$\sigma^{\pm}(\theta,\gamma) = \frac{r_e^2 Z\,(Z+1)}{(\gamma^2-1)^2}\;\frac{\gamma^2}{4\mathrm{Sin}^4(\theta/2)}\;\left[1-\frac{\gamma^2-1}{\gamma^2}\,\mathrm{Sin}^2(\theta/2)\right.$$

$$\left.\mp\,\pi\alpha Z(\gamma^2-1)^{1/2}/\gamma\;\mathrm{Sin}(\theta/2)(1-\mathrm{Sin}(\theta/2))\right] \qquad (5.16)$$

where r_e = classical radius of an electron and $Z(Z+1)$ replaces Z^2 in original Mott's[6] expression to account for the scattering of incident particles by orbital electrons also. The factor 'F' in (Eq. 5.14) is the total density of positrons or electrons.

Now using the theory of Bethe et al.[1] and Rohrlich and Carlson[12], the expression for mean square of the distance traversed by these particles, $(r^2_{av.})^{\pm}$, after the diffusion starts can be obtain from (Eq. 5.14), as:

$$(r^2_{av.})^{\pm} = 1.05 \int \frac{1}{\chi^{\pm}(\gamma)} \left(\left|\frac{d\gamma}{ds}\right|^{\pm}\right)^{-1} d\gamma \quad \ldots \qquad (5.17)$$

Using the values of $\left(\left|\frac{d\gamma}{ds}\right|^{\pm}\right)^{-1}$ from ref. 2,3 and 7 and using (Eqs. 5.15 and 5.16) one can obtain the root mean square distance $r^{\pm}_{av.} = \sqrt{(r^2_{av.})^{\pm}}$ from (Eq. 5.17). Assuming the diffusion

R_p^- and R_{sfp}^- agree for low-Z materials, with the exception of carbon. The difference for intermediate values of Z was of the order of 16% or so and for high-Z materials this difference is 30% and even more for very low energies. After the inclusion of higher order terms in Mott and Massey[6,11] expressions for elastic scattering cross-section the improvement in the values of calculated range was about 6 to 12% in the low Z region and 10 - 18% in the high-Z region. In addition to the modified values of $R_p^{\pm}$ the contribution to range due to diffusion part of the range has been estimated for few absorbers at energies 0.77 MeV and 1.53 MeV. The values of the theoretical range $R_{sfp}^- = R_{p_{mod.}}^- + \sqrt{(r_{av.}^2)}$ at energies E_{max} = 0.77 MeV and 1.53 MeV in Al, Cu, Y, Ag, Ho and Pb, have been compared with the experimental data and shown in table 5.4. The difference in the experimental and theoretical values at energy E_{max} = 0.77 MeV is from -0.01% to about 6% in low-Z materials and from 6% to about 9.5% for high-Z materials. Similarly the difference between the two sets of values at energy E_{max} = 1.53 MeV, is also from -0.50% to 5.3% in low-Z materials and upto 8.4% in high-Z materials. The difference in experimental and theoretical values tends to be more at low energy and high-Z materials and less at high energy and low-Z materials. This trend was also observed in Chapter - III while comparing the values of R_p^- with R_{sfp}^- at different energies and different Z. The agreement between the experimental and theoretical values after incarporating the effects of higher order terms in Mott[6] and Massey[11]

TABLE - 5.4

Comparison of experimental values of R^-_{sfp} (in mg cm^{-2}) at E_{max} = 0.77 MeV and 1.53 MeV with present theoretical values of $R^-_{sfp} = (R^-_{p_{mod}} + \sqrt{(r^2_{av})}^-$ in some absorbers. The values of R^-_p due to Batra and Sehgal[2-4] are also given for comparison.

Material	E_{max} = 0.77 MeV				E_{max} = 1.53 MeV			
	Experimental	Theoretical	% diff.	R^-_p(ref. 2-4)	Experimental	Theoretical	% diff.	R^-_p(ref. 2-4)
Aluminium	296	299	-0.01	297	688	692	-0.5	699
Copper	285	270	+5.2	228	622	589	+5.3	537
Yttrium	268	252	+5.9	206	596	553	+7.2	487
Silver	264	239	+9.5	194	580	547	+5.7	458
Holmium	242	219	+9.5	173	536	501	+6.5	407
Gold	235	218	+7.2	163	514	479	+6.8	386
Lead	231	213	+7.8	161	510	467	+8.4	381

expression of elastic scattering cross-section and the effect of diffusion part of the range, is quite good as shown in table 5.4. The present difference in the two sets of values can be explained as due to the errors in the total stopping power expressions[2-4,7] being used as input data for these calculations, which are stated to be about 4% or so. The experimental values also have error of about 4%. Hence the compound effect of these errors might result in the differences of experimental and theoretical values as shown in table 5.4.

Batra and Sehgal[2-4] in their investigations observed that after the energy of the electrons or positrons has attained the critical value, these particles thereafter move randomly or get diffused and diffusion leads to straggling. By incarporating the contribution to the range due to the diffusion of these particles, the straggling effect has been taken care off. This makes these theoretical values comparable with the straggling free practical ranges of these particles, realized in the present experimental work.

While dealing with the improvements in the earlier theoretical approach in this Chapter, only few details of the earlier work have been given, and as such one has to refer to the earlier references.

REFERENCES

1. H.A. Bethe, M.E. Rose and L.P. Smith, Proc. Am. Phil. Soc. 78, 573 (1938).

2. R.K. Batra and M.L. Sehgal, Nuclear Physics A156, 314-20 (1970).

3. R.K. Batra and M.L. Sehgal, Nucl. Inst. Methods 109, 565 (1973).

4. R.K. Batra and M.L. Sehgal, Phys. Rev. B23, No. 9, 4448 (1981).

5. M.J. Berger and S.M. Seltzer, NAS-NRC Publ. No. 1133(1964) and NASA SP-3012 (1964).

6. N.F. Mott, Proc. Roy. Soc. (London) A124, 425 (1929) and A135, 429 (1932).

7. S.K. Rathi, Ph.D. thesis, A.M.U., Aligarh (un-published) (1982).

8. R.M. Curr, Proc. Roy. Soc. A68, 156 (1955).

9. E.J. Williams, Proc. Roy. Soc. (London) A169, 531 (1939), and Phys. Rev. 58, 292 (1940).

10. E.R.B. Elton, Proc. Phys. Soc. A63, 1115 (1950).

11. H.S.W. Massey, Proc. Roy. Soc. (London) A181, 14 (1943).